

Paleogeographic evolution and vertical motion of the central Lesser Antilles forearc since the Early Miocene: A potential driver for land fauna dispersals between the Americas

Cornée Jean-Jacques ^{1,*}, De Min Lyvane ¹, Lebrun Jean-Frédéric ¹, Quillévéré Frédéric ², Melinte-Dobrinescu Mihaela ³, Boudagher-Fadel Marcelle ⁴, Montheil Lény ⁵, Marcaillou Boris ⁶, Thinon Isabelle ⁷, Philippon Mélody ¹

¹ Géosciences Montpellier, CNRS-Université des Antilles-Université de Montpellier, F-97159, Pointe à Pitre, Guadeloupe, France

² Université Claude Bernard Lyon 1, ENS de Lyon, CNRS, UMR 5276 LGL-TPE, F-69622, Villeurbanne, France

³ National Institute of Marine Geology and Geoecology, 23–25 Dimitrie Onciul Street, PO Box 34–51, 70318, Bucharest, Romania

⁴ Office of the Vice-Provost (Research), University College London, 2 Taviton Street, London, WC1H 0BT, UK

⁵ Géosciences Montpellier, CNRS-Université de Montpellier-Université des Antilles, F-34095, Montpellier, France

⁶ Geoazur, Université de La Côte D'Azur, CNRS, Observatoire de La Côte D'Azur, IRD, F-06560, Valbonne, France

⁷ BRGM, 3 Avenue Claude-Guillemain, BP 36009, 45060, ORLÉANS Cedex 2, France

* Corresponding author : Jean-Jacques Cornée, email address : jean-jacques.cornee@umontpellier.fr

Abstract :

Phylogenetic studies of present-day terrestrial organisms suggest that faunal dispersals between South America and the Greater Antilles may have occurred during the Cenozoic through the Lesser Antilles. However, because of the lack of geological data to unravel the areas that may have emerged along the Lesser Antilles trench, the migration paths used by their ancestors remain unknown. Here, we present novel paleogeographic maps of the central Lesser Antilles (extending from Guadeloupe to Martinique islands) which are built on the basis of onshore and offshore stratigraphic correlations (50 seismic lines, biostratigraphy of 9 dredged and 29 field samples, six sedimentary logs). We find that repetitive episodes of uplift and drowning have occurred in the central part of the Lesser Antilles during the Neogene. Offshore, the Marie-Galante Basin comprises three sedimentary megasequences that deposited between: (i) the Oligocene and Early Miocene, including the extinct arc, (ii) the Middle and Late Miocene and (iii) the latest Miocene and Holocene. These sediments infill a NNW-SEE trending forearc rift that opened during the Early Miocene. The megasequences are separated by subaerial regional unconformities that affect the rift shoulders. Onshore, we show that the lower part of the carbonate platform in Guadeloupe and La Désirade has deposited during the late Messinian. In Martinique, we refine the age of the carbonate deposits belonging to the extinct arc to the Chattian-Burdigalian, and evidence a major subaerial unconformity corresponding to the Middle Miocene. We propose that between Anguilla and Martinique, from north to south, large archipelagos, which are now drowned, have existed during the

early Middle Miocene and the latest Miocene. We suggest that during the Miocene, the Lesser Antilles may have been used as a pathway for land-faunal dispersals from South America.

Highlights

► The Marie Galante Basin comprises three Eocene to present-day seismic megasequences. ► The Marie Galante Basin is an intra-arc rift with two Miocene uplifts. ► Martinique displays an early Middle Miocene uplift. ► ArChipelagos existed by the early Middle and latest Miocene in the Lesser Antilles. ► The Lesser Antilles can be a pathway for Cainozoic terrestrial fauna migrations.

Keywords : Lesser antilles, Neogene, Paleogeography, Guadeloupe Archipelago, Rifting, Seismic stratigraphy, Fauna dispersal

39
40 50 1. INTRODUCTION
41
42

43 51 Subduction zones experience intense strain inducing significant vertical motions in the overriding
44
45
46 52 plate. Back-arc, arc and forearc domains undergo cycles of hundred to thousand metres scaled uplift
47
48 53 and subsidence over temporal scales of 100 ka to 10 Ma (Lallemand and Le Pichon, 1987; Fisher et
49
50
51 54 al., 1998; Sak et al., 2004; Clift and Vanucchi, 2004; Menant et al., 2020). In addition to tectonically-
52
53 55 controlled vertical motion, magmatism along the arc can contribute to crustal thickening, both pro-
54
55 56 cesses leading to land uplift (Ma et al., 2022; Montheil et al., 2022). Along intra-oceanic subduction
57
58 57 zones, these processes may thus result in cyclic rise or demise of islands or isthmus, building or
59
60
61
62
63
64
65

58 destroying terrestrial connections and possibly connecting/disconnecting nearby continental land-
159 masses. These prompt paleogeographic changes control the existence of emerged pathways for ter-
2 restrial fauna and flora. The temporality of the formation and disappearance of such pathways partly
3 60 dictate the dispersal or isolation of terrestrial species, strongly influencing their biological evolution
4 5
6 61 and biodiversity. The Antilles (*sensu lato*) intra-oceanic subduction zone has evolved in between the
7 8
8 62 North and South America landmasses since the mid Cretaceous (*e.g.*, Pindell and Kennan, 2009;
9 10
11 63 Boschman et al., 2014) and has been identified worldwide as one of the thirty-five biodiversity
12 13
13 64 hotspots (Myers et al., 2000). This subduction zone thus constitutes a fabulous natural laboratory to
14 15
15 65 shed light on the relationships between paleogeography, tectonics, magmatism and biological history.
16 17
18 66

19
20
21 67 In the Greater and Lesser Antilles, many Cenozoic terrestrial organisms originated from South
22 23
23 68 America (*e.g.*, Hedges, 1996; Itturalde-Vinent and Mac Phee, 1999; Blackburn et al., 2020; Marivaux
24 25
25 69 et al., 2020), while others find their ancestors in North America (*e.g.*, Marivaux et al., 2021). How
26 27
28 70 and when these terrestrial organisms have spread from to reach the isolated Antilles islands remains
29 30
30 71 highly debated. For some authors, a land bridge existed between the South American continent and
31 32
32 72 the Greater Antilles during the late Eocene (between 35 and 33 Ma). These authors either suggested
33 34
34 73 that this land bridge was located along the currently submerged Aves Ridge, a remnant of the Late
35 36
36 73 Cretaceous-Paleocene arc now in back arc position (GAARLandia hypothesis, Itturalde-Vinent and
37 38
38 74 Mac Phee, 1999; Cala-Riquelme et al., 2022) or along the northern Lesser Antilles (GrANoLA land,
39 40
40 75 Philippon et al., 2020) (Fig. 1). Others suggested the existence of an isthmus in the southern Lesser
41 42
42 76 Antilles (late Eocene – Present-day arc) (Bourgade, 2020) and/or long-distance overseas dispersals
43 44
44 77 (Ali, 2012; Ali and Hedges, 2021) (Fig. 1B).
45 46
46 78
47
48 78

49
50
51 79 In the Lesser Antilles, the fossil record of terrestrial organisms is presently limited to Upper Pleis-
52 53
53 80 tocene deposits (*e.g.*, Hedges, 1996; Davalos, 2004; Fabre et al., 2014). The origin, pattern of dis-
54 55
55 81 persal and timing of isolation of these organisms remain unknown. For example, colonization of the
56 57
57 82 fossil Oryzomyine rodents in Guadeloupe, Marie-Galante, Antigua and Barbuda took place during
58 59
59 82
60
61
62
63
64
65

83 the Late Miocene (Brace et al., 2015) and subfossil genera exhibit peculiar distributions in the differ-
 184 ent islands of the Lesser Antilles (Durocher et al., 2020). Based on mitochondrial DNA (mtDNA)
 2
 385 analyses, Surget-Groba and Thorpe (2013) demonstrated that the appearance of the lizard geckos
 4
 5
 686 *Sphaerodactylus vincenti* and *Anolis roquet* occurred at *ca* 12.5 Ma and high divergence rates have
 7
 887 been evidenced between northern Martinique-Dominica and southern Martinique-southern Lesser
 9
 10
 1188 Antilles populations. Moreover, molecular clock data showed that the common ancestor of other
 12
 1389 *Anolis* lizards from the central and southern Lesser Antilles originated from South America and that
 14
 15
 1690 speciation events began prior to 25 Ma (Bourgade, 2020). For this author, Martinique would have
 17
 1891 been a refuge for insular terrestrial faunas as soon as 45 Ma. This island that remained emerged since
 19
 20
 2192 *ca* 25 Ma might have been a centre of dispersion for species in the Antillean arc since 12 Ma. Molec-
 22
 2393 ular clock data further showed that amphisbaenid lizards should have migrated from the Amazon
 24
 2594 Basin to Hispaniola (Grabosky et al., 2022). These authors suggested that it occurred through the
 26
 27
 2895 Lesser Antilles during the late Early Miocene or Middle Miocene thanks to both overwater dispersals
 29
 3096 by the North Brazilian Current and ephemeral formations of islands during glacio-eustatic sea level
 31
 32
 3397 drops.

34
 35
 3698 Philippon et al. (2020) and Cornée et al. (2021) recently provided evidences for major changes in
 37
 3899 the paleogeography of the northern Lesser Antilles (*i.e.*, north of Guadeloupe) and its potential role
 39
 40
 41100 in the dispersal of terrestrial organisms. To understand whether or not past emergent landmasses ex-
 42
 43101 isted in the central Lesser Antilles as suggested by molecular phylogenetic studies, we reconstruct
 44
 45
 46102 the paleogeographic evolution of the central Lesser Antilles since the late Oligocene-Early Miocene
 47
 48103 interval, from north to south between the Marie-Galante Basin and the Martinique Island (Figs. 1 and
 49
 50104 2). Our study is based on offshore data acquired during the KaShallow Program (Lebrun , 2009) and
 51
 52
 53105 new field investigations onshore Guadeloupe, La Désirade and Martinique.

54
 55
 56106 2. GEOLOGICAL SETTING OF THE CENTRAL LESSER ANTILLES (GUADELOUPE, DOM-
 57
 58
 59107 INICA, MARTINIQUE)

60
 61
 62
 63
 64
 65

108 2.1. GEODYNAMICAL SETTING

1109 The Lesser Antilles subduction zone results from the westward subduction of the North and South
 1110 America lithosphere beneath the mantle stationary Caribbean plate, at a speed of 18-20 km.Ma⁻¹
 1111 (Dixon et al., 1998; DeMets et al., 2010; Boschman et al., 2014) (Fig. 1). To the north and to the
 1112 south, the Caribbean plate is bounded by two transform faults. To the east, the plate boundary consists
 1113 in the highly curved Lesser Antilles trench, along which the Lesser Antilles volcanic arc has devel-
 1114 oped since the Eocene (Martin-Kaye, 1969; Stein et al., 1982; Bouysse and Westercamp, 1990;
 1115 Bouysse et al., 1990; Pindell and Barret, 1990; Mann et al., 1995). This arc shows a peculiar north-
 1116 south dichotomy. North of Martinique, an extinct Eocene-Oligocene arc is exposed in the forearc on
 1117 the islands of Antigua, Saint-Barthélemy and Saint-Martin (*e.g.*, Bouysse and Mascle, 1994; Legen-
 1118 dre et al., 2018; Noury et al., 2021; Montheil et al., 2022). This extinct arc is sealed by shallow water
 1119 carbonate platforms whose ages range between the late Oligocene and the Holocene. From Marti-
 1120 nique southward, the modern arc remains at the location of the extinct arc (Fig. 1A).

31 32 21 2.2. GEOLOGY OF GUADELOUPE ARCHIPELAGO

33 The Guadeloupe Archipelago (Fig. 2) consists of (i) to the West, the islands of Basse-Terre and
 34 Les Saintes composed of subaerial volcanic rocks that have formed since 4.3 Ma in the Early Pliocene
 35 (Andréieff et al., 1989; Bouysse et al., 1990; Samper et al., 2007; Zami et al., 2014; Favier et al.,
 36 2019) and (ii) to the East, the islands of Marie-Galante, Grande-Terre and La Désirade, made of
 37 Pliocene to Pleistocene carbonate platform deposits unconformably lying on Miocene sedimentary
 38 rocks or Upper Jurassic igneous rocks (*e.g.*, Andréieff et al., 1989; Bouysse et al., 1993; Neill et al.,
 39 2010 ; Corsini et al., 2011; Cornée et al., 2012; Münch et al., 2013, 2014). Offshore in the Marie-
 40 Galante Basin, several submerged flat top shallow banks or plateaus occur (Fig. 2D). Les Saintes
 41 Plateau surrounds the volcanic island, the Colombie Bank rests between Basse-Terre and Marie-Ga-
 42 lante and the Flandres Bank is located east of La Désirade. To the east, the north-south trending
 43 Karukéra Spur separates the Marie-Galante Basin (west) from the outer-forearc Barbados accretion-
 44 ary wedge (east).

134 2.2.1. Onshore setting

135 The carbonate platform of Grande-Terre consists of more than 100 m- thick deposits organized
 136 into four transgressive-regressive sedimentary cycles, namely Sequences 1 to 4 (Andréieff et al.,
 137 1983, 1989; Garrabé, 1983; Léticée et al., 2005; Cornée et al., 2012; Münch et al., 2014) (Fig. 3). The
 138 sequences comprise red algal and coral-rich beds which deposited between the Zanclean and the Ca-
 139 labrian. The sequences are bounded by erosional unconformities that attest for emersion of the island.
 140 In Grande-Terre, these sequence boundaries are accurately dated to the Piacenzian (SB0 and SB1)
 141 and the Calabrian (SB2 and SB3) (Münch et al., 2014) (ages on Fig. 3). A coral reef terrace that
 142 formed during Marine Isotope Stage (MIS) 5e locally fringes the island.

143 Marie-Galante and La Désirade carbonate platforms share a common stratigraphy with that of
 144 Grande-Terre (Fig. 3). In Marie-Galante the platform is 150- m thick. Due to poor exposure, SB0 and
 145 SB1 are not clearly identified in the red algal deposits but the change to coral rich unit as well as SB2
 146 and SB3 are correlated with those exposed in Grande-Terre (Bouysse et al., 1993; Léticée, 2008;
 147 Münch et al., 2013). The Marie-Galante platform rests unconformably above ten m-thick upper Tor-
 148 tonian tilted tuffaceous marls (Fig. 3). Uplifted and tilted marine terraces formed during MIS5e and
 149 MIS7e rim the southeastern part of the island (Battistini et al., 1986; Feuillet et al., 2004). In La
 150 Désirade (Fig. 3) the 100- to 120- m thick Pliocene to Lower Pleistocene red algal to coral rich shal-
 151 low carbonate deposits (Westercamp, 1980; Léticée, 2008; Lardeaux et al., 2013; Münch et al., 2014)
 152 rest above a deformed Upper Jurassic magmatic basement (Westercamp, 1980; Bouysse et al., 1983;
 153 Mattinson et al., 2008; Cordey and Cornée, 2009; Neill et al., 2010; Corsini et al., 2011). SB1, SB2
 154 and SB3 are also identified, suggesting that the three islands of the Guadeloupe Archipelago experi-
 155 enced synchronous episodes of emersions (Fig. 3). La Désirade Island is also surrounded by a flight
 156 of four uplifted marine terraces formed during the Pleistocene interglacial stages MIS 5e (+10m),
 157 MIS 9e (+35m), MIS 15 to MIS 17 (+71m), and MIS 19 to MIS 25 (+90m) (Battistini et al., 1986;
 158 Feuillet et al., 2004; Léticée et al., 2019).

159 2.2.2. Offshore setting

160 Les Saintes consist of 3 to 2 Ma and 0.9 Ma old volcanic islands (Zami et al., 2014) that underwent
 161 high temperature hydrothermalism (Vérati et al., 2018; Favier et al., 2019, 2021). The submerged part
 162 of the volcanoes is covered by a *ca* 250 m- thick coral reef plateau. Leclerc and Feuillet (2019) sug-
 163 gested that this fringing reefal plateau has been built during glacial cycles of the Middle to Late
 164 Pleistocene (since less than 360 ka, MIS9).

165 The submerged plateau south of Grande-Terre and La Désirade rests between 10 and 20 m below
 166 sea level (bsl). Münch et al. (2013) correlated the plateau seismic units with the Grande-Terre car-
 167 bonate Sequences 3 and 4 and argued that the South Grande-Terre Plateau has been recently tectoni-
 168 cally drowned along the E-W trending fault bounding the southern coast of the island.

169 From seismic interpretations across the Colombie Bank (Münch et al., 2013), a first sequence of
 170 outer ramp to basin sediments has been attributed to the Lower Pleistocene (Calabrian, between 1.1
 171 and 1.5 Ma) and correlated with carbonate Sequence 4 in the island of Marie-Galante (Fig. 3). The
 172 second sequence of the bank (*ca* 0.1 stwt- thick, Fig. 8 in Münch et al. 2013) rests conformably upon
 173 the first one and displays seismic characteristics of reefal build-ups. This indicates that when the
 174 island of Marie-Galante emerged by the end of the Calabrian, the Colombie Bank remained below
 175 sea level with shallow-water deposits (Fig. 3 and Fig. 10 in Münch et al., 2013).

176 The Flandres Bank is a narrow carbonate platform that culminates at 40 m bsl at the northernmost
 177 tip of the Karukéra Spur. The platform rests unconformably upon the igneous basement of the spur.
 178 The carbonate deposits comprise two sequences. The first sequence remains undated, fills the base-
 179 ment depressions and is topped by a flat erosional surface. The second (0.02s twt- thick) is made of
 180 Holocene reefal deposits (Andréieff et al., 1980; Münch et al., 2013; De Min et al., 2015).

181 The Karukéra Spur is a submerged north-south trending horst that borders the eastern part of the
 182 Marie-Galante Basin (Fig. 2). The basement of the spur is composed of igneous rocks like those of

183 La Désirade Island (Andréieff et al., 1980). De Min (2014) and De Min et al. (2015) characterized
 184 seven seismic units organized into four depositional megasequences above the basement (Fig. 3).

2
 3
 485 • Megasequence 1 (S1 and S2 in Fig. 3 and MG-MS1 in Fig. 4) infills basement depressions
 5 and retrogrades upslope. The uppermost part of the megasequence exhibits Lower Miocene
 6
 786 shallow-water limestones. Megasequence 1 is sub-divided into two units and is framed by two
 8
 987 erosional unconformities, SB1 at bottom and SB2 at top.

10
 1188
 12
 13
 1489 • Megasequence 2 (S3 in Fig. 3 - MG-MS2 in Fig. 4) is made of Middle (?) to Upper Miocene
 15 basin deposits organized into a transgressive system tract, topped by an erosional unconform-
 16
 1790 ity SB3 dated to the latest Miocene.

18
 1991
 20
 21
 2292 • Megasequence 3 (S4 in Fig. 3 - MG-MS3 in Fig. 4) consists of Lower to Upper Pliocene basin
 23 marls and reefal deposits.

24
 2593
 26
 27
 2894 • Megasequence 4 (S5 to S7 in Fig. 3 - upper part of MG-MS3 in Fig. 4) is made of Gelasian-
 29
 3095 Calabrian to recent deposits.

31
 32
 3396 During the 1970' and 1980', the Arcante Project (Bouysse and Guennoc, 1983) was devoted to the
 34 Marie-Galante Basin. The team collected regional scale geophysical data and 14 rock samples (Fig.
 35
 3697 S1). The authors described large amplitude vertical motions affecting the forearc related to transient
 37
 3898 events due to subduction of a buoyant ridge. They suggested large forearc emersion during the Oli-
 39
 4099 gocene, followed by a westward (landward) migration of the volcanic islands as the consequence of
 41
 424300 slab breakoff (Bouysse et al., 1990 and references therein). During the early 2000', the AGUADO-
 44
 45201 MAR project team (Deplus et al., 1998; Feuillet et al., 2002) acquired new seismic and bathymetric
 46
 474802 data. They described the Marie-Galante Basin as a forearc transverse basin connecting the Montser-
 49
 50203 rat-Harvers strike slip fault that runs along the arc to the trench. The SismAntilles/Thales Was Right
 51
 525204 program (Hirn, 2001; Kopp et al., 2011; Evain et al., 2011; Laigle et al., 2013) provided crustal scale
 53
 5455205 structure images revealing a rather thick, igneous inner forearc crust (25-28km) beneath the Marie-
 56
 575806 Galante Basin.

59
 60207
 61
 62
 63
 64
 65

208 2.3. GEOLOGY OF MARTINIQUE AND DOMINICA

~~2~~¹209 Martinique Island comprises three main volcanic and sedimentary units (Bellon et al., 1984; An-
~~3~~³
~~4~~⁴210 dréïeff et al., 1988; Westercamp et al., 1989, 1990; Germa et al., 2011), showing a westward decrease
~~5~~⁵
~~6~~⁶211 in ages. From east to west the island exposes (i) an ancient (latest Oligocene-Early Miocene) arc
~~7~~⁷
~~8~~⁸212 dating 24.8 ± 0.4 to 20.8 ± 0.4 Ma (K/Ar, Germa et al., 2011); (ii) an intermediate arc with submarine
~~9~~⁹
~~10~~¹⁰213 volcanoclastic sediments and numerous dykes to the east and subaerial magmatism to the west (16.12
~~11~~¹¹
~~12~~¹²214 ± 0.23 - 7.09 ± 0.10 Ma; K/Ar, Germa et al., 2011); (iii) a recent arc (2.36 Ma to present-day; Germa
~~13~~¹³
~~14~~¹⁴215 et al., 2011). The oldest arc also presents some intercalated shallow marine carbonate patches that
~~15~~¹⁵
~~16~~¹⁶216 were emplaced during volcanic quiescence episodes (La Caravelle, Sainte-Anne, Macabou) and that
~~17~~¹⁷
~~18~~¹⁸217 have deposited during the late Oligocene and possibly the Aquitanian (Andréïeff et al., 1988;
~~19~~¹⁹
~~20~~²⁰218 Westercamp et al., 1989). Offshore from the northeastern shelf of Martinique northward, the Oligo-
~~21~~²¹
~~22~~²²219 cene-Early Miocene ancient arc stands beneath the reefal platform of America and Dien Bien Phu
~~23~~²³
~~24~~²⁴220 Banks (Fig. 1) dating from Pliocene-Pleistocene at least to Holocene (Andréïeff et al, 1980; Leclerc
~~25~~²⁵
~~26~~²⁶221 et al., 2015).
~~27~~²⁷
~~28~~²⁸
~~29~~²⁹
~~30~~³⁰
~~31~~³¹
~~32~~³²

~~33~~³³
~~34~~³⁴222 Dominica Island is composed of four subaerial volcanic units which date Late Miocene (6.8-5.2
~~35~~³⁵
~~36~~³⁶223 Ma) to present (*e.g.*, Lindsay et al., 2005; Smith et al., 2013). Sparse outcrops of undated “raised
~~37~~³⁷
~~38~~³⁸224 limestone” deposits are reported along the western coast, resting onto Upper Pliocene – Lower Pleis-
~~39~~³⁹
~~40~~⁴⁰225 tocene (3.7-1.8 Ma) volcanoclastic deposits. Offshore, a narrow shelf occurs around the island with
~~41~~⁴¹
~~42~~⁴²226 Holocene reefal carbonate deposits.
~~43~~⁴³
~~44~~⁴⁴
~~45~~⁴⁵
~~46~~⁴⁶

~~47~~⁴⁷227 3. METHODS

~~48~~⁴⁸
~~49~~⁴⁹

~~50~~⁵⁰228 We present a dataset acquired during the KaShallow cruise (Lebrun, 2009) including high-resolu-
~~51~~⁵¹
~~52~~⁵²229 tion seismic reflection lines, high resolution multibeam bathymetry and collected rock samples from
~~53~~⁵³
~~54~~⁵⁴230 the Marie-Galante Basin (Fig. 2). The dataset is complemented with seismic and bathymetric data
~~55~~⁵⁵
~~56~~⁵⁶231 from the Aguadomar (Deplus, 1998) and SismAntilles 1 and 2 cruises (Hirn 2001; Hirn et al., 2007;
~~57~~⁵⁷
~~58~~⁵⁸232 Laigle et al., 2007).
~~59~~⁵⁹
~~60~~⁶⁰
~~61~~⁶¹
~~62~~⁶²
~~63~~⁶³
~~64~~⁶⁴
~~65~~⁶⁵

233 3.1. SEISMIC REFLEXION PROFILES

1
 234 In this study we interpreted *ca* 6500 km of seismic reflection lines of various resolution and pen-
 3
 235 etration including KaShallow 1 HR seismic data (sparker source) and SismAntilles 1 multichannel
 5
 236 seismic reflection data (4400-8800Ci airguns array source) not shown here. The KaShallow 2 seismic
 7
 237 source was an array of six 24-35Ci GI Airguns recorded with a 72 channel – 450 m long streamer (9
 8
 10 or 18-fold stack - far field peak frequency 40-70hz – characteristic penetration *ca* 1-1.5stwt - second
 11
 12 two-way-travel-time). The Aguadomar cruise seismic lines were shot with 2 GI airguns of 45/105ci
 13
 14 239 recorded on a 50 m long 6 channels streamer (3-fold stack) and acquired at high speed. This provided
 15
 16 240 a mid-resolution seismic data with a far field peak frequency of *ca* 30-50Hz and a characteristic pen-
 17
 18 241 etration *ca* 1-2stwt. The cruise aimed at mapping the basin relief, thus lines are rather distant one
 19
 20 242 from the other and oriented N-S, except south of Marie-Galante where they are oriented E-W. Pro-
 21
 22 243 cessing of these data included band pass filtering, predictive deconvolution, simple velocity analysis
 23
 24 244 and nmo corrections, stack and constant water velocity time migration.
 25
 26
 27
 28
 29
 30

31 246 We determine the seismic facies following conventional seismic facies analysis as first established
 32
 33 247 during the late 70's (Mitchum et al. 1976, Vail et al. 1977, Roksandic 1978, Xu and Haq 2022 and
 34
 35 248 references there in) and interpret the sedimentary sequences based on the nomenclature of Catuneanu
 36
 37 249 et al. (2011). We defined 14 facies illustrating the first order seismic stratigraphy of the basin (sup-
 38
 39 250 plementary Fig. S2) based on regional setting, external form, internal configuration, reflection ampli-
 40
 41 251 tude, dominant frequency and reflection continuity of the units. The seismic facies (supplementary
 42
 43 252 data Fig. S2) are interpreted in terms of igneous and sedimentary facies based on dredged samples
 44
 45 253 collected from several of the seismic units (supplementary Fig. S1). We found that the basin com-
 46
 47 254 prised six seismic units organised in 3 Megasequences (MG-MS) bounded by regional, partly ero-
 48
 49 255 sional, unconformities (MG-SB). We investigated the seismic lines of the Marie-Galante Basin refer-
 50
 51 256 ring to the seismic units defined by De Min et al. (2015) across the Karukéra Spur. We cross-corre-
 52
 53 257 lated all the seismic lines through the basin and spur. We present the line Aguadomar-116-34-119-
 54
 55 258 KaShallow2-080 (Fig. 4 and Fig. S3) to illustrate the structure of the basin along an E-W transect,
 56
 57
 58
 59
 60
 61
 62
 63
 64
 65

259 perpendicular to the western border of the Karukéra Spur, across the Arawak Sub-basin to upslope
 260 the Kubuli Sub-basin. The line KaShallow2-026-060-061-062 (Fig. 5 and Fig. S4) provides a NNW-
 261 SSE trending cross section along the Arawak Sub-basin, from the South of the Grande-Terre shelf to
 262 the southeastern Arawak Sub-basin. The line trends parallel to the gully shape of the basin (*i.e.* in the
 263 direction of the sedimentary transport). The line KaShallow2-051-052 (Fig. 6 and Fig. S5), in the
 264 southeastern part of the basin, shows its sedimentary organization and the seismic facies in its deepest
 265 part. Finally, the line KaShallow2-090 (Fig. 7 and Fig. S6) extends from the northern Dominica shelf
 266 to the southern Grande-Terre shelf, west of Marie-Galante. It trends N-S across the upper part of the
 267 Kubuli Sub-basin and crosscuts perpendicularly the N80-100° main fault system of the upslope basin.
 268 Despite a large number of studied seismic lines, their variable quality and variations in depth pene-
 269 tration did not allow to build continuous isochron maps throughout the basin.

3.2. DREDGES, PISTON CORE AND ROV SAMPLING

270 The Karukéra Spur megasequences were dated using descriptions and analyses of ancient dredges
 271 collected during the cruises Arcante 1 (Andréieff et al., 1980) and new samples collected during the
 272 KaShallow2 cruise (De Min, 2014; De Min et al., 2015) (Fig. 2C and Fig. S2). In the Marie-Galante
 273 Basin, sixteen other sites were sampled during the KaShallow 2 cruise using a Kullenberg piston
 274 corer (samples “KS”) and eleven others with a CNEXO-Ville rock sampler (samples “CR”) (Fig. 2C
 275 and supplementary material Fig. S1). Correlated with seismic units, these samples were used to cal-
 276 ibrate the age and the paleoenvironment of the sedimentary megasequences. Many of the samples
 277 yielded Late Pleistocene to Holocene ages. In this work, we only document the results of new and
 278 ancient dredges that yielded older deposits (late Oligocene to Middle Pleistocene) based on their
 279 foraminiferal and calcareous nannofossil contents (Fig. S1). During the KaShallow program, we also
 280 performed ROV dives and sampled two sites, east and west of the northern coast of Marie-Galante,
 281 along one of the most prominent fault scarps in the basin (samples “BMG” and “BC”, respectively,
 282 Münch et al., 2013) (Fig. 2C and Fig. S1). Dredge KS09_038 on the Karukéra Spur was also reinves-
 283 tigated to better characterize its foraminiferal content. Ten soft samples were hand-washed over a 65

285 μm screen and 5 standard smear-slides were prepared for foraminiferal and calcareous nannofossil
 286 biostratigraphic analyses, respectively.

2
 3

287 3.3. ONSHORE ROCK SAMPLE ANALYSES

4
 5
 6

7 288 In Martinique, we logged four sections in the carbonate deposits at La Caravelle, Tartane, Grand
 8
 9
 10 289 Macabou and Petit Macabou, the two later outcrops being separated in the field by 500 m (Fig. S7).

11
 12

13 290 Twenty-three thin sections were prepared to analyse the foraminiferal content and depositional set-
 14
 15 291 tings of the onshore sediments.

16
 17

18 292 In Guadeloupe Archipelago, we further refined the age of the carbonate platform of Grande-Terre
 19
 20 293 by sampling the lowermost part of a recently drilled borehole at Morne à l'Eau and reinvestigated the
 21
 22 294 lower part of the La Désirade platform with new samples from Pointe Frégule, in the western part of
 23
 24
 25 295 the island. We prepared four and sixteen thin-sections, respectively (Fig. S8).

26
 27

28 296 Carbonate microfacies were characterized following the nomenclature of Flügel (2006). The stand-
 29
 30 297 ard planktonic foraminifera zonal scheme and bio-event calibrations used in this study are from Wade
 31
 32
 33 298 et al. (2011) and BouDagher-Fadel (2018a). For larger benthic foraminifera, bio-event calibrations
 34
 35 299 are from BouDagher-Fadel et al. (2010), BouDagher-Fadel and Price (2010, 2013) and BouDagher-
 36
 37
 38 300 Fadel (2018b). For calcareous nannofossils, we used bio-event calibrations published by Raffi et al.
 39
 40 301 (2006). Foraminiferal taxa with biostratigraphic significance found in these thin sections are illus-
 41
 42
 43 302 trated in Figures S3 and S4.

44
 45

46 303 4. RESULTS

47
 48

49 304 4.1. SEISMIC STRATIGRAPHY OF THE MARIE-GALANTE BASIN

50
 51

52 305 Three sedimentary seismic megasequences MG-MS, up to 2 stwt- thick, limited by regional un-
 53
 54
 55 306 conformities MG-SB, are recognized resting above an acoustic basement (Figs. 4, 5, 6, 7, high-reso-
 56
 57
 58 307 lution seismic lines in Figures S3, S4, S5, S6). From bottom to top, these are:

59
 60

61 308 4.1.1. The basement

62
 63

64
 65

309 The basement (grey in Figs. 4 and 6) comprises transparent to discontinuous, low amplitude and
 310 low frequency reflectors displaying a chaotic structure (Facies 1 – Fig. S2 and Fig. 6). The basement
 311 is topped by the regional prominent MG-SB1 unconformity (dot red line in Figs. 4 and 6). At Ka-
 312 rukéra Spur and beneath the Petite-Terre Sub-basin, MG-SB1 is sharp and underlined by a high am-
 313 plitude and continuous reflector (*e.g.*, Fig. 4A - CDP8300 to 11000 at *ca* 3,8 stwt). In the southeastern
 314 part of the Arawak Sub-basin, MG-SB1 shows few high amplitude, low frequency, continuous and
 315 parallel reflectors suggesting that a thin sedimentary unit rests conformably upon the basement (Fa-
 316 cies 3 – Fig. S2 and Fig. 4). To the west beneath the Kubuli Sub-basin, the basement is generally
 317 hidden by multiples reflections and is too deep to be imaged. The basement crops out in La Désirade
 318 and all along the N70° trending crest dominating the *ca* 5000 m deep V-shaped La Désirade Valley
 319 (Fig. 2 and Fig. 5 in De Min et al., 2015).

320 At the basin scale, the basement gently deeps southward along the Karukéra Spur (Fig. 5 in De
 321 Min et al., 2015). In the Petite-Terre Sub-basin southward and from the Karukéra Spur westward, the
 322 basement steps down toward the Arawak Sub-basin along N90° south-dipping or N150° and N0°
 323 west-dipping normal faults, respectively (Figs. 2B and 4, CDP8200 to 13000; Fig. 8). It rests at 4.4
 324 stwt below a 2stwt- thick sedimentary pile in the western Arawak Sub-basin (Fig. 4, CDP 4400).
 325 Wide angle seismic data (Kopp et al., 2011) show that the basement unconformity corresponds to the
 326 4.5 km/s “mid crust” boundary that extends further westward beneath the Kubuli Sub-basin at a con-
 327 stant depth. This indicates that *ca* 3.5 stwt- thick seismic units rest above the basement upslope of the
 328 Kubuli Sub-basin.

329 Dredges from the southern flank of La Désirade Valley recovered igneous basement rocks with
 330 facies similar to those cropping out onshore La Désirade (dredges ST18 to ST22, ST 28, 44D; Arcante
 331 1 and 2 cruises - Andréieff et al., 1980; Bouysse and Guennoc, 1983) (Fig. 2), *i.e.* Upper Jurassic
 332 magmatic rocks that underwent Albian greenschist metamorphism (*e.g.*, Corsini et al., 2011).

333 4.1.2. Megasequence MG-MS1:

334 The MG-MS1 complete sequence can be described in the central and southern parts of the Arawak
 335 Sub-basin and in the southern Karukéra Spur (Figs. 4 and 6 and Fig. 5 in De Min et al 2015). At
 336 Karukéra Spur, MG-MS1 is 0.60-0.80 stwt- thick at maximum (600 to 700 m- thick). It reaches 1.3
 337 stwt- thick (*ca* 1400 m- thick) in the south-central part of the basin (Fig. 4 at CDP 4400). MG-MS1
 338 comprises two main units with discontinuous to locally continuous, sub-parallel, medium to low am-
 339 plitude and medium frequency reflectors (Facies F4 and F4' – Fig. S2 and Fig. 4). The lower unit
 340 (blue in Figs. 4 and 6, and Fig. 8 in De Min et al. 2015) infills topographic depressions above MG-
 341 SB1 and is thicker in the Arawak Sub-basin than over the spur. The upper unit (orange in Figs. 4, 5
 342 and 6, and Fig. 7 in de Min et al., 2015) rests conformably above the lower one and displays an
 343 aggradational pattern (Fig. 4 from CDP 8100 eastward and Fig. 6A). Over the Karukéra Spur and in
 344 the Arawak Sub-basin northward, MG-MS1 retrogrades onto the erosional basement surface MG-
 345 SB1 (Fig. 5 and 10 in De Min et al. 2015). In the Kubuli Sub-basin and south of Grande-Terre, MG-
 346 SB1 is too deep to be observed.

347 At the top of MG-MS1, MG-SB2 is a marbled erosional surface all over the basin. In the southern
 348 Arawak Basin, MG-SB2 entails deep into MG-MS1, locally down to the basement (Fig. 6, line
 349 K09_52). This deep incision was a submarine passage toward the 5500 m deep outer forearc Marti-
 350 nique Basin to the east (Fig. 2). Over the Karukéra Spur and across the Arawak Sub-basin, MG-SB2
 351 displays local reliefs and MG-MS1 shows truncations below few strong amplitude, low frequency
 352 and continuous reflector (Facies F5 – Fig. S2 and Fig. 6A), suggesting that MG-SB2 is subaerial.
 353 Westward in the Kubuli Sub-basin, MG-SB2 becomes shallower and is mostly conformable with the
 354 underlying deposits. The unit boundary is underlined by low angle onlaps (Facies F6 – Fig. S2 and
 355 Fig. 4B). This architecture suggests that MG-SB2 is submarine. MG-SB2 is vertically offset and tilted
 356 against the N90°E trending Morne Piton Fault by *ca* 1 stwt down to the north (Fig. 5, line K09-60).
 357 MG-MS1 is absent over the northernmost Karukéra Spur, Petite-Terre Sub-basin and in La Désirade
 358 (Fig. 2A).

359 The westward lateral facies variation of MG-MS1 is a remarkable feature. The well bedded units
 360 of the Arawak Sub-basin changes into a weakly reflective more or less layered seismic facies in the
 2
 361 Kubuli Sub-basin (Facies F6 and F7 – Fig. S2 and Fig. 4B). The facies transition occurs around the
 4
 362 deepest part of the boundary between the Arawak and Kubuli Sub-basins (Fig. 4 *ca* CDP4400-4500).
 5
 7
 363 Closer to Dominica Island, where MG-SB2 is shallower, Aguadomar profiles (with deeper penetra-
 9
 10
 364 tion than the KaShallow seismic lines) confirm that the seismic facies of MG-MS1 is poorly reflec-
 12
 1365 tive. Such facies, lacking of internal reflections, is also observed close to the active arc beneath the
 14
 15
 366 Rodrigue Plateau and in the Les Saintes Channel (brown colour in Fig. 7, and Facies F2 – Fig. S2).
 16
 17
 1867 We interpret this facies as volcanoclastic deposits or magmatic intrusions from the remnant and pre-
 19
 20
 368 sent day arc (Fig. 8). We dredged rock samples from the uppermost part of MG-MS1. Dredge
 21
 22
 2369 KS09_38 in the Karukéra Spur yielded reefal deposits (De Min et al., 2015, sample location on Fig.
 24
 25
 370 2C and Fig. 4 at cdp14500-K09-80) with larger benthic foraminifera (including *Miolepidocyclina*
 26
 27
 371 *mexicana*, *Heterostegina antillea*, *Miogypsina tani* and *M. triangulata*) which together indicate that
 28
 29
 3072 deposition occurred during the Chattian-Aquitania interval (27.82-20.4 Ma) (Fig. S1). There, both
 31
 32
 3373 the high amplitude and continuity of the seismic reflectors at the top of MG-MS1 (Facies F5 – Fig.
 34
 3574 S2 and Fig. 6) contrast with the lower amplitude and very continuous reflectors of the overlying
 36
 37
 375 megasequence MG-MS2 (Facies F9 – Fig. S2 and Fig. S6). This suggests a high impedance contrast
 38
 39
 4076 between MG-MS1 and MG-MS2. We conclude that the deposits with this strong amplitude facies on
 41
 42
 4377 top of MG-MS1 correspond to a shallow carbonate platform from which sample KS09_38 was col-
 43
 44
 4578 lected. The topmost part of MG-MS1 also crops out on the Morne Piton fault escarpment, immedi-
 46
 47
 4879 ately east of Marie-Galante. ROV samples BMG2 and BMG4 (Fig. 2C and Fig. 5 at CDP3200-K09-
 48
 49
 5080 60) yielded calcareous marls with abundant Early Miocene calcareous nannofossils and planktonic
 51
 52
 5381 foraminifera (Burdigalian, between 18.50 and 17.30 Ma) (Fig. S1). Dredges 41D and 43D collected
 53
 54
 5582 east of Grande-Terre (Fig. 2C) yielded Lower Miocene basin and middle Oligocene outer platform
 55
 56
 5783 deposits (Andréieff et al., 1980) (Fig. S1), thus confirming the existence of basin deposits of this age.
 58
 59
 6084 We conclude that by the end of the Early Miocene, a shallow carbonate platform covered the Karukéra
 60
 61
 62
 63
 64
 65

385 Spur and eastern Arawak Sub-basin, and that the shallow carbonate platform changes into basin de-
 386 posits westward (Fig. 2A; Facies 7 – Fig. S2).

387 4.1.3. Megasequence MG-MS2

388 MG-MS2 is characterized by a wide variety of types and shapes of seismic reflectors, especially
 389 in the Arawak and Kubuli Sub-basins where subparallel, cross bedded, chaotic or lense-shaped ge-
 390 ometry, high to low amplitude and generally medium to long continuity reflectors occur (Facies 8, 9,
 391 10 and 11 – Fig. S2).

392 In the Karukéra Spur, De Min et al. (2015) provided a detailed description of MG-MS2 (termed
 393 US3 in De Min et al., 2015). There, MG-MS2 is 0,24 to 0,30 stwt- thick (200 to 300 m) (Figs. 5 and
 394 7 in De Min et al., 2015) and thicker to the south than to the north. As a whole, the megasequence
 395 presents one unit with continuous reflectors, intermediate amplitude and high to intermediate fre-
 396 quency, arranged in a retrogradational pattern changing upward in an aggradational one. Rock sam-
 397 ples yielded foraminifer-rich massive oozes indicating a basin depositional environment and, in the
 398 upper part of the megasequence, peri-reefal limestones with Tortonian to Messinian calcareous nan-
 399 nofossils. MG-MS2 is limited at its top by the sequence boundary MG-SB3. MG-SB3 is mostly con-
 400 formable with MG-MS2 but displays a clear angular unconformity with the overlying MG-MS3 when
 401 observed perpendicular to the N120° and N40° faults cross-cutting the spur (Fig. 2B). To the north
 402 of the spur, MG-MS2 is eroded and absent in the hanging walls of the faults.

403 Elsewhere in the Marie-Galante Sub-basins, MG-MS2 is thicker than in the Karukéra Spur, reach-
 404 ing 0,8 stwt- thick (600 to 700 m) (Figs. 4 and 8), and it is lowered to the west along the N150-N0°
 405 faults bounding the spur to the west (Fig. 2B). We distinguish two units in MG-MS2. The lower unit
 406 is thicker in the Arawak Sub-basin than in the Kubuli Sub-basin (Figs. 4 and 5). It displays subparallel
 407 reflectors with variable amplitudes (Facies F8 – Fig. S2 and Fig. 5). In the Arawak Sub-basin, the
 408 lower unit locally shows large and long wavelength incisions filled with well-stratified deposits sug-
 409 gesting erosion by deep-sea currents (Facies F9 – Fig. S2 and Fig. 6 at CDP500-2500). The upper

410 unit rests unconformably upon the irregular surface except upslope of the Kubuli Sub-basin where it
 411 is conformable. The unit is thicker in the Kubuli Sub-basin than in the Arawak Sub-basin. The unit
 2
 3
 412 facies corresponds to the F8 facies too (Fig. S2). Along the eastern slope of the Kubuli Sub-basin, the
 4
 5
 413 upper unit is arranged in a large lens-shaped, south-eastward prograding pattern (Facies F10 – Fig.
 7
 8
 414 S2 and Fig. 5A). Upslope in the Kubuli Sub-basin, the upper unit onlaps and retrogrades onto the unit
 9
 10
 415 boundary and becomes conformable and aggrades upward (Figs. 4 at cdp800-1800). Immediately east
 11
 12
 416 of Marie-Galante, the upper unit shows channel-levee patterns in the footwall of the Morne Piton
 14
 15
 417 fault (Facies F11 – Fig. S2 and Fig. 5B).

17
 18
 19
 20
 21
 22
 23
 24
 25
 26
 27
 28
 29
 30
 31
 32
 33
 34
 35
 36
 37
 38
 39
 40
 41
 42
 43
 44
 45
 46
 47
 48
 49
 50
 51
 52
 53
 54
 55
 56
 57
 58
 59
 60
 61
 62
 63
 64
 65

418 North of the Morne Piton Fault in the Marie-Galante Canyon and the Petite-Terre Sub-basin, the
 419 two units cannot be distinguished. There, MG-MS2 presents poorly continuous but subparallel re-
 420 flectors of medium amplitude (Fig. 5, lines K09-26 and K09-60). MG-MS2 displays few low angle
 421 onlaps onto MG-SB2 and is aggradational. All megasequences (MG-MS1 and MG-MS2) are tilted
 422 to the south against the Morne Piton fault and the N130° faults in the Petite-Terre Sub-basin (Fig. 5).
 423 The thickness of MG-MS2 sediments does not vary against the faults suggesting that they are pre-
 424 tectonic.

425 MG-MS2 lower unit onlaps above MG-SB2 and retrogrades upslope where it becomes concordant
 426 with MG-SB2 and aggrades in the uppermost part of the Kubuli Sub-basin (Fig. 4, line Agua116).
 427 The sequence boundary MG-SB3 on top of MG-MS2 is irregular with local incisions in MG-MS2,
 428 suggesting submarine erosion (*e.g.*, Fig. 4 at cdp8250-8650 and Fig. 5 at K09-61-cdp3400-4200). It
 429 is mostly concordant with sediments in the upper part of the Kubuli Sub-basin (Fig. 4 at cdp700-1800
 430 – Fig. 7 at cdp15000-19000). In the footwall of the Morne Piton Fault and in the Marie-Galante
 431 Canyon (Fig. 5, line K09-60), MG-MS2 is deeply incised and covered by recent canyon deposits. In
 432 the Petite-Terre Sub-basin (Fig. 5, line K09-26), MG-MS2 crops out and is deeply incised. In the
 433 northernmost part of the Petite-Terre Sub-basin and northern Karukéra Spur, the unit is missing, sug-
 434 gesting emergence and erosion (Fig. 8). In the Petit-Cul de Sac Marin Sub-basin (PCSM in Fig. 2A),
 435 a clear angular unconformity with the overlying MG-MS3 suggests that the surface might correspond

436 to MG-SB3 but MG-MS2 is hidden below the multiple (Fig. 7A). In the southern Arawak Sub-basin,
 437 MG-SB3 is mostly conformable with MG-MS2 with only low angle onlaps of MG-MS3 (Fig. 6, line
 2
 3
 438 K09-52).

439 Dredge samples at sites 39D and CR24 (Fig. 2C and located in Fig. 5) provided marls that indicate
 8
 440 a basin depositional environment dating from the Langhian to the Tortonian (Fig. S1). These ages are
 10
 11
 12
 441 consistent with the Upper Miocene basin deposits found by Andréieff et al. (1980) on the basis of
 13
 14
 442 dredge samples 41D and 43D (Fig. 2C) collected in the upper part of the La Désirade Valley. As a
 15
 16
 443 whole, a Middle to Late Miocene age is assigned to MG-MS2.

444 4.1.4. Megasequence MG-MS3

445 MG-MS3 is characterized by well stratified and continuous reflectors (Facies F13, Fig. S2 and
 24
 25
 26
 446 Fig. 7) onlapping above MG-SB3, retrograding and aggrading in most of the basin and over the Ka-
 27
 28
 447 rukéra Spur (Figs. 4 and 5). In the deepest part of the basin, it shows various facies such as well
 29
 30
 448 layered reflectors suggesting clastic deposits (Facies F12 – Fig. S2), local transparent unit slightly
 31
 32
 449 incising in the lower unit suggesting mass transport deposits (F12') or downslope prograding deposits
 33
 34
 450 (Facies F12 – Fig. S2 and Fig. 5). MG-MS3 comprises two units separated by a remarkable unit
 36
 37
 451 boundary locally underlined by truncations, onlaps and a regional high amplitude reflector (Figs. 4D
 38
 39
 452 and 6B). MG-MS3 is up to 0.4 stwt- thick (*ca* 400 m) in the southern Arawak (Fig. 6, line K09-52)
 41
 42
 453 and central Arawak Sub-basin (Fig. 5 at K09-62-CDP150-4000). It progressively thins to *ca* 0.2 stwt
 43
 44
 454 (*ca* 200 m) upslope of the Kubuli Sub-basin and over the Karukéra Spur (Figs. 4 and 5). Along the
 46
 47
 455 Morne Piton Fault scarp, MG-MS3 presents channel-levees incising MG-MS2 (Facies F11 – Fig. S2
 48
 49
 50
 456 and Fig. 5). North of the fault in the Marie-Galante canyon, MG-MS3 displays a cross-bedded and
 51
 52
 457 lens shaped pattern corresponding to canyon deposits (Fig. 5B). In the Petite-Terre Sub-basin, MG-
 53
 54
 458 MS3 only fills narrow depressions. In the PCSM Sub-basin, MG-MS3 shows clear angular onlaps
 55
 56
 459 onto MG-SB3 and the upper unit exhibits channel incisions and infillings (Fig. 7A). At Colombie
 58
 59
 460 Bank, MG-MS3 upper unit comprises three units topping the bank with strong amplitude reflectors

461 at the top and pinnacle-like reliefs, typical of carbonate platforms (Facies F14 – Fig. S2 and Fig. 7).
462 This platform conformably rests upon well stratified, continuous, medium to low amplitude reflectors
2
3
463 of the lower unit (Münch et al., 2013).
4
5

6
7
464 At Rodrigue Plateau, MG-MS3 onlaps onto the plateau or presents a fan shaped pattern when
8
465 observed perpendicular to the N150° normal faults bounding the plateau to the East (ENE-WSW lines
10
11
12
13
14
15
16
17
18
19
20
21
22
23
24
25
26
27
28
29
30
31
32
33
34
35
36
37
38
39
40
41
42
43
44
45
46
47
48
49
50
51
52
53
54
55
56
57
58
59
60
61
62
63
64
65

466 crossing K09-90, Fig. 2A and 2B). At Karukéra Spur, MG-MS3 corresponds to US4 and US5 of De
467 Min et al. (2015). These authors described the two units as well stratified, with continuous reflections.
468 Deposition of the lower unit (US4) is clearly controlled by faults as it is (i) overally retrograding
469 northward, and (ii) tilted eastward. The upper unit (US5) partly covers the basement of the spur. It is
470 organized in a fan shaped pattern against the spur faults and arranged as a thin-sheet unit along the
471 deepest part of the spur. At Flandres Bank, a thin reefal unit (samples CR25 and CR26 – Fig. 2C)
472 caps the spur basement.

473 Both MG-MS3 units were sampled and provided outer shelf marls turning upward into shallow
474 water reefal deposits. At Karukéra Spur, the lower unit (US4 of De Min et al., 2015) was dated Zan-
475 clean to Piacenzian and the upper one (US5) late Gelasian-Calabrian (Fig. S1). The Flandres Bank
476 platform is Late Pleistocene to Holocene (De Min et al., 2015). In the Marie-Galante Canyon, sample
477 KS17 (Fig. 2C) has been deposited during the Zanclean. Albeit the marl samples cannot be correlated
478 to a specific seismic unit, they all indicate a basin environment and may belong to the lower unit of
479 MG-MS3. In the Arawak Canyon, sample KS39 (Fig. 4, line K09-80 at cdp10000; location in Fig.
480 2C) was collected just above the unit boundary. The dredge provided Piacenzian marls (3.36-3.16 Ma
481 interval), suggesting a middle-late Piacenzian age for the unit boundary. Sample KS47 (Fig. 5, line
482 K09-61 at CDP400, location in Fig. 2C) from the channel levee deposits west of Marie-Galante Island
483 provided Piacenzian bioclastic sandstones (location in Fig. 5). At Rodrigue Plateau west of Marie-
484 Galante, samples KS05 (Fig. 7, at CDP10650, location in Fig. 2C), KS07 and KS08 (Fig. 2C) revealed
485 that the plateau is capped by bioclastic limestones with foraminifera. KS07 has deposited during the
486 Early Pleistocene (planktonic foraminiferal Zone PT1a). The Arcante Cruise samples 17V and 18V

487 (Fig. 2C), located along the Les Saintes Plateau, provided Pliocene – Pleistocene outer platform lime-
 488 stones. Around the Colombie Bank, samples BC1 and BC2 (Fig. 7 at CDP5200, location in Fig. 2C)
 2
 3 489 yielded wackestones bearing planktonic foraminifera and volcanic minerals with radiometric ages at
 4
 5 490 1.15 ± 0.12 to 1.33 ± 0.23 Ma (Münch et al., 2014); sample KS13 (Fig. 2C) is a Lower Pleistocene marl;
 7
 8 491 samples Arcante 15D - 16D (Fig. 2C) yielded Pliocene to Pleistocene volcanoclastic calcareous sand-
 9
 10 492 stones that deposited under outer ramp platform to basin environments. Samples CR51, CR53 and
 11
 12 493 CR54 (Fig. 2C), collected from units topping the Colombie Bank, provided bioclastic limestones and
 14
 15 494 corals indicating an inner ramp - reefal platform environment. Other dredges from the Arcante cruise
 16
 17 495 in the La Désirade slope (35D, 41D, 42D, Fig. 2C) yielded Pleistocene marls that relate to the upper
 19
 20 496 unit of MG-MS3.

2497 4.2. ONSHORE

27 498 4.2.1. Carbonate deposits of eastern Martinique

29
 30 499 In La Caravelle Peninsula, the Caravelle and Tartane sections (Fig. 9 and Fig. S7) comprise 4 to
 31
 32 500 21 m- thick red algal packstones and interbedded coral-red algae biostromes, with abundant rhodo-
 34
 35 501 liths. In the Caravelle section, these carbonate rocks rest upon andesitic breccias and lava sills. Foram-
 36
 37 502 iniferal assemblages (including *Miogypsinella elongata*, *Miolepidyclina mexicana*, *Miogypsina gun-*
 38
 39 503 *teri*) and *Paragloborotalia opima* found in the lower part of the section correlate with Zone P21b
 41
 42 504 (early Chattian, 28.82-26.8 Ma). Both foraminiferal assemblages and microfacies indicate an inner to
 43
 44 505 mid ramp, reefal depositional setting. In the Tartane section, similar facies occur above magmatic
 46
 47 506 rocks of the oldest arc. The larger benthic foraminifera are indicative of Zone P22 (Chattian, 26.8-24
 48
 49 507 Ma).

51
 52 508 The Grand Macabou section comprises, from bottom to top (Fig. 9A, B and Fig. S7):

- 53 509 • 0.3 m- thick argillaceous green tuffites;

57
 58
 59
 60
 61
 62
 63
 64
 65

- 510 • 2 m- thick bioturbated red algal grainstones to packstones with planktonic foraminiferal taxa
 511 from Zones M1 and M2 (N4-N5a, Aquitanian, 23.03-20.4 Ma);
 2
 3
 4
 512 • 10 m- thick coral grainstones to rudstones with diverse coral colonies in life position (Fig.
 5
 6
 713 9C). The co-occurrence of the larger benthic foraminifera (*Miogypsina triangulata*, *Mi-*
 8
 914 *olepidocyclina panamensis* and *Archaias angulatus*) correlates with Zones N4-N5a (Aqui-
 10
 11515 tanian, 23.03-20.4 Ma);
 12
 13
 14
 1516 • 10.5 m- thick red algal grainstones to packstones with planar cross-bedding and corals be-
 16
 1717 tween 18 and 19 m above the base of the section. There, the larger benthic foraminiferal as-
 18
 1918 semblages (including *Miolepidocyclina excentrica* and *Miogypsina tani*) correlate with Zone
 20
 21
 2219 N5b-N8a (Burdigalian, 20.4-15.97 Ma). Both foraminiferal assemblages and microfacies in-
 23
 2420 dicate an inner to mid ramp, reefal depositional setting for the whole section;
 25
 26

2721 The Petit Macabou section comprises, from bottom to top (Fig. 9D and 9E and Fig. S7):
 28
 29

- 3022 • 2 m- thick coral buildups that underwent karstification and are covered by reefal breccias.
 31
 32
 3323 Karst features and breccia fragments are coated by iron hydroxydes (Fig. 9D). Both larger
 34
 3524 benthic (*Miogypsina panamensis*, *M. tani*, *A. angulatus*, *Heterostegina antillea*, *Panorbuli-*
 36
 37
 3825 *nella larvata*) and planktonic foraminifera in the reef and the breccia elements indicate that
 39
 4026 deposition occurred during the Aquitanian (23.03-20.4 Ma) within Zones N4-N5b;
 41
 42
 4327 • 8 m- thick debris flows, coarse-grained turbidites and cross-bedded levels (Fig. 9E) composed
 44
 45
 4628 of andesitic fragments. Two beds in their lower part yielded larger benthic (*Miogypsina inter-*
 47
 4829 *media*, *H. antillea*, *Lepidocyclina yurnagunensis*, *Planorbulina larvata*) and planktonic
 49
 50
 5130 foraminifera (*Orbulina universa*, *Sphaeroidinellopsis seminulina*, *Globoquadrina dehiscens*)
 52
 5331 corresponding to Zones N9-N13a (Langhian-Serravalian, 15.97-11.8 Ma).
 54
 55

5632 4.2.2. Carbonate deposits of the Guadeloupe Archipelago

58
 59
 60
 61
 62
 63
 64
 65

533 In Grande-Terre, the Morne à l'Eau borehole (Fig. S8 – location in Fig. 2C) comprises 80 m- thick
 534 red algal grainstones to bindstones, with rhodolith-rich intervals. This succession is interspersed with
 2
 335 coarse-grained volcanoclastic and carbonate beds. Four emergence surfaces with karstic features such
 4
 5
 536 as gullies and microcaves are identified. Referring to the general organization of the Pliocene-Pleis-
 7
 537 tocene platform of Cornée et al. (2012), the lithological succession of the borehole is typical of its
 9
 10
 538 lower part (Sequences 1 and 2 of Cornée et al., 2012). The precise age of the base of the platform
 11
 12
 1339 remains unknown due to the lack of outcrop. The presently oldest known age corresponds to the late
 14
 15
 540 Zanclean planktonic foraminiferal Zone PL2 (La Simonière borehole, in Münch et al., 2014). The
 16
 17
 541 lowermost part of the deposits in the Morne à l'Eau borehole, between 80 and 77.5 m depths, yielded
 18
 19
 542 late Tortonian-Messinian species of *Amphistegina* corresponding to Zones N17-N18 within the 8.6-
 20
 21
 543 5.33 Ma interval. Above, between 71 and 72.2 m depths, we found foraminifera that co-occurred
 22
 23
 544 during the late Tortonian/Messinian-Zanclean interval, between 8.6 and 3.4 Ma. Consequently, in
 24
 25
 545 Grande Terre, the lower part of the Upper Plateaus in Grande-Terre has deposited during the Mes-
 26
 27
 546 sinian (Late Miocene).

347 In La Désirade, at Frégule Cape, the lowest 10 m of the Upper Plateau carbonates above the Ju-
 34
 35
 548 rassic basement yielded larger benthic foraminiferal taxa (Fig. S8 and location on Fig. 2C) that co-
 36
 37
 549 ccurred between the latest Miocene and the Early Pliocene. Comparing the ages obtained in Grande
 38
 39
 550 Terre (8.6-5.33 Ma) and La Désirade islands (5.8-3.4 Ma), the lowermost part of the carbonate plat-
 40
 41
 551 form in the Guadeloupe Archipelago has deposited during the late Messinian (Zone N18, between
 42
 43
 552 5.8 and 5.33 Ma).

4.3. AGE MODEL AND ONSHORE-OFFSHORE CORRELATIONS IN THE GUADELOUPE 50 51 553 ARCHIPELAGO AND MARTINIQUE

54
 55
 555 The age of the MG-SB1 unconformity in the deepest part of the Marie-Galante Basin remains
 56
 556 uncertain (Fig. 10) because of the lack of dredge and borehole samples. However, sample 43D col-
 57
 58
 557 lected nearby La Désirade Valley indicates that this unconformity is older than the Middle Miocene

558 and could be as old as the Eocene considering the 1300-1400-m thickness of MG-MS1. MG-MS1 is
559 topped by a Lower Miocene shallow water carbonate platform to the east but remains in basin condi-
2
360 tions to the west. The western side of the shallow carbonate platform was probably limited by the
4
561 sub-meridian faults bounding the western flank of the Karukéra Spur now buried in the Arawak Sub-
7
562 basin (Fig. 4, at line Agua119). We hypothesise that the facies change that occurs westward and
9
10
563 upslope in the Kubuli Sub-basin (Fig. 4B) may correspond to a lateral change between basin deposits
12
1364 and volcanic and/or volcanoclastic deposits of the ancient late Eocene – late Oligocene arc (Fig. 8).
14
15
165 Indeed, (i) the facies change is observed at the vicinity of the volcanic line of the ancient arc, (ii) MG-
18
17
1866 MS1 deposits are contemporaneous with the activity of the ancient arc, *i.e.* during the late Eocene to
19
20
21567 the latest Oligocene (Germa et al., 2011; Legendre et al., 2018; Bosch et al., 2022), (iii) basin deposits
22
2368 show imbricated, sometimes onlapping or parallel reflectors, with east dipping low amplitude reflec-
24
25
26569 tors that could correspond to the arc trenchward slope. By the end of the Early Miocene, MG-MS1
26
27
2870 emerged to the east, giving rise to the erosional surface MG-SB2 over the Karukéra Spur and eastern
29
30
3171 Arawak Sub-basin, and the basement crops out north of the spur and in La Désirade (Fig. 10). In
31
32
3372 Martinique, the ages of the magmatic rocks belonging to the ancient arc have been considered to
34
35
3673 range between 24.8 ± 0.4 and 20.8 ± 0.4 Ma (latest Chattian-Aquitainian) (Germa et al., 2011), but
36
37
3874 the arc activity started earlier, during the early Chattian, as shown by the age of the carbonate deposits
38
39
4075 resting upon volcanic rocks at La Caravelle (Fig. S7 and Fig. 10).

41
42
4376 In the Marie-Galante Basin, foraminiferal and calcareous nannofossil assemblages indicate that
44
45
4677 the age of the unconformity MG-SB2 ranges between the late Burdigalian (top of MG-MS1) and the
47
4878 Langhian-Late Miocene interval (oldest known age of MG-MS2). To the south, in Martinique, we
49
50
5179 also recognized a subaerial unconformity between the Burdigalian limestone deposits at Grand Ma-
51
52
5380 cabou and the Middle Miocene volcanoclastic deposits at Petit Macabou (Fig. 9 and Fig. S7). Conse-
54
55
5681 quently, an erosional unconformity corresponding to the latest Burdigalian-Langhian interval occurs
56
57
5882 in the central Lesser Antilles (Fig. 10).

583 MG-MS2 sediments further indicate that the entire Marie-Galante Basin remained deep during the
 584 Middle and the Late Miocene (Fig. 10). Faults along the western side of the Karukéra Spur enhanced
 2
 385 the spur relief, leading to thinner and more conformable and stratified deposits over the spur than in
 4
 586 the basin. The Arawak Sub-basin was fed by south-eastward directed turbiditic prograding systems
 7
 587 indicative of sediment transport from the upslope of the Kubuli Sub-basin. In the westernmost part
 9
 10
 588 of this sub-basin, sediments are intruded by the volcanic formation of the arc (Fig. 7 – *e.g.*, Agoucha
 11
 12
 1389 volcano). In the Petite-Terre Sub-basin and probably beneath the South Grande-Terre platform, MG-
 14
 15
 590 MS2 is tilted to the south along the N110° and N130° trending faults, and eroded. In the southern
 16
 17
 1891 Arawak Sub-basin, the southern tip of the spur is downthrown and opens a passage for the sediments
 19
 20
 592 toward the outer fore-arc basins. During deposition of MG-MS2, the sediments infilled this passage
 21
 22
 593 (Fig. 6 at line K09-52).

24
 25
 2594 In the Marie-Galante Basin, the age of unconformity MG-SB3 (Fig. 10) is estimated to range be-
 27
 28
 295 tween the Late Miocene (Serravalian-Tortonian, youngest age for MG-MS2) and the Early Pliocene
 29
 30
 3196 (Zanclean, oldest age of MG-MS3). Onshore, in the Marie-Galante Island, upper Tortonian ($8.57 \pm$
 32
 33
 3497 0.43 Ma, Münch et al., 2014) tuffaceous marls are unconformably overlain by Pliocene to Lower
 34
 35
 3598 Pleistocene shallow water carbonate deposits (Upper Plateaus; Bouysse et al., 1993; Münch et al.,
 36
 37
 3899 2013). Based on our investigations, the lowermost part of these carbonates deposited during the late
 39
 40
 4100 Messinian in the Morne à l'Eau borehole and in La Désirade Island (Fig. S4). Consequently, onshore
 42
 43
 4401 data allow to refine the age of the MG-SB3 to the Messinian, while it was previously considered to
 44
 45
 4602 be late Tortonian-early Zanclean (Bouysse et al., 1993; Münch et al., 2013). Offshore, the main in-
 46
 47
 4803 ternal unit boundary within MG-MS3 can be assigned to the middle Piacenzian. Indeed, the lower
 49
 50
 5104 unit correlates with the Zanclean and the lower part of the upper unit with the late Piacenzian (Arawak
 51
 52
 5305 and Kubuli Sub-basins). Onshore this unit boundary correlates with the middle Piacenzian emersion
 54
 55
 5606 surface occurring within the carbonate platform in Grande-Terre, Marie-Galante and La Désirade
 56
 57
 5807 (SB1, Fig. 3). In Grande-Terre, this surface is overlain by the index unit named Pliocene Volcano-
 59
 6008 sedimentary unit (PVS) (Cornée et al., 2012; Lardeaux et al., 2013; Münch et al., 2014).

609 MG-MS3 (Fig. 10) dates latest Miocene to present. During this period, the Karukéra spur recorded
610 a general drowning and tilting trenchward. The Arawak and Kubuli Sub-basins continued to fill with
611 clastic deposits in a basin environment. On the margins of these sub-basins, reefal platforms were
612 built up (La Désirade, Grande-Terre, Marie-Galante). By the middle Piacenzian, all the basin recorded
613 a transient emergence event of its shallow platforms (unit boundary in MG-MS3) that is also recorded
614 in La Désirade and Grande-Terre Islands Grande-Terre (SB1 surface in Cornée et al., 2012 and
615 Münch et al., 2014; Figs. 3 and 10). During deposition of the upper unit of MG-MS3, the islands of
616 La Désirade, Grande-Terre and Marie-Galante emerged while the Colombie bank evolved from a
617 slope to a shallow water reefal platform. Concomitantly, subaerial volcanism along the present-day
618 volcanic arc developed, first in Dominica since the Messinian then in Les Saintes and northern Basse-
619 Terre during the Zanclean. Shallow reefal platforms built up around these new islands.

620 To summarize, MG-MS1 has deposited on an erosional surface at the top of an igneous basement.
621 It dates Eocene (?) to late Burdigalian and is partly contemporaneous with volcanism since the early
622 Chattian at least. An uplift episode occurred at the Burdigalian-Langhian transition, then MG-MS2
623 deposited in a rift basin between the Langhian and the Messinian. By the latest Messinian, a second
624 uplift occurred, then MG-MS3 deposited between the latest Messinian and the Holocene.

625 5. DISCUSSION

626 5.1. DEPOSITIONAL SETTINGS AND PALEOGEOGRAPHIC EVOLUTION SINCE THE LATE-EARLY MIO- 627 CENE IN THE GUADELOUPE ARCHIPELAGO, DOMINICA AND MARTINIQUE

628 Our correlations of onshore and offshore data (Fig. 10) allow us to reconstruct the paleogeographic
629 evolution of the whole Guadeloupe Archipelago, Dominica and Martinique with emerged and
630 drowned areas, starting from the late Oligocene - Early Miocene (uppermost part of MG-MS1) (Fig.
631 11). We do not restore tectonic motions back in time and present our reconstruction based on the
632 present-day geographic maps. However, the relative position of the studied islands should have been

633 very close to the present-day one since the Lower Miocene (*e.g.*, Pindell and Kennan, 2009; Bosch-
 634 man et al., 2014).

635 *During the late Oligocene-Early Miocene (ca 25-17 Ma, uppermost part of MG-MS1, Fig. 11A),*
 636 the Karukéra Spur and possibly western Grande-Terre were capped by shallow-water carbonate de-
 637 posits evolving eastward to basin deposits. Westward, the Karukéra Spur was larger than today,
 638 bounded to the west by N150° west dipping faults now buried beneath the Arawak Sub-basin (Fig. 4,
 639 at line Agua119). Further west, basin deposits dominate in the Arawak Sub-basin. The shallow water
 640 areas, with a similar water depth than the banks today surrounding the islands of the Lesser Antilles,
 641 were located at the hinge between the inner forearc and the deep outer-forearc deep basins. The only
 642 emergent area along the Karukéra Spur at this time was a small island in the footwall of a NE-SW
 643 trending normal fault. Following the interpretation of Boucard et al. (2021), the V-shaped basins
 644 found along the Lesser Antilles, among which the La Désirade Valley, were actively opening prior to
 645 the Late Miocene. Because MG-MS1 onlaps northward on the Karukéra Spur and is missing in its
 646 northern part and in La Désirade, we suggest that the hinge of the N70° trending basin wall was
 647 cropping out too, as an emerged (or very shallow) narrow area parallel to the scarp. The southern
 648 extent of the Karukéra shallow platform is unknown because of the deep erosion that entails its south-
 649 ern part. The facies transition in the Kubuli Sub-basin may indicate the presence of volcanoclastic
 650 deposits from volcanoes of the remnant arc. This arc would have extended from Martinique to Anti-
 651 gua, passing at the longitude of the Kubuli Sub-basin and Marie-Galante Island. In Martinique, Bur-
 652 digalian carbonates of the Macabou area indicate a drowning of the subaerial upper Oligocene-Lower
 653 Miocene volcanic arc.

654 *By the Early-Middle Miocene transition (ca 17-16 Ma, unconformity MG-SB2, Fig. 11B), the Ka-*
 655 *rukéra Spur and possibly eastern Grande-Terre were emergent. We did not find evidence for shallow*
 656 *water carbonate platforms around the emergent areas, only marly deposits in the Marie-Galante Ba-*
 657 *sin, which remained below sea level. In Martinique, an uplift occurred between the late Early Miocene*

658 and the Middle Miocene, responsible for an emersion surface and a localized erosion of the Burdi-
 659 galian deposits.

660 *During the early Middle Miocene (ca 16-13 Ma - lower unit of MG-MS2, Fig. 11C), the Marie-*
 661 *Galante Basin and previously emergent areas underwent a drastic drowning. Faults bounding the Ka-*
 662 *rukéra Spur to the west offset MG-SB2 down to the west. Shallow-water carbonate deposits are re-*
 663 *stricted to the western margin of the Karukéra Spur along the summit of a narrow horst. At the same*
 664 *time, mid to outer platform volcanoclastics were emplaced in shallow-water banks, east of Grande-*
 665 *Terre and the Karukéra Spur. Dredges and seismic profiles analyses evidence a deepening to possibly*
 666 *1000 m paleowater depth for the deepest part of the Marie-Galante Basin, most probably accommo-*
 667 *dated by large NNW-SSE parallel to the trench normal faults responsible for the present-day config-*
 668 *uration of the basin. As the Arawak Sub-basin deepened, large submarine channels where then carved,*
 669 *and gravity-driven deposits (e.g., mass flows, turbidites) were emplaced. In its deepest part, SSE-*
 670 *ward prograding turbiditic deep-sea fans and lobes developed, and contouritic facies occurred along*
 671 *the steep western edge of the Karukéra Spur. South of the Karukéra Spur and probably thanks to*
 672 *faults transverse to the spur that drown its southern part, submarine erosion entailed deep into the*
 673 *previous units and opened a passage for the sediments toward the deep outer forearc basins. Upslope*
 674 *in the Kubuli Sub-basin, MG-MS2 capped the volcanoclastic deposits of the remnant arc. In Marti-*
 675 *nique, the oldest arc was also drowned, contemporaneously with the onset of volcanic activity of the*
 676 *Middle Miocene arc. New subaerial volcanic centres developed, and submarine volcanoclastics were*
 677 *deposited at their foot above the previously emergent areas of the Macabou area. North of Martinique,*
 678 *the Middle Miocene corresponds to a period of volcanic quiescence.*

679 *During the late Middle and Late Miocene (ca 13-7 Ma - upper unit of MG-MS2, Fig. 11D) the*
 680 *configuration of the Marie-Galante Basin persisted. In the basin, deep-sea fans and lobes prograded*
 681 *SSE-ward toward the deepest part of the basin, fed by canyons that entailed the Kubuli Sub-basin*
 682 *around the present-day Marie-Galante Island. In the northern part of the Karukéra Spur, sedimenta-*
 683 *tion recorded a new episode of uplift attested by shallow-water carbonate deposits while its southern*

684 part remained in deeper marine conditions, suggesting a regional tilt of the spur toward the SSE. At
 685 the same time, an intensive volcanic activity occurred in Martinique (Germa et al., 2011).

686 *During the latest Miocene (ca 7-5.8 Ma - MG-SB3, Fig. 11E), the physiography of the Guadeloupe*
 687 *Archipelago changed substantially. The whole area recorded a regional uplift. As a result, Grande-*
 688 *Terre, the northern Karukéra Spur, the Petite-Terre Sub-basin, Marie-Galante and the Rodrigue Plat-*
 689 *teau constituted tens of kilometres wide islands. The Arawak and Kubuli Sub-basins continued to*
 690 *deepen SSE-ward with turbiditic and contouritic deposits. The N110° Morne Piton fault system, cross*
 691 *cutting the Marie-Galante island, was incipient as attested by onlaps of MG-MS3 onto the uplifted*
 692 *MG-SB3 when observed perpendicular to the fault. Contemporaneously, aerial volcanism resumed*
 693 *in eastern Dominica between 7 and 5.3 Ma while volcanic activity decreased in Martinique.*

694 *During the latest Miocene - Early Pliocene (5.8-3.4 Ma - lower unit of MG-MS3, Fig. 11F) a*
 695 *second drowning episode occurred in the Guadeloupe archipelago. The former emerged islands un-*
 696 *derwent shallow carbonate sedimentation, dominated by red algal facies, as well as mid platform fine-*
 697 *grained deposits (Grande-Terre, La Désirade, northern Karukéra Spur, Marie-Galante, Rodrigue and*
 698 *Les Saintes Plateaus). The Marie-Galante Island carbonate platforms built up along the N110° Morne*
 699 *Piton fault scarp shoulder. Sedimentation of MG-MS3 in the Arawak and Kubuli Sub-basins was*
 700 *retrogradational and aggradational above MG-SB3, attesting for distal clastic basin infilling. As the*
 701 *Morne Piton Fault scarp developed, the main canyon system feeding the Arawak Sub-basin progres-*
 702 *sively jumped at the toe of the fault scarp forming the present-day Marie-Galante Canyon. To the*
 703 *north of this canyon, the Petite-Terre Sub-basin remained as an elevated area. It was not covered by*
 704 *MG-MS3 but incised by deep canyons controlled by the N130° fault system. Only the northern tip of*
 705 *Karukéra Spur remained emerged. The spur then progressively tilted eastward. Submarine and aerial*
 706 *volcanism resumed all along the present-day arc since ca 4 Ma in Les Saintes Channel (Henri et al.,*
 707 *2022) and in Northern Basse-Terre (Favier et al., 2019). In Dominica, volcanism was active during*
 708 *the Early Pliocene and in Martinique both submarine and aerial volcanisms built the central part of*
 709 *the island. By the end of the Early Pliocene, a short uplift episode led to the emersion of western*

710 Grande-Terre. This event is recorded in the offshore basins by a low angle unconformity (unit bound-
 711 ary in MG-MS3).

712 *During the Late Pliocene-Early Pleistocene (ca 3.4-1 Ma - MG-MS3 upper unit, Fig. 11G), the*
 713 Karukéra Spur continued to tilt ESE-ward. A carbonate platform covered most of its northern half
 714 while the southern one deepened to a thousand of meters below sea level. The Rodrigue Plateau was
 715 covered by MG-MS3 deposits and a carbonate platform started to build up around the active volca-
 716 noes of Les Saintes. A coral carbonate platform covered Grande-Terre, Marie-Galante Island and La
 717 Désirade. In the Marie-Galante Basin, deep-sea deposition occurred. Aerial volcanoes developed in
 718 central Dominica, Les Saintes, northern Basse-Terre and western Martinique.

719 *Since the Middle Pleistocene (< 1Ma, Fig. 11H), the configuration of the Marie-Galante Basin has*
 720 remained close to its present configuration. The bathymetry reached *ca* 2000 m bsl in the Arawak
 721 Sub-basin and the Karukéra Spur was a submerged shoal. A narrow carbonate platform was emplaced
 722 on the Flandres Bank while the southern part of the spur deepened to *ca* 1700 m bsl. Concomitantly,
 723 La Désirade Island raised up to 270 m above sea level. The carbonate platforms were subsequently
 724 dissected by normal faults: N150° faults in La Désirade, N90°, N130° and N40° faults in Grande-
 725 Terre and N110° faults in Marie-Galante. Uplift in the PCSM Sub-basin, between Marie-Galante and
 726 Basse-Terre, led to the development of the carbonate platform of the Colombie Bank along the shoul-
 727 der of the Morne Piton Fault. In Les Saintes, a carbonate platform built up around the now extinct
 728 volcanoes. Volcanic activity continued in central and southern Guadeloupe and in Dominica. La Sou-
 729 frière active volcano in Guadeloupe is nowadays the summit of the Lesser Antilles with an elevation
 730 of 1497 m above sea level. Analyses of marine terrace elevations have evidenced vertical motions
 731 during the last 1 Ma. These studies showed that La Désirade is still uplifting, although the motion is
 732 slowing down (Léticée et al., 2019). Marie-Galante is rising too, part of the movement being due to
 733 the active Morne Piton Fault (Feuillet et al., 2004). Grande-Terre remained stable or has slowly drowned
 734 to the West (Feuillet et al., 2002). Both the submerged Les Saintes and Martinique platforms subsided
 735 (Leclerc et al., 2016; Leclerc and Feuillet., 2019). Geodesic data have further suggested a general 1

736 – 2 mm. yr⁻¹ regional subsidence of the arc and a slow uplift of La Désirade (Van Rijsingen et al.,
 737 2022).

738 5.2. CORRELATION WITH THE NORTHERN LESSER ANTILLES AND VERTICAL MOTIONS IN THE 739 NORTHERN AND CENTRAL LESSER ANTILLES

1740 We evidence a major unconformity MG-SB2 extending from the Marie-Galante Basin to Marti-
 1741 nique corresponding to the latest Burdigalian-Langhian interval (Figs. 10 and 11B). This unconform-
 1742 ity is subaerial all along the Karukéra Spur. The spur was probably a N-S elongated island on the
 1743 eastern border of the Marie-Galante Basin. Such an unconformity was also identified in the northern
 1744 Lesser Antilles from the Anguilla Bank to the Antigua Bank where it is recognized as the SB4 un-
 1745 conformity (Fig. 10) corresponding to the latest Burdigalian-early Langhian interval (Cornée et al.,
 1746 2021). Recent seismic investigations have shown that SB4 is also present to the east in the outer
 1747 forearc, offshore St Barthélemy and Antigua, in V-shaped basins that are oblique to the trench (Le-
 1748 gendre et al., 2018; Philippon et al., 2020; Boucard et al., 2021). Consequently, we propose that the
 1749 unconformity MG-SB2 of the Marie-Galante Basin may be coeval with the regional unconformity
 1750 SB4 of the northern Lesser Antilles and with the Middle Miocene unconformity of Martinique. This
 1751 unconformity appears therefore of regional extent and may be related to a major event. In the northern
 1752 Lesser Antilles, SB4 has been interpreted as resulting from a forearc uplift with temporary emersion
 1753 of extensive archipelagos (Boucard et al., 2021; Cornée et al., 2021), like in the central Lesser Antilles
 1754 (Fig. 12A). During the Middle and Late Miocene, the northern and the central Lesser Antilles sub-
 1755 sided and most of archipelagos disappeared (Fig. 12B). The subsidence of the Lesser Antilles forearc
 1756 has been related to basal tectonic erosion of the upper plate during subduction (Münch et al., 2014;
 1757 De Min et al., 2015; Boucard et al., 2021). Boucard et al. (2021) suggested that this process is respon-
 1758 sible for the landward arc retreat that occurred between the latest Oligocene and the Pliocene. Our
 1759 interpretation that the sediments of MG-MS2 capped the volcanoclastic deposits of MG-MS1 in the
 1760 Kubuli Sub-basin corroborates the hypothesis that the central Lesser Antilles arc also retreated west-
 1761 ward during this interval.

762 In the Guadeloupe archipelago, we evidence a second major unconformity MG-SB3, estimated to
 763 be late Messinian based on our onshore-offshore correlations (Fig. 10). At that time, new islands were
 2
 364 formed in the western part of the Marie-Galante Basin and along the shallowest part of the Karukéra
 4
 5
 665 Spur to the north. In the northern Lesser Antilles, the SB5 unconformity similarly corresponds to the
 7
 866 late Messinian/early Zanclean interval, as for example in Barbuda (Cornée et al., 2021). Conse-
 9
 10
 1167 quently, we propose that MG-SB3 correlates with SB5 (Fig. 10). During the late Messinian, new
 12
 1368 archipelagos appeared from the Anguilla Bank to Martinique, coeval with new subaerial volcanic
 14
 15
 16769 activity that started to build the first islands of the present-day arc (Fig. 12). MG-SB3 (= SB5 of the
 17
 18770 northern Lesser Antilles) has been related to transient uplift of the Lesser Antilles forearc during basal
 19
 20
 21771 erosion processes (De Min, 2014; Münch et al., 2014; De Min et al., 2015; Boucard et al., 2021).
 22
 23772 Subsequently, the Lesser Antilles forearc subsided from the Zanclean (Early Pliocene). Finally, a
 24
 25
 26773 latest uplift episode led to the emergence of the present-day islands of Grande-Terre, Marie-Galante
 27
 28774 and La Désirade at *ca* 1.2 Ma (Cornée et al. 2012; Münch et al. 2014) whereas the Karukéra Spur
 29
 30
 31775 recorded continuous subsidence. Over the whole studied time interval, islands first occurred to the
 32
 33776 east at the Karukéra Spur. Later, new islands developed further west from Grande-Terre to Marie-
 34
 35
 36777 Galante while the spur subsided. Such a temporal evolution may be related to tectonic erosion of the
 37
 38778 margin that induced a westward migration of the flexural bulge of the upper plate, resulting in a
 39
 40
 41779 landward migration of the emerged areas.

42
 4380 Eustatic sea level changes did not play a significant role in the appearance or drowning of Neogene
 44
 45
 46781 islands. Indeed, their amplitude is limited to some tens of meters (Miller et al., 2020). Moreover,
 47
 4882 when islands were formed during the latest Burdigalian-early Langhian and the latest Messinian (Fig.
 49
 50
 51783 11B and E), the sea level was rising and not falling. Thanks to high resolution and good coverage of
 52
 5384 available geophysical and chronostratigraphic constraints, our study allows: (i) a better understanding
 54
 55
 56785 of the regional causes responsible for cycles of drowning and uplift of forearc crustal blocks and (ii)
 57
 58786 to figure out the periodicity of these cycles. Although our dataset is restricted to the central Lesser
 59
 60
 61
 62
 63
 64
 65

787 Antilles since the late-Early Miocene, we show that uplift and subsidence affecting the forearc oc-
 788 curred several times, during about 2-4 million years. Peri-Pacific forearcs show similar tectonic cy-
 2 cles with a comparable frequency and an amplitude of several hundreds of meters (Menant et al.,
 3 789 2020). These drowning/uplift “cycles” are attributed to transient underplating of sediments at the base
 4 790 of the forearc, responsible for uplift and followed by basal erosion responsible for subsidence/drown-
 5 791 ing (Menant et al., 2020). The accurate quantification of the amplitude of these vertical motions af-
 6 792 fecting the Lesser Antilles forearc still remain unravelled and this could be achieved through deep-
 7 793 sea drillings. At regional scale, from the northern (Cornée et al., 2021) to the central Lesser Antilles
 8 794 (this work), the subduction arc region (*sensu lato*) also recorded Ma- long alternating episodes of
 9 795 drowning and uplift (Fig. 12).

2497 5.3. THE LESSER ANTILLES: A MIOCENE PATHWAY FOR TERRESTRIAL FAUNA MIGRATIONS BE- 25 TWEEN THE GREATER ANTILLES AND SOUTH AMERICA? 26 798

2999 Based on the results obtained in this work and the recently published paleogeographic data col-
 30 lected from the northern part of the Lesser Antilles (Philippon et al., 2020; Cornée et al., 2021), we
 31 find that islands have episodically existed in the region during the Miocene. This is especially the
 32 800 case during the early Middle Miocene and the latest Miocene, when important uplift events occurred
 33 801 in the northern Lesser Antilles forearc, *i.e.* the Kalinago and the Marie-Galante rift basins. These
 34 802 former emerged lands were separated from each other by tens to a hundred of kilometres wide sea-
 35 ways, and were likely about ten times larger than the present-day islands.
 36 803
 37 804
 38 805
 39 806
 40 807
 41 808
 42 809
 43 810
 44 811

811 In which manner terrestrial animals, and especially those who are intolerant to salinity (*e.g.*, am-
 48 phibians), dispersed from continental areas to oceanic islands is still a debated topic. Several pro-
 49 807 cesses have been proposed, as for example land bridges, large floating islands, small-sized natural
 50 808 vegetation rafts, swimming, storms, birds, low salinity paths in oceans (*e.g.*, Measey et al., 2006; Ali
 51 809 and Huber, 2010; Townsend et al., 2011; Ali and Hedges, 2021; Ali et al., 2021). Here, we demon-
 52 810 strate that along the Lesser Antilles subduction zone, between Anguilla to the north and Martinique
 53 811

812 to the south, no continuous land bridge has occurred since *ca* 17-16 Ma. Besides Quaternary glacio-
813 eustatic sea level changes that may have triggered episodic emergences (Cornée et al., 2021), we
2
814 evidence that wide archipelagos punctually emerged and drowned as a consequence of large-scale
4
5
815 tectonic processes.
7

8
816 Blackburn et al. (2020) discussed the mechanisms of dispersal of some early Oligocene frogs from
10
11
817 South America to Puerto Rico, and they consider that further studies are necessary to understand the
12
13
818 origins of the Greater Antilles fauna. Based on an updated compilation of the diversity of 35 terrestrial
14
15
819 vertebrate clades (within amphibians, mammals and reptiles) and the geological work of Garroq et
16
17
820 al. (2021) in the Aves Ridge, Ali and Hedges (2021) concluded that the GAARlandia hypothesis has
18
19
20
821 to be rejected and that the mechanisms of dispersal should be re-evaluated in the Caribbean. From
21
22
822 molecular phylogenetic analyses of the spider *Antillatus*, a clade endemic of the current Greater An-
23
24
25
823 tilles which originated in the northern part of South America, Cala-Riquelme et al. (2022) concluded:
26
27
824 (i) that their common ancestor first occurred in Hispaniola about 25 Ma ago and migrated through the
28
29
30
825 GAARlandia landbridge; (ii) that Hispaniola should have been a nucleus of terrestrial dispersal to-
31
32
33
826 ward Cuba and Puerto Rico prior to their separation; and (iii) that multiple dispersal and island-spe-
34
35
36
827 ciation events occurred during the Middle and Late Miocene, when these islands were formed. Based
37
38
828 on genomic phylogeny studies, Schools et al. (2022) proposed that diploglossid lizards dispersed
39
40
41
829 twice from South America to the Greater Antilles, first during the Oligocene and then during the
42
43
830 Miocene. Additional recent findings have shown that during the late Eocene, the GrANoLA landmass
44
45
831 emerged as a result of a regional compressional event that affected the northern part of the Antilles
46
47
48
832 from Puerto Rico to St. Barthélemy (Philippon et al., 2020) (Fig. 1B). Both the estimated age of the
49
50
833 GrANoLA and paleontological data confirm that large islands, hundreds- kms wide, have existed in
51
52
53
834 the northeastern Caribbean, connecting the Greater and Lesser Antilles (Fig. 1B). Moreover, the
54
55
835 northern Lesser Antilles (from Antigua to Anguilla) may also have played a role later during the
56
57
58
59
60
61
62
63
64
65

836 Cenozoic because the region underwent several episodes of emergence of archipelagos, notably dur-
837 ing the late Oligocene, the early Middle Miocene, at the Miocene-Pliocene transition, and during the
2
338 most severe glacials of the Quaternary (Cornée et al., 2021) (Fig. 1B).

639 In the southern Lesser Antilles, molecular phylogeny studies of current insular frog and lizard
8
840 species (Bourgade, 2020; Grabosky et al., 2022) suggest that ephemeral archipelagos played a role in
10
11841 connecting South America, Martinique and Hispaniola. Nevertheless, geological data are crudely
12
13842 missing in these areas to better constrain such a hypothesis. The initial dispersal of some reptiles and
15
16843 amphibians from South America to the Lesser Antilles (*e.g.*, Prates et al., 2015) has been explained
17
18844 by the hypothetical existence of the Isthmus of Matina (connecting Martinique to Tobago) during the
20
21845 middle Eocene (Bourgade, 2020). The later author also hypothesized the existence of a Matigwana
22
23846 Island (connecting Martinique to St Lucia) during the late Eocene-early Oligocene. Matigwana has
24
25
26847 been proposed as a refuge where the speciation and increasing endemism of some lizards (Prates et
27
28848 al., 2015) and now extinct rodents might have occurred (Bourgade, 2020). South of St Lucia, the
29
30849 presence of wide emerged islands during the Neogene is also highly suspected. In St Vincent-Les
32
33850 Grenadines-Grenada islands, Eocene and Miocene deep-sea deposits are cropping out, indicating that
34
35
36851 severe vertical motion affected these islands (Speed et al., 1993; Donovan and Jackson, 2013).

38
39852 Our study shows that tectonics played a significant role in the uplift and emergence of archipelagos
40
41853 in the central Lesser Antilles during the early Middle Miocene and the latest Miocene. Such uplifted
42
43854 islands may have also existed in the southern Lesser Antilles as suggested by molecular phylogenetic
45
46855 data (Bourgade, 2020; Grabosky et al., 2022). The resulting proximity between emerged landmasses
47
48856 may have favoured short distance oversea dispersals of some terrestrial fauna and their subsequent
49
50
51857 speciation, at least during the Miocene. Consequently, besides long-distance oversea or land bridge
52
53858 hypotheses, we propose that the diachronous vertical motions along the arc and resulting emersion
54
55
56859 episodes and changing paleogeography of the Lesser Antilles may also have played a significant role
57
58860 in the dispersal and speciation of terrestrial fauna during the Miocene. Our hypothesis needs now to
59
60
61
62
63
64
65

861 be further tested by new paleontological research in the Lesser Antilles and new geological investi-
 862 gations in the southern Lesser Antilles. This would notably allow to better constrain the paleo-geo-
 2 graphic evolution and the potential connection or land proximity between the southern Lesser Antilles
 3 863 and South America. Such constraints are necessary to precise the kinematic reconstructions that will
 4
 5 864 allow to refine the paleo-locations of past islands in the Lesser Antilles since the late Eocene.
 6
 7
 8 865

11 866 6. CONCLUSIONS

13
 14
 15 867 Our integrated study of seismic lines, together with biostratigraphic analyses of dredged and core
 16
 17 868 samples and correlations with new onshore data from Guadeloupe and La Désirade, show that the
 18
 19 869 Marie-Galante Basin comprises three sedimentary megasequences lying above an Upper Jurassic de-
 20
 21 870 formed basement: an Eocene (?) to upper Burdigalian megasequence (MG-MS1), a Middle Miocene
 22
 23 871 to Upper Miocene megasequence (MG-MS2) and an uppermost Miocene to present-day me-
 24
 25 872 gasequence (MG-MS3). The MG-SB2 sequence boundary dates late Burdigalian-Langhian and is
 26
 27 873 also identified onshore in Martinique. The age of the MG-SB3 sequence boundary dates late Mes-
 28
 29 874 sinian. The opening of the Marie-Galante Basin has been controlled by NNW-SSE trending normal
 30
 31 875 faults that have been active since the Oligocene. The megasequences are separated by regional un-
 32
 33 876 conformities which have been partly erosional and subaerial in the shoulders of the main fault systems
 34
 35 877 of the Marie-Galante Basin and the Karukéra Spur. Our paleogeographic reconstructions reveal that
 36
 37 878 tectonically-controlled archipelagos took place between Anguilla Bank and Martinique during the
 38
 39 879 early Middle Miocene (MG-SB2) and the latest Miocene (MG-SB3), and that magmatic activity has
 40
 41 880 occurred since the latest Miocene. Such emergence periods exhibit a cyclic pattern of several million
 42
 43 881 years. This suggests that repeated episodes of underplating/erosion at the plate interface may have
 44
 45 882 accounted for part of the vertical motion in the forearc. The Miocene archipelagos were much wider
 46
 47 883 than today, with islands of tens to hundred kilometres wide, separated by narrower seaways. Consid-
 48
 49 884 ering the available biodiversity in the southern Lesser Antilles, we suggest that short distance over-
 50
 51 885 water dispersals may also have driven migrations and speciation of terrestrial fauna in the Lesser
 52
 53 886 Antilles during the Neogene.
 54
 55
 56
 57
 58
 59
 60
 61
 62
 63
 64
 65

887

888

Acknowledgments

3

889

6

890

8

891

10

892

11

893

13

894

14

895

15

896

16

897

18

898

19

899

20

900

21

901

22

902

23

903

24

904

25

905

26

906

27

907

28

908

29

909

30

31

32

33

34

35

36

37

38

39

40

41

42

43

44

45

46

47

48

49

50

51

52

53

54

55

56

57

58

59

60

61

62

63

64

65

Authors thank the Parc Naturel Régional de Martinique for field support in the Caravelle botanical and geological reserve and for sampling authorizations. We thank Olivia Urity for help during field trips in Martinique and B. Leru for scientific discussions. We are indebted to the crew and the scientific party of the KaShallow cruise (<https://doi.org/10.17600/9020010>). We are also indebted to the French BRGM who allowed us to study the Morne à l'Eau borehole (Project FEDER C3AF), and to C. Deplus for providing Aguadomar cruise data.

This work has been funded by the French KaShallow cruise program (<https://doi.org/10.17600/9020010>) and the INSU-SYSTER program OBLISUB. The Région Guadeloupe supported L. De Min PhD grant.

We would like to dedicate this work to our colleague Professor Marcelle Boudagher-Fadel who passed away on June, 29th, 2022. She provided invaluable information about foraminifers, leading to an improved understanding of the stratigraphy and paleoenvironments in the Caribbean region, among many other places. We also want to thank our colleague Jean-Len Léticée who passed away on December, 21st, 2022 for his pioneering PhD work (2008) on the Grande-Terre carbonate platform.

Data Availability

Bathymetric and seismic data are available at Sismar data repository from the cruises DOI : Aguadomar cruise - <https://doi.org/10.17600/98010120> - KaShallow cruise <https://doi.org/10.17600/9020010> – SismAntilles 2 cruise <https://doi.org/10.17600/7010020>

909 **References**

- 1
2 910 Ali, J.R., 2012. Colonizing the Caribbean: is the GAARLandia land-bridge hypothesis gaining a
3
4 911 foothold? *J. Biogeogr.* 39, 431–433. <https://doi.org/10.1111/j.1365-2699.2011.02674.x>.
5
6
- 7 912 Ali J.R. and Hedges S.B., 2021. Colonizing the Caribbean: new geological data and an updated land
8
9 913 vertebrate colonization record challenge the GAARlandia landbridge hypothesis. *J. Biogeogr.*,
10
11
12 914 48, 2699-2707. <https://doi.org/10.1111/jbi.14234>
13
14
- 15 915 Ali J. and Huber M., 2010. Mammalian biodiversity on Madagascar controlled by ocean currents.
16
17 916 *Nature*, 463, 653-656. <https://doi.org/10.1038/nature08706>
18
19
- 20 917 Ali J.R., Fritz U. and Vargas-Ramírez M., 2021. Monkeys on a free-floating island in a Colombian
21
22 918 river: further support for over-water colonization. *Biogeographia*, 36.
23
24 919 <https://doi.org/10.21426/B636051761>
25
26
27
- 28 920 Andréieff P., Bouysse P. and Westercamp D., 1980. Reconnaissance géologique de l'arc insulaire
29
30 921 des Petites Antilles, résultats d'une campagne à la mer de prélèvements de roches entre St Lucie
31
32 922 et Anguilla. Rapport 80SGN086MAR 1979, 227-270, BRGM ed., Orléans (F).
33
34
35
- 36 923 Andréieff P., Bouysse P. and Westercamp D., 1983. Révision géologique de l'île de Marie-Galante
37
38 924 (Petites Antilles). *Bull. Soc. géol. Fr.*, XXV, 805-810. [https://doi.org/10.2113/gssgfbull.S7-
39
40
41 925 XXV.6.805](https://doi.org/10.2113/gssgfbull.S7-XXV.6.805)
42
43
- 44 926 Andréieff P., Baubron J.C. and Westercamp D., 1988. Histoire géologique de la Martinique (Petites
45
46 927 Antilles): biostratigraphie (foraminifères), radiochronologie (potassium–argon), évolution vol-
47
48 928 cano-structurale. *Géol. Fr.*, 2-3, 39-70.
49
50
51
- 52 929 Andréieff P., Bouysse P. and Westercamp D., 1989. Géologie de l'arc insulaire des Petites Antilles
53
54 930 et évolution géodynamique de l'Est-Caraïbe. Thèse de doctorat d'Etat, Université de Bordeaux1,
55
56 931 Bordeaux, France. <https://www.theses.fr/1987BOR10638>
57
58
59
60
61
62
63
64
65

- 932 Battistini R., Hirschberger F., Hoang C. T. and Petit M., 1986. La basse terrasse corallienne pleisto-
 933 cene (Eémien) de la Guadeloupe: morphologie, datations $^{230}\text{Th}/^{234}\text{U}$, néotectonique. Rev.
 2 géomorph. Dyn., 25, 1-10.
 3
 4
 5
 6
 7 935 Bellon H., Pelletier B. and Westercamp, D., 1984. Données géochronométriques relatives au volca-
 8 nisme martiniquais. C. R. Ac. Sci., Paris, 279, 457–460.
 9
 10
 11
 12 937 Blackburn DC, Keeffe RM, Vallejo-Pareja MC, Vélez-Juarbe J. 2020. The earliest record of Carib-
 13 bean frogs: a fossil coquí from Puerto Rico. Biol. Lett. 16: 20190947.
 14
 15 938 <http://doi.org/10.1098/rsbl.2019.0947>
 16
 17 939
 18
 19
 20 940 Bosch D., Zami F., Philippon M., Lebrun J.-F., Münch P., Cornée J.-J., Legendre L. and Lemoyne
 21 A. 2022. Evolution of the northern part of the Lesser Antilles arc - Geochemical constraints from
 22 941 St Barthélemy Island lavas. Geochem., Geophys. Geosyst., 23, e2022GC010482.
 23
 24
 25 942 <https://doi.org/10.1029/2022GC010482>
 26
 27 943
 28
 29
 30 944 Boschman L. M., van Hinsbergen D. J. J., Torsvik T. H., Spakman W. and Pindell J. L., 2014. Kin-
 31 ematic reconstruction of the Caribbean region since the Early Jurassic. Earth Sci. Rev., 138, 102-
 32 945 136. <https://doi.org/10.1016/j.earscirev.2014.08.007>
 33
 34
 35 946
 36
 37
 38 947 Boucard M., Lebrun J.-F., Marcaillou B., Laurencin M., Klingelhoefer, F., Laigle, M., Lallemand,
 39 S., Schenini L., Graindorge D., Cornée J.-J., Münch, P., Philippon M., and the ANTITHESIS 1,
 40 948 3 Teams, 2021. Paleogene V-shaped basins and Neogene subsidence of the Northern Lesser An-
 41 949 tilles forearc. Tectonics, 40, e2020TC006524. <https://doi.org/10.1029/2020TC006524>
 42
 43 950
 44
 45
 46
 47
 48 951 BouDagher-Fadel K., 2008. Evolution and significance of larger benthic foraminifera. In: WIG-
 49 NALL P.B. (Ed), Developments in Paleontology and stratigraphy, 21, 540 pp., Amsterdam, Else-
 50 vier. [https://doi.org/10.1016/S0920-5446\(08\)00012-5](https://doi.org/10.1016/S0920-5446(08)00012-5)
 51
 52
 53 953
 54
 55
 56 954 BouDagher-Fadel M. K., 2015. Biostratigraphic and Geological Significance of Planktonic Forami-
 57 nifera (Updated 2nd Edition). London, UCL Press, 298 pp.
 58
 59 955 <https://doi.org/10.14324/111.9781910634257>
 60
 61 956
 62
 63
 64
 65

- 957 BouDagher-Fadel M.K., 2018a. Revised Diagnostic First and Last Occurrences of Mesozoic and
958 Cenozoic Planktonic Foraminifera. UCL Office of the Vice-Provost Research, Professional Pa-
959 pers Series, 2, 1-5.
960 Boudagher-Fadel M. K., 2018b. Evolution and Geological Significance of Larger Benthic Forami-
961 nifera. London, UK: UCL Press. <https://doi.org/10.14324/111.9781911576938>
- 962 BouDagher-Fadel M.K. and Price G.D., 2010. American miogypsinidae: An analysis of their phy-
963 logeny and biostratigraphy. *Micropaleontology*, 56, 567-586. [https://www.jstor.org/sta-
964 ble/40983741](https://www.jstor.org/stable/40983741)
- 965 BouDagher-Fadel M.K. and Price G.D., 2013. The phylogenetic and palaeogeographic evolution of
966 the miogypsinid larger benthic foraminifera. *J. Geol. Soc.*, 170, 185-208.
967 <https://doi.org/10.1144/jgs2011-149>
- 968 BouDagher-Fadel M.K., Price G.D. and Koutsoukos E.A.M., 2010. Foraminiferal biostratigraphy
969 and paleoenvironments of the Oligocene-Miocene carbonate succession in Campos Basin, south-
970 eastern Brazil. *Stratigraphy*, 7, 283-299.
- 971 Bourgade M., 2020. History of Squamate Lizard Dactyloidae from the Eastern Caribbean, Origins
972 of *Anolis* from Martinique, Zannoli Matinik (*Dactyloa roquet*). Unpublished data publically
973 available at <https://hal.archives-ouvertes.fr/hal-02469738>
- 974 Bouysse P., 1988. Opening of the Grenada back-arc basin and evolution of the Caribbean plate dur-
975 ing the Mesozoic and early Paleogene. *Tectonophysics*, 149, 121-143.
976 [https://doi.org/10.1016/0040-1951\(88\)90122-9](https://doi.org/10.1016/0040-1951(88)90122-9)
- 977 Bouysse P. and Guennoc P., 1983. Données sur la structure de l'arc insulaire des Petites Antilles
978 entre St Lucie et Anguilla. *Mar. Geol.* 53, 131– 166. [https://doi.org/10.1016/0025-
979 3227\(83\)90038-5](https://doi.org/10.1016/0025-3227(83)90038-5)

- 980 Bouysse P. and Mascle, A., 1994. Sedimentary Basins and Petroleum Plays around the French An-
981 tilles. In: MASCLE, A. (Ed.), Hydrocarbon and Petroleum Geology of France. Special Publica-
2 tion of the Europ. Assoc. Petrol. Geoscient., 4. Springer. [https://doi.org/10.1007/978-3-642-](https://doi.org/10.1007/978-3-642-78849-9_32)
382 [78849-9_32](https://doi.org/10.1007/978-3-642-78849-9_32).
4
5
683
7
8
984 Bouysse P. and Westercamp D., 1990. Subduction of Atlantic aseismic ridges and Late Cenozoic
10 evolution of the Lesser Antilles Island arc. *Tectonophysics* 175, 349–380.
11
12
13
1485 [https://doi.org/10.1016/0040-1951\(90\)90180-G](https://doi.org/10.1016/0040-1951(90)90180-G)
15
16
1987 Bouysse P., Schmidt-Effing R. and Westercamp D., 1983. La Désirade island (Lesser Antilles) re-
18 visited: Lower Cretaceous radiolarian cherts and arguments against an ophiolitic origin for the
1988 basal complex. *Geology*, 11, 244-247. [https://doi.org/10.1130/0091-7613\(1983\)11<244:LDI-](https://doi.org/10.1130/0091-7613(1983)11<244:LDI-LAR>2.0.CO;2)
20 [LAR>2.0.CO;2](https://doi.org/10.1130/0091-7613(1983)11<244:LDI-LAR>2.0.CO;2)
21
22
23
2490
25
26
2791 Bouysse P., Westercamp D. and Andréïeff P., 1990. The Lesser Antilles Island arc. *Proc. Ocean*
28 *Drill. Program Sci. Results* 110, 29–44.
29
3092
31
32
3393 Bouysse P., Garrabé F. and Mauboussin T., 1993. Carte géologique de la France (1/50 000), Feuille
34 Marie-Galante et îlets de la Petite-Terre (Guadeloupe). Service géologique national. – BRGM,
3594 Orléans, France.
36
37
3895
39
40
4196 Bouysse P., Garrabé F., Mauboussin T. and Andréïeff P., 1993. Carte géologique du département de
42 la Guadeloupe : Marie-Galante et les îlets de Petite-Terre) 1/50000, Service Géologique National
4397 edn., BRGM, Orléans, France.
44
45
4698
47
48
4999 Bouysse P., Andréïeff P., Richard M., Baubron J., Mascle A., Maury R. and Westercamp D., 1985.
50 Aves swell and northern Lesser Antilles ridge: Rock-dredging results from Arcante 3 cruise. *In*:
1000 *Géodynamique des caraïbes*, symposium, 65-76, Paris, Technip Ed.
51
52
53
54
55
56
1002 Brace S., Turvey S. T., Weksler M., Hoogland M. L. P. and Barnes I., 2015. Unexpected evolution-
57 ary diversity in a recently extinct Caribbean mammal radiation. *Proc. Roy.Soc. London, B*, 282,
58 20142371. <https://doi.org/10.1098/rspb.2014.2371>
59
60
61
62
63
64
65

- 1005 Cala-Riquelme F., Wienczek P., Florez-Daza E., Binford G.J., and Agnarsson I, 2022. Island-to-Is-
1006 land Vicariance, Founder-Events and within-Area Speciation: The Biogeographic History of the
2
3
1007 *Antillattus* Clade (Salticidae: Euophryini). *Diversity*, 14, 224. <https://doi.org/10.3390/d14030224>
4
5
1008 Catuneanu O., Galloway W.E., Kendall C.G.S., Miall A.D., Posamentier H.W. and Tucker M.E.,
6
8
1009 2011. Sequence stratigraphy: methodology and nomenclature. *Newsl. Stratigr.*, 44, 173-245.
10
11
1010 <https://doi.org/10.1127/0078-0421/2011/0011>
12
13
14
1011 Church R. E. and Allison K. R., 2004. The Petroleum Potential of the Saba Bank Area, Netherlands
15
16
1012 Antilles. *Search and Discovery Article # 10076*. Posted December 20, 2004
18
19
1013 Clift P.D. and Vannucchi P., 2004. Controls on tectonic accretion versus erosion in subduction
21
22
1014 zones: Implications for the origin and recycling of the continental crust. *Rev. Geophys.*, 42,
23
24
1015 RG2001. <https://doi.org/10.1029/2003RG000127>
26
27
1016 Cordey F. and Cornée J.-J., 2009. Late Jurassic radiolarians from La Désirade basement complex
29
30
1017 (Guadeloupe, Lesser Antilles Arc) and tectonic implications. *Bull. Soc. géol. Fr.*, 180, 399-409.
31
32
1018 <https://doi.org/10.2113/gssgfbull.180.5.399>
34
35
1019 Cornée J.-J., Léticée J.-L., Münch P., Quillévére F., Lebrun J.-F., Moissette P., Braga J.C., Melinte-
37
38
1020 Dobrinescu M., De Min L., Oudet J., Randrianasolo A., 2012. Sedimentology, paleoenviron-
39
40
1021 ments and biostratigraphy of the Pliocene-Pleistocene carbonate platform of Grande-Terre (Gua-
41
42
1022 deloupe, lesser Antilles fore-arc). *Sedimentology*, 59, 1426-1451. <https://doi.org/10.1111/j.1365->
44
45
1023 [3091.2011.01311.x](https://doi.org/10.1111/j.1365-3091.2011.01311.x)
46
47
48
1024 Cornée J.-J., Münch P., Philippon M., Boudagher-Fadel M., Quillévére F., Melinte-Dobrinescu M.,
49
50
1025 Lebrun J.F., Gay A., Meyer S., Montheil L., Lallemand S., Marcaillou B., Laurencin M., Legen-
52
53
1026 dre L., Garroq C., Boucard M., Beslier M.-O., Laigle M., Schenini L., Fabre P.-H., Antoine P.-
54
55
1027 O., Marivaux L. and the GARANTI and ANTITHESIS Scientific Parties, 2021. Lost islands in
57
58
59
60
61
62
63
64
65

- 1028 the northern Lesser Antilles: possible milestones in the Cenozoic dispersal of terrestrial organ-
1029 isms between South-America and the Greater Antilles. *Earth Sci. Rev.*, 217, 103617.
2
3
1030 <https://doi.org/10.1016/j.earscirev.2021.103617>
4
5
6
1031 Corsini M., Lardeaux J.M., Vérati C., Voitus E. and Balagne M., 2011. Discovery of Lower Creta-
8
1032 ceous synmetamorphic thrust tectonics in French Lesser Antilles (La Désirade Island, Guade-
10
11
1033 loupe): Implications for Caribbean geodynamics. *Tectonics*, 30, TC4005.
12
13
1034 <https://doi.org/10.1029/2011TC002875>
15
16
1035 Dávalos L. M., 2004. Phylogeny and biogeography of Caribbean mammals. *Biol. J. Linnean Soc.*,
18
1036 81, 373-394. <https://doi.org/10.1111/j.1095-8312.2003.00302.x>
20
21
22
1037 Delsuc F., Kuch M., Gibb G. C., Karpinski E., Hackenberger D., Szpak P., Martinez J. G., Mead J.
23
24
1038 I., McDonald H. G., MacPhee R. D. E., Billet G., Hautier L. and Poinar H. N., 2019. Ancient mi-
26
1039 togenomes reveal the evolutionary history and biogeography of sloths. *Current Biology*, 29,
28
1040 2031-2042. <https://doi.org/10.1016/j.cub.2019.05.043>
31
32
1041 De Min L., 2014. Sismo-stratigraphie multi-échelle d'un bassin avant-arc: Architecture du bassin de
34
1042 Marie-Galante, Petites Antilles. Sciences de la Terre. Thèse de doctorat, Université des Antilles
36
1043 et de la Guyane (UAG), Pointe à Pitre, Guadeloupe, France.
38
39
1044 <https://www.theses.fr/2014AGUY0799>
41
42
1045 De Min L., Lebrun J. F., Cornée J. J., Münch P., Léticée J. L., Quillévéré F., Melinte-Dobrinescu
44
1046 M., Randrianasolo A., Marcaillou B. and Zami F., 2015. Tectonic and sedimentary architecture
46
1047 of the Karukéra spur: A record of the Lesser Antilles fore-arc deformations since the Neogene.
49
50
1048 *Mar. Geol.*, 363, 15–37. <https://doi.org/10.1016/j.margeo.2015.02.007>
51
52
53
1049 DeMets, C., Gordon, R.G., Argus, D.F., 2010. Geologically current plate motions. *Geophys. J. Int.*
54
55
1050 181, 1-80. <https://doi.org/10.1111/j.1365-246X.2009.04491.x>
57
58
1051 Deplus C., 1998. Aguadomar Cruise, N/O L'Atalante, <https://doi.org/10.17600/98010120>
60
61
62
63
64
65

- 1052 Dixon T.H., Farina F., DeMets C., Jansma P., Mann P. and Calais E., 1998. Relative motion be-
1053 tween the Caribbean and North American Plates and related boundary zone deformation from a
2 decade of GPS observations. *J. Geophys. Res.*, 103, 15157-15182.
3
1054 <https://doi.org/10.1029/97JB03575>
4
5
1055
6
7
8
1056 Donovan S.K. and Jackson T.A., 2013. The Miocene of Carriacou, the Grenadines, Lesser Antilles.
9
10
1057 *Geology Today*, 29, 150–158. <https://doi.org/10.1111/gto.12017>
11
12
13
14
1058 Durocher M., Nicolas V. and Perdirakis S., 2020. Archaeobiogeography of extinct rice rats (*Ory-*
15
16
1059 *zomyini*) in the Lesser Antilles during the Ceramic Age (500 BCE–1500 CE). *The Holocene*, 31,
17
18
1060 433-445. <https://doi.org/10.1177/0959683620972785>
19
20
21
22
1061 Evain M., Galve A., Charvis P., Laigle M., Kopp H., Bécél A., Weinzierl W., Hirn A., Flueh E.R.
23
24
1062 and Gallard J., 2011. The Lesser Antilles Thales scientific party, 2013. Structure of the Lesser
25
26
1063 Antilles subduction forearc and backstop from 3D seismic refraction tomography. *Tectonophys-*
27
28
1064 *ics*, 603, 55–67. <https://doi.org/10.1016/j.tecto.2011.09.021>
29
30
31
32
1065 Fabre P.-H., Vilstrup J. T., Raghavan M., Der Sarkissian C., Willerslev E., Douzery E. J. P. and Or-
33
34
1066 lando L., 2014. Rodents of the Caribbean: origin and diversification of hutias unravelled by next-
35
36
1067 generation museomics. *Biol. Lett.*, 10, 20140266. <https://doi.org/10.1098/rsbl.2014.0266>
37
38
39
40
1068 Favier A., Lardeaux J.-M., Legendre L., Vérati C., Philippon M., Corsini M., Münch P. and Venta-
41
42
1069 lon S., 2019. Tectono-metamorphic evolution of shallow crustal levels within active volcanic
43
44
1070 arcs. Insights from the exhumed Basal Complex of Basse-Terre (Guadeloupe, French West In-
45
46
1071 dies). *Earth Sci. Bull.*, 190,10. <https://doi.org/10.1051/bsgf/2019011>
47
48
49
50
1072 Favier A., Lardeaux J. M., Corsini M., Vérati C., Navelot V., Géraud Y., Diraison M., Ventalon
51
52
1073 S. and Voitus E., 2021. Characterization of an exhumed high-temperature hydrothermal system
53
54
1074 and its application for deep geothermal exploration: An example from Terre-de-Haut Island
55
56
1075 (Guadeloupe archipelago, Lesser Antilles volcanic arc). *J. Volcanol. Geotherm. Res.*, 418,
57
58
59
1076 107256. <https://doi.org/10.1016/j.jvolgeores.2021.107256>
60
61
62
63
64
65

- 1077 Feuillet N., Manighetti I., Tapponnier P. and Jacques E., 2002. Arc parallel extension and localiza-
1078 tion of volcanic complexes in Guadeloupe, Lesser Antilles, J. Geophys. Res., 107, 2331.
2
3
1079 <https://doi.org/10.1029/2001JB000308>
4
5
- 1080 Feuillet N., Tapponnier P., Manighetti I., Villemant B., and King G.C.P., 2004. Differential uplift
8
1081 and tilt of Pleistocene reef platforms and Quaternary slip rate on the Morne-Piton normal fault
10
1082 (Guadeloupe, French West Indies). J. Geophys. Res.: Solid Earth, 109, B02404.
11
12
13
1083 <https://doi.org/10.1029/2003JB002496>
14
15
- 1084 Feuillet N., Leclerc F., Tapponnier P., Beauducel F., Boudon G., Le Friant A., Deplus C., Lebrun
18
1085 J.-F., Nercessian A., Saurel J.-M. and Clément V., 2010. Active faulting induced by slip parti-
20
1086 tioning in Montserrat and link with volcanic activity: New insights from the 2009 GWADASEIS
21
1087 marine cruise data. Geophys. Res. Lett., 37, L00E15. <https://doi.org/10.1029/2010GL042556>
22
23
24
25
26
- 1088 Feuillet N., Beauducel F., Jacques E., Tapponnier P., Delouis B., Bazin S., Vallée M. and King G.
28
1089 C. P., 2011. The Mw = 6.3, November 21, 2004, Les Saintes earthquake (Guadeloupe): Tectonic
29
1090 setting, slip model and static stress changes J. Geophys. Res., 116, B10301.
30
31
32
1091 <https://doi.org/10.1029/2011JB008310>
33
34
35
36
- 1092 Fisher D.M., Gardner T.W., Marshall J.S., Sak P.B. and Protti M., 1998. Effect of subducting sea-
37
1093 floor roughness on fore-arc kinematics, Pacific coast, Costa Rica. Geology, 26, 467-470.
38
39
40
1094 [https://doi.org/10.1130/0091-7613\(1998\)026<0467:EOSSFR>2.3.CO;2](https://doi.org/10.1130/0091-7613(1998)026<0467:EOSSFR>2.3.CO;2)
41
42
43
44
- 1095 Flügel E., 2006. Microfacies of carbonate rocks: analysis, interpretation and application. Springer,
45
1096 Berlin.
46
47
48
49
50
- 1097 Garrabé F., 1983. Evolution sédimentaire et structurale de la Grande-Terre de Guadeloupe, Thèse
51
1098 de Doctorat, Université de Paris 11, Orsay , France, 178 pp.
52
53
54
55
- 1099 Garrocq C., Lallemand S., Marcaillou B., Lebrun J.-F., Padron C., Klingelhoefer F., Laigle M.,
56
1100 Munch P., Gay A., Shenini L., Beslier M.-O., Cornée J.-J., Mercier De Lepinay B., Quillevere F.
57
1101 and Boudagher-Fadel M., 2021. Genetic relations between the Aves Ridge and the Grenada
58
59
60
61
62
63
64
65

- 1102 back-arc basin, East Caribbean Sea. *J. Geophys. Res., Solid Earth*, 126, e2020JB020466.
- 1103 <https://doi.org/10.1029/2020JB020466>
- 1104 GEBCO, 2014. Gridded bathymetric data. <https://www.gebco.net/>
- 1105 Germa A., Quidelleur X., Labanieh S., Chauvel C. and Lahitte, P., 2011. The volcanic evolution of
- 1106 Martinique Island: insights from K–Ar dating into the Lesser Antilles arc migration since Oligo-
- 1107 cene. *J. Volcanol. Geotherm. Res.*, 208, 122–135. <https://doi.org/10.1016/j.jvolge->
- 1108 [ores.2011.09.007](https://doi.org/10.1016/j.jvolge-ores.2011.09.007)
- 1109 Graboski R., Grazziotin F.G., Mott T. and Trefaut Rodrigue M., 2022. The phylogenetic position of
- 1110 Ridley's worm lizard reveals the complex biogeographic history of New World insular amphis-
- 1111 baenids. *Molec. Phylogen. Evol.* 173, 107518. <https://doi.org/10.1016/j.ympev.2022.107518>
- 1112 Hedges S. B., 1996. Historical biogeography of West Indian vertebrates. *Ann. Rev. Ecol. System.*,
- 1113 27, 163-196. <https://doi.org/10.1146/annurev.ecolsys.27.1.163>
- 1114 Henri M., Quidelleur X., Le Friant A., Komorowski J.-C., Escartín J., Deplus C., Mevel C., 2022.
- 1115 K-Ar Geochronology and geochemistry of underwater lava samples from the Subsaintes cruise
- 1116 offshore Les Saintes (Guadeloupe): Insights for the Lesser Antilles arc magmatism, *Marine Ge-*
- 1117 *ology*, 450, 106862, <https://doi.org/10.1016/j.margeo.2022.106862>
- 1118 Hirn A., 2001. SISMANTILLES 1 cruise, RV Le Nadir. <https://doi.org/10.17600/1080060>
- 1119 Iturralde-Vinent M.A. and MacPhee R.D.E., 1999. Palaeogeography of the Caribbean region: impli-
- 1120 cations for Cenozoic biogeography. *Bull. Am. Mus. Nat. Hist.*, 238, 1–95.
- 1121 Kopp H., Weinzirl W., Becel A., Charvis P., Flueh E.R., Gailler A., Galve A., Hirn A., Kandilarov
- 1122 A., Klaeschen D., Laigle M., Papenberg C., Planert L., Roux E. and Trail and Thales teams,
- 1123 2011. Deep structure of the central Lesser Antilles Island Arc: Relevance for the formation of
- 1124 continental crust. *Earth Planet. Sci. Lett.*, 304, 121-134.
- 1125 <https://doi.org/10.1016/j.epsl.2011.01.024>

- 1126 Laigle M., Lebrun J.-F. and Hirn A., 2007. SISMANTILLES 2 cruise, RV L'Atalante,
 1127 <https://doi.org/10.17600/7010020>
 2
 3
- 1428 Laigle M., Becel A., de Voogd B., Sachpazi M., Bayrakci G., Lebrun J.-F., Evain M. and the “Tha-
 5
 1129 les Was Right” Seismic Reflection working group, 2013. Along-arc segmentation and interaction
 8
 1430 of subducting ridges with the Lesser Antilles Subduction forearc crust revealed by MCS imaging.
 10
 1131 Tectonophysics, 603, 32-54. <http://doi.org/10.1016/j.tecto.2013.05.028>
 12
 13
- 1432 Lallemand S. and Le Pichon X., 1987. Coulomb wedge model applied to the subduction of sea-
 15
 1433 mounts in the Japan Trench. Geology, 15, 1065-1069. [https://doi.org/10.1130/0091-
 18
 1434 7613\(1987\)15<1065:CWMATT>2.0.CO;2](https://doi.org/10.1130/0091-7613(1987)15<1065:CWMATT>2.0.CO;2)
 20
 21
- 1435 Lardeaux J.-M., Münch P., Corsini M., Cornée J.-J., Vérati C., Lebrun J.-F., Quillévéré F., Melinte-
 23
 1436 Dobrinescu M., Léticée J-L., Fietzke J., Mazabraud Y., Cordey F. and Randrianasolo A., 2013.
 26
 1437 La Désirade Island (Guadeloupe, French West Indies): a key target for deciphering the role of
 28
 1438 reactivated tectonic structures in Lesser Antilles arc building. Bull. Soc. géol. Fr., 184, 21-34.
 29
 1439 <https://doi.org/10.2113/gssgfbull.184.1-2.21>
 33
 34
- 1440 Lebrun J.F., 2009. KaShallow2 Cruise, R/V Le Suroît. <https://doi.org/10.17600/9020010>
 36
 37
- 1441 Lebrun J.F. and Lallemand S., 2017. GARANTI cruise, R/V L'Atalante.
 39
 1442 <https://doi.org/10.17600/17001200>
 42
 43
- 1443 Leclerc F. and Feuillet N., 2019. Quaternary coral reef complexes as powerful markers of long-term
 45
 1444 subsidence related to deep processes at subduction zones: Insights from Les Saintes (Guade-
 47
 1445 loupe, French West Indies): Geosphere, 15, 983–1007. <https://doi.org/10.1130/GES02069.1>.
 48
 50
- 1446 Leclerc F., Feuillet N. and Deplus C., 2016. Interactions between active faulting, volcanism, and
 52
 1447 sedimentary processes at an island arc: Insights from Les Saintes channel, Lesser Antilles arc.
 55
 1448 Geochem. Geophys. Geosyst., 17, 2781-2802. <https://doi.org/10.1002/2016GC006337>
 57
 58
 59
 60
 61
 62
 63
 64
 65

- 1149 Leclerc F., Feuillet N., Perret M., Cabioch G., Bazin S., Lebrun J.-F. and Saurel J.M., 2015. The
 1150 reef platform of Martinique: Interplay between eustasy, tectonic subsidence and volcanism since
 2 Late Pleistocene. *Marine Geology*, 369, 34–51. <https://doi.org/10.1016/j.margeo.2015.08.001>
 3
 4
 5
 6
 1152 Legendre L., Philippon M., Münch P., Léticée J. L., Noury M., Maincent G., Cornée J.-J., Caravati
 8
 1153 A., Lebrun J.-F. and Mazabraud Y., 2018. Trench bending initiation: Upper plate strain pattern
 10 and volcanism. Insights from the Lesser Antilles arc, St. Barthélemy island, French West In-
 11
 12
 13
 14
 15
 16
 1156 Léticée J.-L., 2008. Architecture d'une plateforme carbonatée insulaire plio-pleistocène en domaine
 18
 19
 20
 21
 22
 23
 24
 25
 26
 27
 28
 29
 30
 31
 32
 33
 34
 35
 36
 37
 38
 39
 40
 41
 42
 43
 44
 45
 46
 47
 48
 49
 50
 51
 52
 53
 54
 55
 56
 57
 58
 59
 60
 61
 62
 63
 64
 65

- 1173 Mann P., Taylor F.W., Lawrence Edwards R. and Ku T.,1995. Actively evolving microplate for-
 1174 mation by oblique collision and sideways motion along strike-slip faults: An example from the
 2 northeastern Caribbean plate margin. *Tectonophysics*, 246, 1-69. [https://doi.org/10.1016/0040-](https://doi.org/10.1016/0040-1951(94)00268-E)
 3 1175 [1951\(94\)00268-E](https://doi.org/10.1016/0040-1951(94)00268-E)
 4
 5
 6 1176
 7
 8
 9 1177 Marivaux L., Vélez-Juarbe J., Merzeraud G., Pujos F., Viñola López L. W., Boivin M., Santos-Mer-
 10 cado H., Cruz E. J., Grajales A., Padilla J., Vélez-Rosado K. I., Philippon M., Léticée J.-L.,
 11 1178 Münch P. and Antoine P.-O., 2020. Early Oligocene chinchilloid caviomorphs from Puerto Rico
 12 and the initial rodent colonization of the West Indies. *Proc. Roy. Soc. B*, 287, 20192806.
 13
 14 1179 <https://doi.org/10.1098/rspb.2019.2806>
 15
 16 1180
 17
 18 1181
 19
 20
 21 1182 Marivaux L., Vélez-Juarbe J., Lazaro W. Vinola Lopez L.W., Fabre P.-H., Pujos F., Santos-Mer-
 23 cado H., Cruz E.J., Grajalez Perez A.M., Velez-Rojado K.I., Cornée J.-J., Philippon M., Münch
 24 1183 P. and Antoine P.-O., 2021. An unpredicted ancient colonization of the West Indies by North
 25 American rodents: dental evidence of a geomorph from the early Oligocene of Puerto Rico. *Pa-*
 26 1184 *pers in Paleontology*, 7, 1-19. <https://doi.org/10.1002/spp2.1388>
 27
 28
 29 1185
 30
 31 1186
 32
 33
 34 1187 Martin-Kaye P.H.A., 1969. A summary of the geology of the Lesser Antilles. *Overseas Geol.*
 35 *Miner. Resour.*, 10, 172-206.
 36
 37 1188
 38
 39
 40 1189 Mattinson J.M., Pessagno E.A. Jr., Montgomery H. and Hopson C.A., 2008. Late Jurassic age of
 41 oceanic basement at La Désirade Island, Lesser Antilles arc. In: J. WRIGHT and J. SHERVAIS,
 42 1190 (Eds), *Ophiolites, arcs, and batholiths: a tribute to Cliff Hopson.* – GSA Spec. Pap., 438, 175-
 43
 44 1191 190.
 45
 46
 47 1192
 48
 49
 50 1193 Measey G.J., Vences M., Drewes R.C., Chiari Y., Melo M. and Bourles B., 2006. Freshwater paths
 51 across the ocean: molecular phylogeny of the frog *Ptychadena newtoni* gives insights into am-
 52 1194 phibian colonization of oceanic islands. *J. Biogeogr.*, 34, 7-20. [https://doi.org/10.1111/j.1365-](https://doi.org/10.1111/j.1365-2699.2006.01589.x)
 53
 54 1195 [2699.2006.01589.x](https://doi.org/10.1111/j.1365-2699.2006.01589.x)
 55
 56
 57 1196
 58
 59
 60
 61
 62
 63
 64
 65

- 1197 Menant A., Angiboust S., Gerya T., Lacassin R., Simoes M. and Grandin R., 2020. Transient strip-
 1198 ping of subducting slabs controls periodic forearc uplift. *Nature Comm.*,
 2
 1199 11:1823.<https://doi.org/10.1038/s41467-020-15580-7>
 4
 5
- 1200 Miller K. G., Browning J. V., Schmelz W. J., Kopp R. E., Mountain G. S. and Wright J.D., 2020.
 8
 1201 Cenozoic sea-level and cryospheric evolution from deep-sea geochemical and continental margin
 10
 1202 records. *Sci. Adv.*, 6, eaaz1346. <https://doi.org/10.1126/sciadv.aaz1346>
 12
 13
- 1203 Mitchum R.M., Vail P.R. and Todd R.G., 1976. Regional seismic interpretation using sequences
 16
 1204 and eustatic cycles. *AAPG Bull.*, 60, pp. 699-699.
 18
 19
- 1205 Montheil L., Philippon M., Cornée J.-J., BouDagher-Fadel M., van Hinsbergen D.J.J., Camps P.,
 21
 1206 Maffione M., Audemard F., Brons B., Van der Looij K.J.R. and Münch P., 2022. Geological ar-
 23
 1207 chitecture and history of the Antigua volcano and carbonate platform: was there an Oligo-Mio-
 26
 1208 cene lull in Lesser Antilles arc magmatism? *Geol. Soc. Amer. Bull.*
 28
 1209 <https://doi.org/10.1130/B36465.1>
 30
 31
- 1210 Münch P., Lebrun J.-F., Cornée J.-J., Thinon I., Guennoc P., Marcaillou B., Randrianasolo A. and
 34
 1211 the KaShallow TEAM, 2013. Pliocene to Pleistocene carbonate systems of the Guadeloupe ar-
 36
 1212 chipelago, French Lesser Antilles: a land and sea study. *Bull. Soc.géol. Fr.*, 184, 99-110.
 37
 1213 <https://doi.org/10.2113/gssgfbull.184.1-2.99>
 41
 42
- 1214 Münch, P., Cornée, J.-J., Lebrun, J.F., Quillévéré, F., Vérati, C., Melinte-Dobrinescu, M., Demory,
 44
 1215 F.,Smith, M.J., Jourdan, X., Lardeaux, J.-M., De Min L., Léticée J.-L. and Randrianasolo A.,
 46
 1216 2014. Pliocene to Pleistocene vertical movements in the forearc of the Lesser Antilles subduc-
 49
 1217 tion: insights from chronostratigraphy of shallow-water carbonate platforms (Guadeloupe archi-
 51
 1218 pelago). *J. Geol. Soc. London*, 171, 329-341. <https://doi.org/10.1144/jgs2013-005>
 52
 54
 55
- 1219 Myers N., Russell A., Mittermeier R.A., Mittermeier C.G., da Fonseca G.A.B. and Kent J., 2000.
 57
 1220 Biodiversity hotspots for conservation priorities. *Nature*, 403, 853-858.
 59
 1221 <https://doi.org/10.1038/35002501>
 62
 63
 64
 65

- 1222 Neill I., Gibbs J.A., Hastie A.R. and Kerr A.C., 2010. Origin of the volcanic complexes of La Dé-
 1223 sirade, Lesser Antilles: Implications for tectonic reconstruction of the Late Jurassic to Cretaceous
 2 Pacific - proto Caribbean margin. – *Lithos*, 120, 407-420. [https://doi.org/10.1016/j.li-](https://doi.org/10.1016/j.lithos.2010.08.026)
 1224 [thos.2010.08.026](https://doi.org/10.1016/j.lithos.2010.08.026)
 3
 4
 5
 6
 7
 8
 1226 Noury M., Philippon M., Cornée J.-J., Bernet M., Bruguier O., Montheil L., Legendre L., Dugamin
 10
 11
 1227 E., Bonno M. and Münch P., 2021. Evolution of a shallow volcanic arc pluton during arc migra-
 12
 13
 1228 tion: A tectono-thermal integrated study of the St. Martin granodiorites (northern Lesser Antil-
 15
 16
 17
 1229 les). *Geochem., Geophys., Geosyst.*, 22, e2020GC009627.
 18
 19
 20
 21
 1230 <https://doi.org/10.1029/2020GC009627>
 22
 23
 1231 Philippon M., Cornée J.-J., Münch P., van Hinsbergen D.J.J., BouDagher-Fadel M., Gailler L.,
 24
 25
 1232 Quillévéré F., Boschman L., Montheil L., Gay A., Lebrun J.-F., Lallemand S., Marivaux L. and
 26
 27
 1233 Antoine P.O., 2020. Eocene intra-plate shortening responsible for the rise of a fauna pathway in
 28
 29
 1234 the northeastern Caribbean realm. *Plos-ONE*, 15, e0241000. [https://doi.org/10.1371/jour-](https://doi.org/10.1371/journal.pone.0241000)
 30
 31
 1235 [nal.pone.0241000](https://doi.org/10.1371/journal.pone.0241000)
 32
 33
 34
 1236 Pindell J.L. and Barrett S.F., 1990. Geological evolution of the Caribbean region: a plate tectonic
 35
 36
 1237 perspective. In: G. Dengo and J.E. Case, Eds, *The Caribbean region, the geology of North Amer-*
 38
 39
 1238 *ica. Geol. Soc. Amer.*, Boulder, CO, 405-432. <https://doi.org/10.1130/DNAG-GNA-H.405>
 40
 41
 42
 1239 Pindell J. L. and Kennan L., 2009. Tectonic evolution of the Gulf of Mexico, Caribbean and north-
 43
 44
 1240 ern South America in the mantle reference frame: an update. In: *The origin and evolution of the*
 45
 46
 1241 *Caribbean Plate*, *Geol. Soc., London, Spec. Public.*, 328, 1-55. [https://doi:10.1144/SP328.1](https://doi.org/10.1144/SP328.1)
 47
 48
 49
 50
 1242 Prates I., Trefaut Rodriguez M., Melo-Sampaio P.R. and Carnaval A.C., 2015. Phylogenetic rela-
 51
 52
 1243 tionships of Amazonian anole lizards (*Dactyloa*): Taxonomic implications, new insights about
 53
 54
 1244 phenotypic evolution and the timing of diversification. *Evolution*, 82, 258-268.
 55
 56
 1245 <https://doi.org/10.1016/j.ymp.2014.10.005>
 57
 58
 59
 60
 61
 62
 63
 64
 65

- 1246 Raffi I., Backman J., Fornaciari E., Pälke H., Rio D., Lourens L. and Hilgen F., 2006. A review of
1247 calcareous nannofossil astrobiochronology encompassing the past 25 million years. *Quat. Sci.*
2
348 *Rev.* 25, 3113–3137. <https://doi.org/10.1016/j.quascirev.2006.07.007>
4
5
649 Roksandic M.M., 1978. Seismic facies analysis concepts. *Geophys. Prospect.*, 26, 383-398.
7
8
950 <https://doi.org/10.1111/j.1365-2478.1978.tb01600.x>
10
11
1251 Sak P.B., Fisher D.M and Gardner T.W., 2004. Effects of subducting seafloor roughness on upper
13
14
152 plate vertical tectonism: Osa Peninsula, Costa Rica. *Tectonics*, 23, TC1017.
15
16
1253 <https://doi.org/10.1029/2002TC001474>
18
19
2054 Samper A, Quidelleur X, Lahitte P, Mollex D. 2007. Timing of effusive volcanism and collapse
21
22
2355 events within an oceanic arc island: Basse-Terre, Guadeloupe archipelago (Lesser Antilles Arc).
23
24
2556 *Earth Planet. Sci. Letters* 258, 175–191. <https://doi.org/10.1016/j.epsl.2007.03.030>
26
27
2857 Schools M., Kasprowicz A. and Hedges S.B., 2022. Phylogenomic data resolve the historical bioge-
29
30
3158 ography and ecomorphs of Neotropical forest lizards (Squamata, Diploglossidae). *Molec. Phy-*
31
32
3259 *logen. Evol.*, 175, 107577. <https://doi.org/10.1016/j.ympev.2022.107577>
34
35
3660 Smith A.L., Roobol M.J., Mattioli G.S., Frywell J.E., Daly G.E. and Fernandez L.A., 2013. Vol-
37
38
3961 canic geology of the Mid-Arc Island of Dominica, Lesser Antilles. The surface expression of an
39
40
4162 Island-Arc batholith. *Geol. Soc. Amer., Spec. Pap.*, 496, 1-29. <https://doi.org/10.1130/2013.2496>
42
43
4463 Speed R.C., Smith-Horowitz P.L., Perch-Nielsen K.V.S., Saunders J.B. and Sanfilippo A.B., 1993.
45
46
4664 Southern Lesser Antilles arc platform: Pre-LateMiocene stratigraphy, structure, and tectonic evo-
47
48
4965 lution. *Geol. Soc. America, Spec. Pap.*, 277, 1–98.
49
50
51
5266 Stein S., Engeln J.F., Wiens D.A., Fujita K. and Speed, R.C., 1982. Subduction seismicity and tec-
53
54
5567 tonics in the Lesser Antilles arc. *J. Geophys. Res.*, 87 (NB10), 8642–8664.
55
56
5768 <https://doi.org/10.1029/JB087iB10p08642>
57
58
59
60
61
62
63
64
65

- 1269 Surget-Groba Y. and Thorpe R.S., 2013. A likelihood framework analysis of an island radiation:
 1270 phylogeography of the Lesser Antillean gecko *Sphaerodactylus vincenti*, in comparison with the
 2
 1271 anole *Anolis roquet*. J. Biogeogr., 40, 105-116. [2699.2012.02778.x](https://doi.org/10.1111/j.1365-

 3

 4

 5

 1272 <a href=)
 6
 7
 8
 1273 Townsend T.M., Tolley K.A., Glaw F., Böhme W. and Vences M., 2011. Eastward from Africa:
 9
 10
 11
 1274 palaeocurrent-mediated chameleon dispersal to the Seychelles islands. Biol. Lett., 7, 225-228.
 11
 12
 13
 1275 <https://doi.org/10.1098/rsbl.2010.0701>
 13
 14
 15
 16
 1276 Vail P. R., Mitchum R. M. and Thompson S., 1977, Seismic stratigraphy and global changes of sea
 17
 18
 19
 1277 level, Part 3: Relative changes of sea level from coastal onlap. In: Payton C.W. (Ed.), Seismic
 19
 20
 21
 1278 Stratigraphy—Applications to Hydrocarbon Exploration, AAPG Mem., 26, 83-97.
 21
 22
 23
 24
 1279 Van Rijnsingen E.M., Calais E., Jolivet R., de Chabaliér J.B., Robertson R., Ryan G.A., Symithe S.,
 24
 25
 26
 27
 1280 2022. Ongoing tectonic subsidence in the Lesser Antilles subduction zone. Geophys. J. Int., 231,
 27
 28
 29
 1281 319–326. <https://doi.org/10.1093/gji/ggac192>
 29
 30
 31
 32
 1282 Vérati C., Lardeaux J. M. Favier A., Corsini M., Philippon M. and Legendre, L., 2018. Arc-related
 32
 33
 34
 1283 metamorphism in the Guadeloupe archipelago (Lesser Antilles active island arc): First report and
 34
 35
 36
 1284 consequences. Lithos, 320-321, 592-598. <https://doi.org/10.1016/j.lithos.2018.08.005>
 36
 37
 38
 39
 40
 1285 Wade B.S., Pearson P.N., Berggren W.A. and Paëlike H., 2011. Review and revision of Cenozoic
 40
 41
 42
 1286 tropical planktonic foraminiferal biostratigraphy and calibration to the geomagnetic polarity and
 42
 43
 44
 1287 astronomical time scale. Earth Sci. Rev., 104, 111-142. [rev.2010.09.003](https://doi.org/10.1016/j.earsci-

 44

 45

 46

 47

 1288 <a href=)
 47
 48
 49
 50
 1289 Westercamp D., 1980. La Désirade, carte géologique à 1: 25 000 et notice explicative. Service Géo-
 50
 51
 52
 1290 logique National, Bureau de Recherches Géologiques et Minières, Orléans, France.
 52
 53
 54
 55
 56
 1291 Westercamp D., Andréïeff P., Bouysse P., Cottez S., and Battistini,R., 1989. Notice explicative,
 56
 57
 58
 1292 Carte géol. France (1/50 000), feuille MARTINIQUE. Bureau de recherche géologiques et mi-
 58
 59
 60
 1293 nières, Orléans, France.
 59
 60
 61
 62
 63
 64
 65

- 1294 Xu G., Haq, B.U., 2022. Seismic facies analysis: Past, present and future, Earth-Science Reviews
1295 224, 103876. <https://doi.org/10.1016/j.earscirev.2021.10387>
2
3
- 1296 Zami F., Quidelleur X., Ricci J., Lebrun J.-F. and Samper A., 2014. Initial sub-aerial volcanic activ-
5
6
7
8
1298 ity along the central Lesser Antilles inner arc: New K–Ar ages from Les Saintes volcanoes. J.
Volcanol. Geother. Res., 287, 12–21. <https://doi.org/10.1016/j.jvolgeores.2014.09.011>

1299

13

14

15

16

17

18

19

20

21

22

23

24

25

26

27

28

29

30

31

32

33

34

35

36

37

38

39

40

41

42

43

44

45

46

47

48

49

50

51

52

53

54

55

56

57

58

59

60

61

62

63

64

65

1300

1
201 **Figure captions**

1302

1303 Figure 1. A) Geodynamic setting of the eastern Caribbean. Bathymetry from the GEBCO (2014); AB:

5

1304 America Bank; DB: Dien Bien Phu Bank; TBR: Tiburon Ridge. B) Possible pathways for past

8

1305 dispersals of terrestrial fauna in eastern Caribbean. White box: studied area. 1: Aves Ridge,

10

1306 Paleogene; 2: Orinoco – southern Antilles, *e.g.*, Bourgade (2020); 3: Northern Lesser Antilles,

12

1307 Paleogene, Neogene

15

1308 Figure 2. Seismic lines location, structural setting, location of dredges and toponomy in the Marie-

18

1309 Galante Basin. Background relief map is from the GEBCO (2014); high resolution relief is a

20

1310 digital terrain model from multibeam bathymetric data acquired during the Aguadomar, Sis-

21

1311 mAntilles 2 and KaShallow cruises (French Oceanographic Fleet); Islands relief is from the

25

1312 SRTM (<https://doi.org/10.5066/F7PR7TFT>). A) Location of seismic reflection data; pink and

26

1313 yellow bold lines are section presented in Figs. 4 to 7 and supplementary material Figs. S3 to

30

1314 S6. Dashed bold lines are seismic lines over the Karukéra Spur, referred in text and published

31

1315 by De Min et al. (2015). B) Structural map re-interpreted from Feuillet et al. (2002), De Min et

35

1316 al. (2015) and Leclerc et al. (2016) ; ticks lines are normal faults. Orange bold line is the north-

36

1317 ern boundary of MG-MS1 megasequence. Dashed bold line indicates the western extent of the

40

1318 MG-MS1 carbonate platform as it can be interpreted from seismic facies. C) Rock samples

42

1319 location. M_aL: Morne à l'Eau drill, PF: Pointe Frégule outcrop. D) Toponymy : island names

43

1320 are in bold. CB: Colombie Bank, GT: Grande-Terre, LSP Les Saintes Plateau, PCSM: Petit Cul

47

1321 de Sac Marin, RP Rodrigue Plateau.

48

1322 Figure 3. Synthetic lithostratigraphic logs, major unconformities, correlations and ages across car-

51

1323 bonate platforms of the Guadeloupe archipelago islands and adjacent submerged Karukéra spur

53

1324 and Colombie Bank.

55

56

57

58

59

60

61

62

63

64

65

1325 Figure 4. Line drawing and interpreted section of the seismic lines Aguadomar 116 -34 and 119 and
 1326 KaShallow K09_80 extending from the Rodrigue Plateau (west) to the Karukéra Spur (east).
 2
 1327 Location in Fig. 2A. The cross-section illustrates the architecture of the Kubuli and Arawak
 4
 5
 1328 Sub-basins, including the westward deepening of the basement beneath MG-MS1, the lateral
 7
 1329 facies transition of MG-MS1 deposits toward the remnant arc and the eastward prograding ar-
 9
 10
 1330 chitecture of MG-MS2 and MG-MS3. Black rectangles outline location of facies illustrated and
 12
 1331 described in supplementary material Figure S2, as well as location of enlargements A, B, C and
 14
 15
 1332 D illustrating some characteristic parts of the seismic lines that are described in the text. An
 16
 17
 1333 uninterpreted section and a larger line drawing image are available in supplementary material
 19
 20
 1334 Figure S3.

22
 23
 1335 Figure 5. Line drawing and interpreted section of the seismic lines KaShallow K09_26-60-61-62 in
 24
 25
 1336 the central part of the Marie-Galante Basin. Location in Figure 2A. The cross-section illustrates
 27
 1337 the transition between the South Grande-Terre Plateau downslope toward the Arawak Sub-ba-
 28
 29
 1338 sin extending NNW-SSE between the Kubuli Sub-basin outer slope and the faulted Karukéra
 30
 1339 Spur eastern border. Black rectangles outline location of facies illustrated and described in sup-
 34
 35
 1340 plementary material Figure S2, as well as location of zooms A and B illustrating some charac-
 37
 1341 teristic parts of the seismic line that are described in the text. An uninterpreted section and a
 39
 40
 1342 larger line drawing image are available in supplementary material Figure S4.

42
 43
 1343 Figure 6. Line drawing and interpreted section of the seismic lines KaShallow K09_51-52 in the
 44
 45
 1344 south-eastern part of the Arawak Sub-basin. Location in Figure 2A. The cross-section illustrates
 47
 1345 the deep incision of MG-SB2 in the southern Arawak Sub-basin, the peculiar facies of MG-
 48
 49
 1346 MS1 uppermost unit and significant internal incision into MG-MS2 in the northern Arawak
 50
 1347 Sub-basin. Black rectangles outline location of facies illustrated and described in supplemen-
 54
 55
 1348 tary material Figure S2, as well as location of zooms A and B illustrating some characteristic
 57
 1349 parts of the seismic line that are described in the text. An uninterpreted section and a larger line
 59
 60
 1350 drawing image are available in supplementary material Figure S5.

1351 Figure 7. Line drawing and interpreted section of the seismic line KaShallow K09_90 in the western
 1352 part of Marie-Galante Basin. Location in Figure 2A. The cross section illustrates the landward
 1353 most part of the Kubuli Sub-basin with volcanic intrusions, cross cuts the Colombie Bank car-
 1354 bonate platform northward through the Morne-Piton Fault into the Petit Cul de Sac Marin Sub-
 1355 basin. Black rectangles outline location of facies illustrated and described in supplementary
 1356 material Figure S2, as well as location of enlargement A illustrating some characteristic parts
 1357 of the seismic line that are described in the text. An uninterpreted section and a larger line
 1358 drawing image are available in supplementary material Figure S6.

1359 Figure 8. 3D representation of the Marie-Galante Basin seen from the south-east illustrating the rela-
 1360 tionships between the upper plate igneous crust, the remnant and active arc and the Marie-
 1361 Galante Basin sedimentary infill. M-G.: Marie-Galante Island.

1362 Figure 9. Field views of the Martinique outcrops. Upper left panel: simplified geological map of
 1363 Martinique with organization of the remnant, intermediate and present day arcs. Locations of
 1364 La Caravelle, Tartane, Grand and Petit Macabou sections are indicated. A) simplified strati-
 1365 graphic organization of Caravelle Peninsula and Macabou areas carbonate platform intercalated
 1366 within the remnant arc formation (not to scale). Grand Macabou area: B) Aquitanian, coral-rich
 1367 part of the section; C) detailed view of a coral-rich bed. Petit Macabou area: D) top of karstified
 1368 and bored Aquitanian coral-rich bed with iron coatings (arrows; oblique view); E) Middle Mi-
 1369 ocene cross bedded volcanoclastic deposits with larger benthic foraminifera. See also supple-
 1370 mentary material Figure S7 for detailed cross sections, stratigraphic and depositional settings
 1371 descriptions, as well as larger benthic foraminifera determinations and biostratigraphic age cal-
 1372 ibrations.

1373 Figure 10. Age model reconstructed from correlations of onshore and offshore sedimentary sequences
 1374 between the northern and central Lesser Antilles. Naming from authors: MS: megasequence;
 1375 S: sequence; U: unit; SB and UB: sequence and unit boundary, respectively. GT: Grande-Terre,
 1376 MG: Marie-Galante, Des: La Désirade.

1377 Figure 11. Paleogeographic maps of the Marie-Galante Basin area since the late Oligocene-Early
 1378 Miocene to present. Each step is interpreted based on the sedimentary architecture of the basin
 2 as determined on the seismic line and described in the text. A) At the top of MG-MS1, B) during
 1379 MG-SB2 sequence boundary stand, C and D) during deposition of MG-MS2 lower and upper
 5 units respectively, E) during MG-SB3 stand, F and G) during deposition of MG-MS3 lower and
 1380 upper units respectively, and H) since the Middle Pleistocene. Dredge samples from the various
 7 units are indicated at each step. Samples description is reported in supplementary material Fig-
 1381 ure S1.
 9
 10
 1382
 12
 1383
 14
 15
 1384
 17

1385 Figure 12. Three steps cartoon illustrating the changing paleogeography of the central and northern
 20 Lesser Antilles during the Miocene, interpreted from this work and Cornée et al. (2021). Max-
 1386 imum extent of islands occurred during the late-Early Middle Miocene and the latest Miocene
 22 offering wide lands for species dispersion, while general drowning during the Middle to Late
 1387 Miocene and since the Early Pliocene reduced islands superficies and increased sea distance
 25 leading to isolate populations and driving speciations.
 1388
 27
 1389
 29
 1390
 32
 33

1391

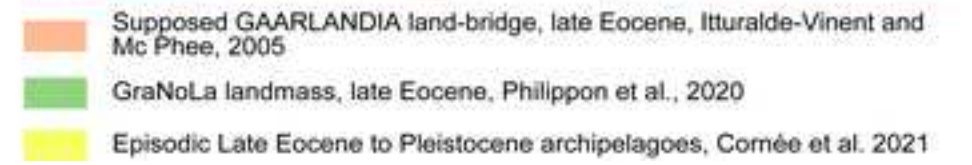
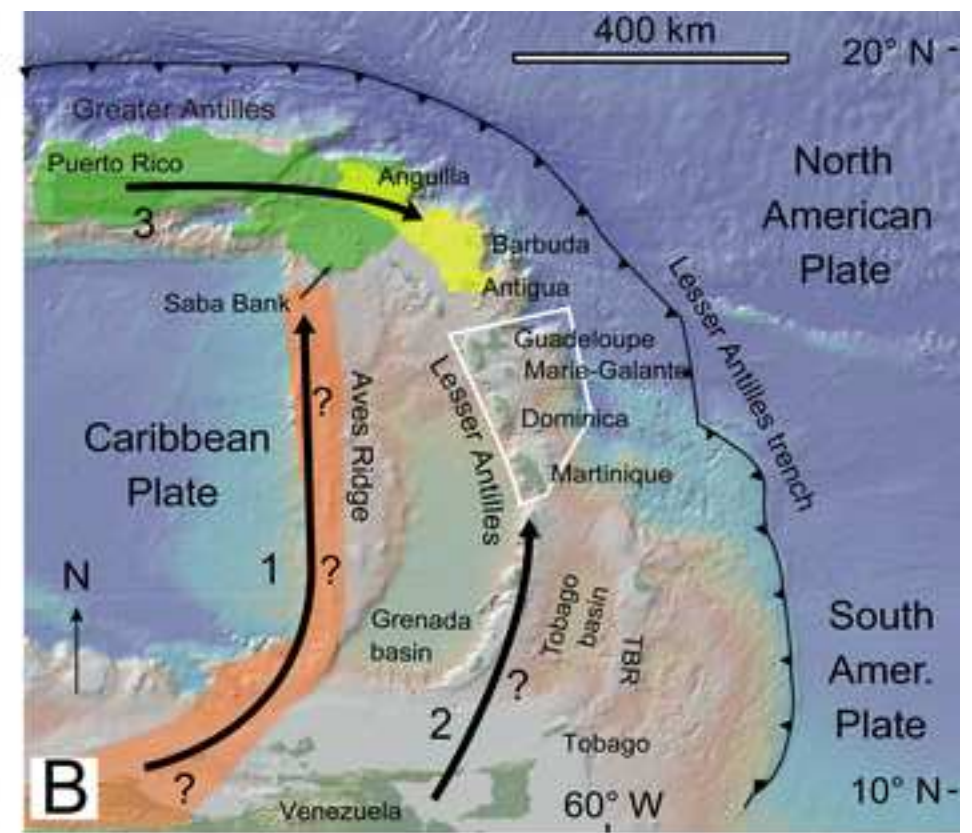
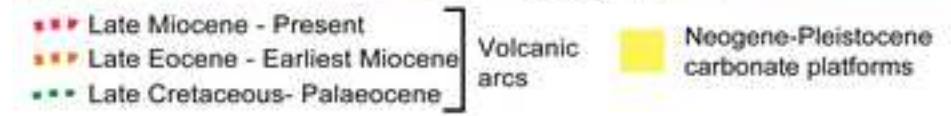
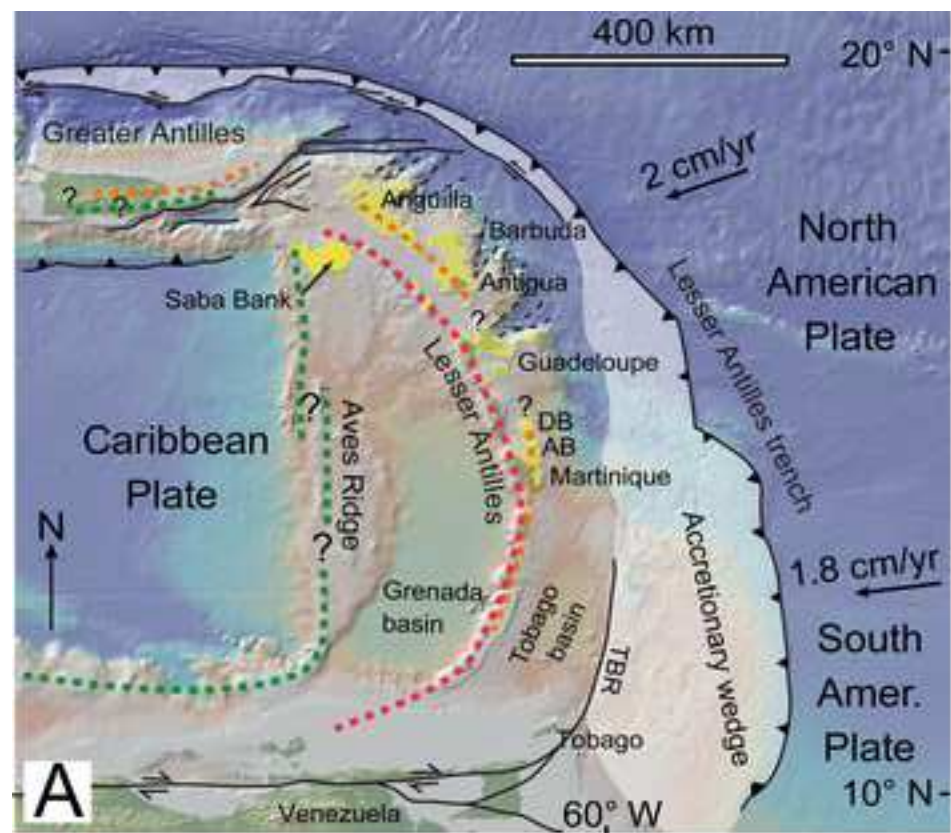
1392 **Supplementary data**

1393 Figure S1: micropaleontological analysis and depositional environments of samples dredged in the
 41 Guadeloupe archipelago (Arcante and KaShallow cruises).
 1394
 43
 44

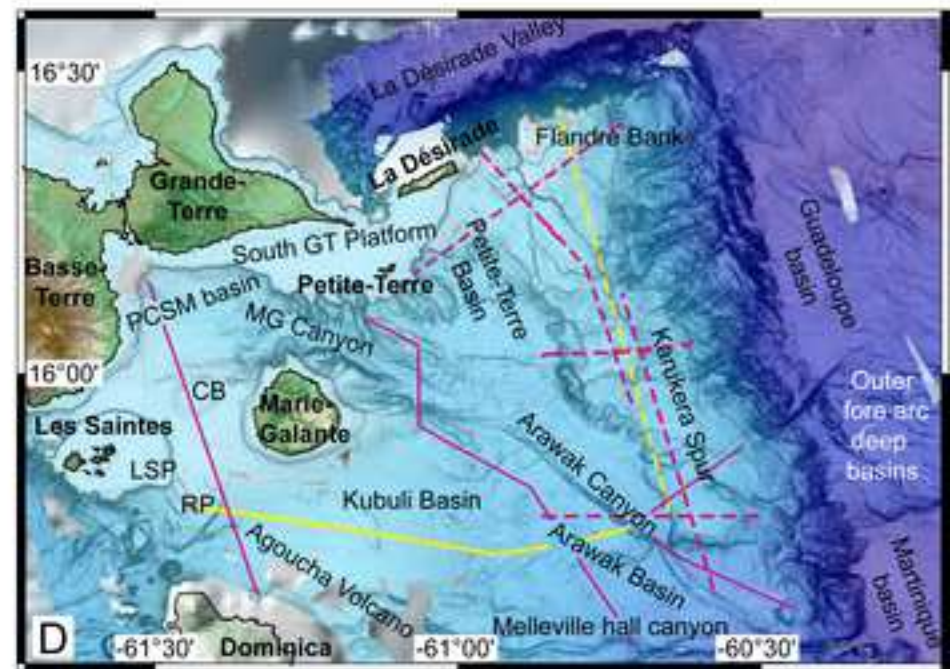
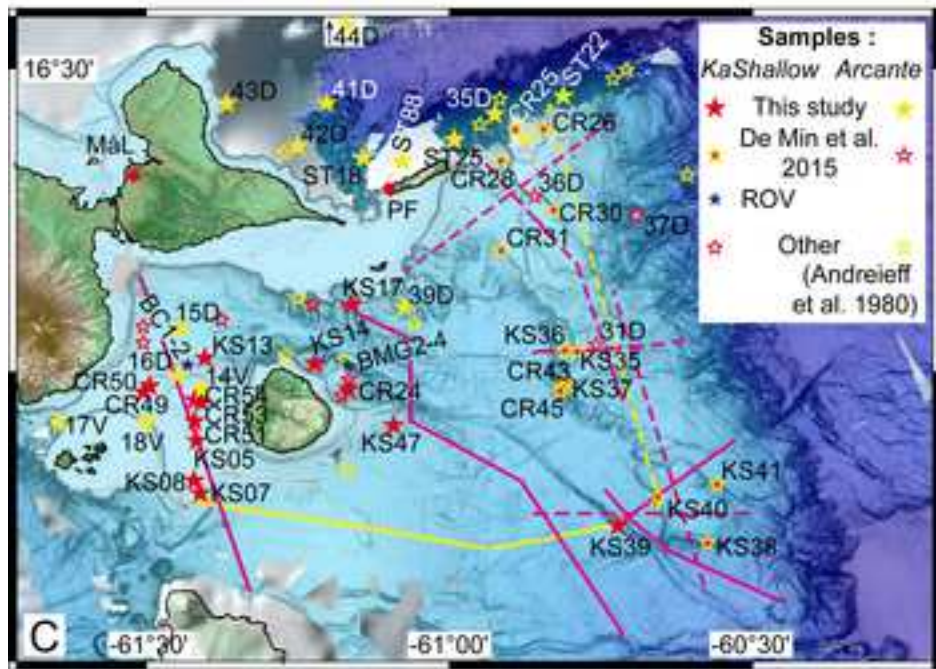
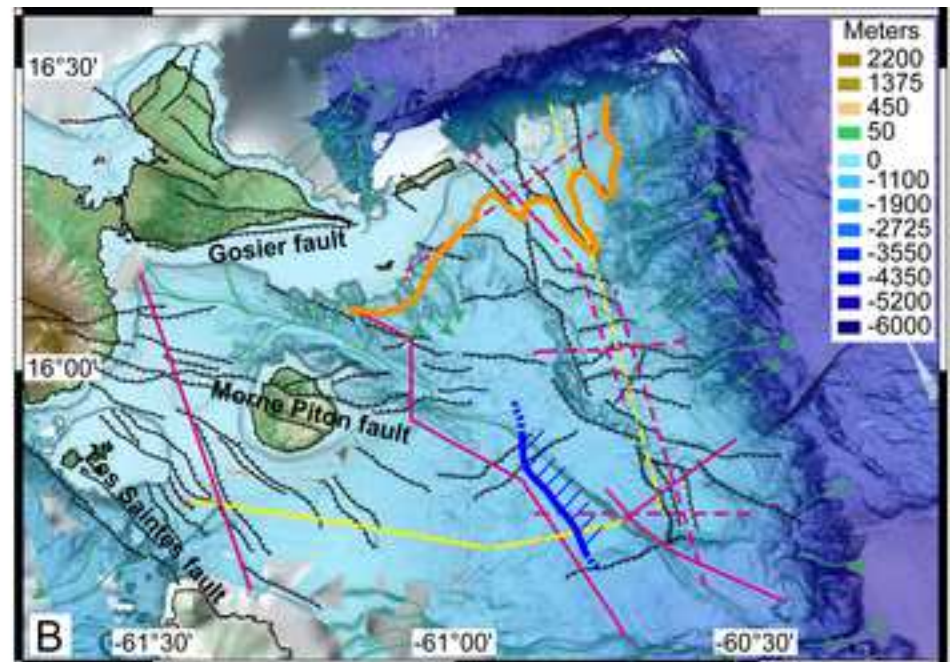
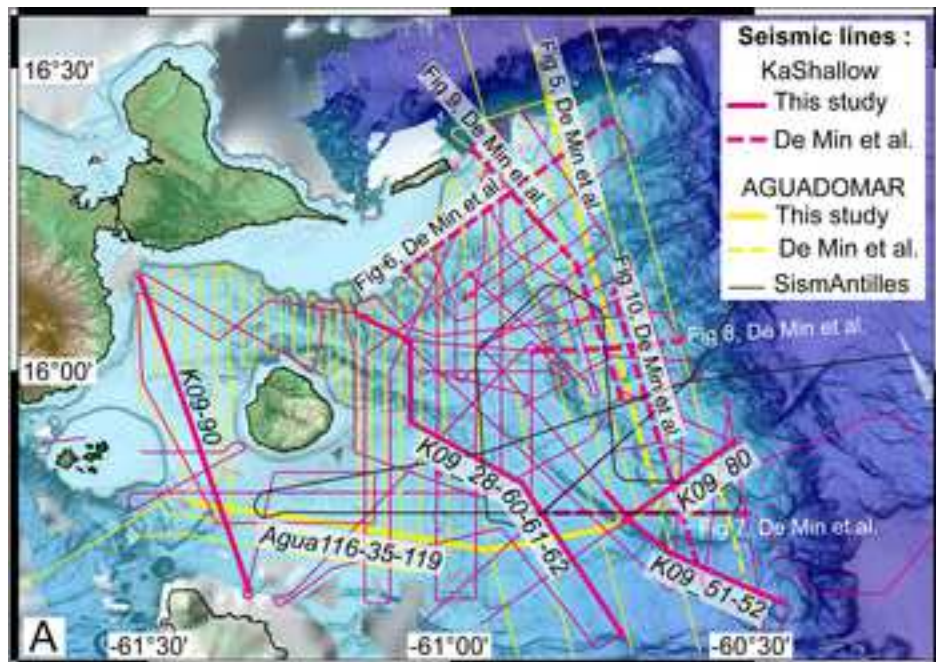
1395 Figure S2: illustration of the seismic facies from the Marie-Galante Basin and Karukéra Spur, their
 46 description and interpretation. Each facies is identified on seismic lines of Figures 4 to 7. In-
 1396 terval between black horizontal lines is 0.2s twt except for facies 14, 0,1s twt. Yellow-black
 50 images are high resolution seismic data from the KaShallow 2 cruise; Red-Blue images are
 52 medium resolution seismic data from the Aguadomar cruise; Grey image is from very high
 1397 resolution (sparker source) seismic line from the KaShallow 1 cruise (in Münch et al. 2013).
 54
 1398
 56
 1399
 57
 1400
 59
 60
 61
 62
 63
 64
 65

- 1401 Figure S3: Aguadomar seismic lines 116-034-119 and KaShallow 2 K09_80 (top) and interpreta-
 1402 tion (bottom) from the Rodrigue Plateau to the Karukéra Spur across the Kubuli and Arawak
 2
 1403 Sub-basins. Location in Figure 2A.
 3
 4
 5
 1404 Figure S4: KaShallow 2 seismic lines - K09_26-60-61-62 (top) and interpretation (bottom) from
 6
 7
 8
 1405 the South Grande-Terre Plateau to the southern Arawak Basin. Location in Figure 2A.
 9
 10
 11
 1406 Figure S5: KaShallow 2 seismic lines - K09_51-52 (top) and interpretation (bottom) across the
 12
 13
 14
 1407 south-western part of the Arawak basin. Location in Figure 2A.
 15
 16
 17
 1408 Figure S6: KaShallow 2 seismic line KS09_90 (top) and interpretation (bottom) across the western
 18
 19
 1409 Kubuli Sub-basin, the Colombie Bank and the Petit Cul de Sac Marin Sub-basin. Location in
 20
 21
 1410 Figure 2A.
 22
 23
 24
 1411 Figure S7: cross-sections, stratigraphy, depositional settings, larger benthic foraminifera and bio-
 25
 26
 27
 1412 stratigraphic age calibrations of the carbonate deposits in eastern Martinique (Caravelle, Tar-
 28
 29
 1413 tane, Grand Macabou and Petit Macabou).
 30
 31
 32
 1414 Figure S8: photographs of some of the larger benthic foraminifera in sample KS38 south of the Ka-
 33
 34
 35
 1415 rukéra Spur (location in Figure 2C). Cross-sections, stratigraphy, depositional settings, larger
 36
 37
 1416 benthic foraminifera (and photographs) and biostratigraphic age calibrations of the lower part
 38
 39
 40
 1417 of the carbonate deposits (Upper Plateaus) in Guadeloupe Morne à l'Eau borehole (location in
 41
 42
 1418 Figure 2C) and La Désirade at Pointe Frégule (location in Figure 2C).
 43
 44
 45
 46
 47
 48
 49
 50
 51
 52
 53
 54
 55
 56
 57
 58
 59
 60
 61
 62
 63
 64
 65

1
2
3
4
5
6
7
8
9
10
11
12
13
14
15
16
17
18
19
20
21
22
23
24
25
26
27
28
29
30
31
32
33
34
35
36
37
38
39
40
41
42
43
44
45
46
47
48
49



1
2
3
4
5
6
7
8
9
10
11
12
13
14
15
16
17
18
19
20
21
22
23
24
25
26
27
28
29
30
31
32
33
34
35
36
37
38
39
40
41
42
43
44
45
46
47
48
49



Grande Terre Marie Galante La Désirade Karukéra Spur

Andréieff et al. (1989)

Westercamp (1980)

Léticée et al. (2005)

Lardeaux et al. (2013)

Cornée et al. (2012)

Münch et al. (2014)

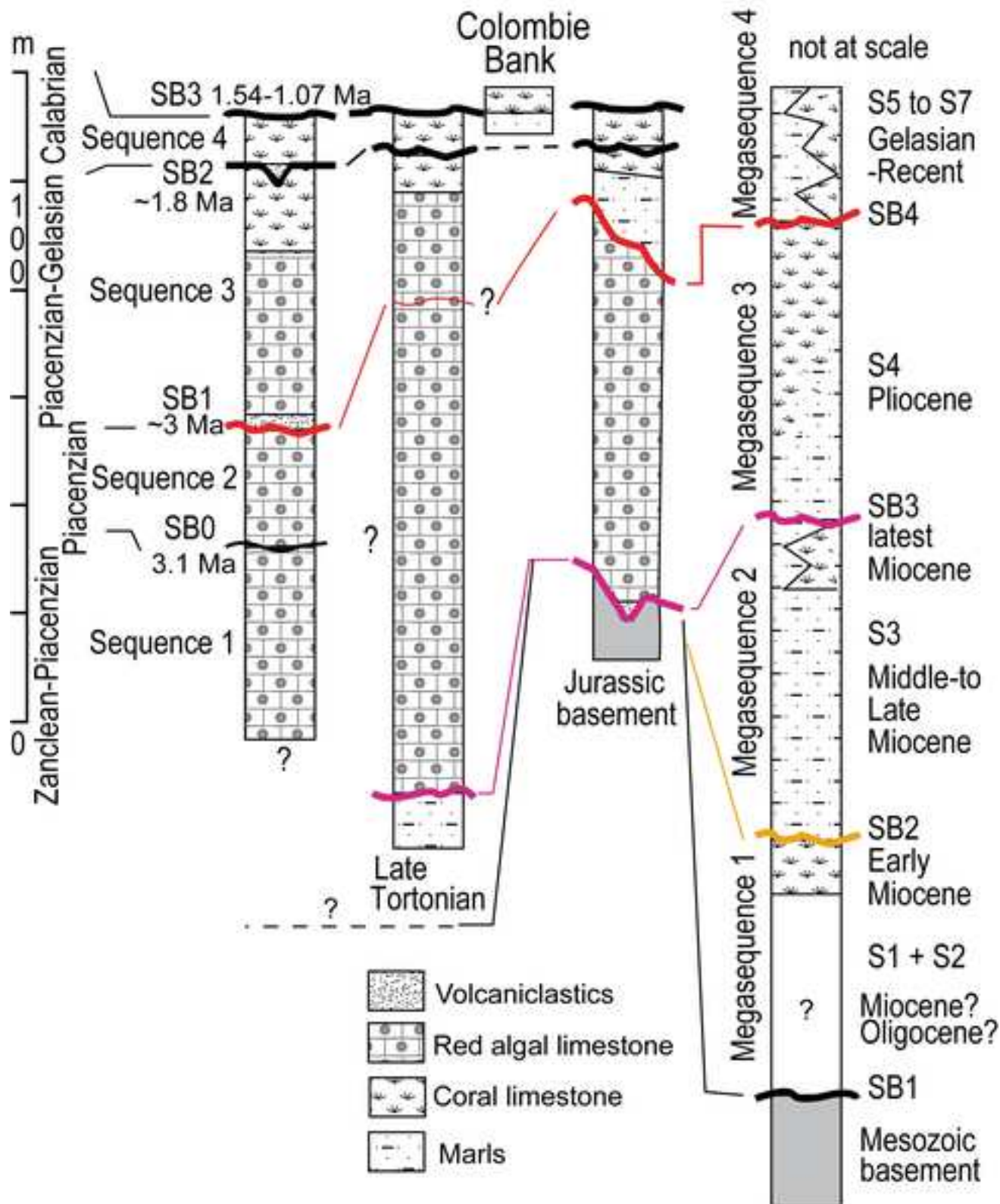
Simplified from

Münch et al. (2014) Bouysse et al. (1993)

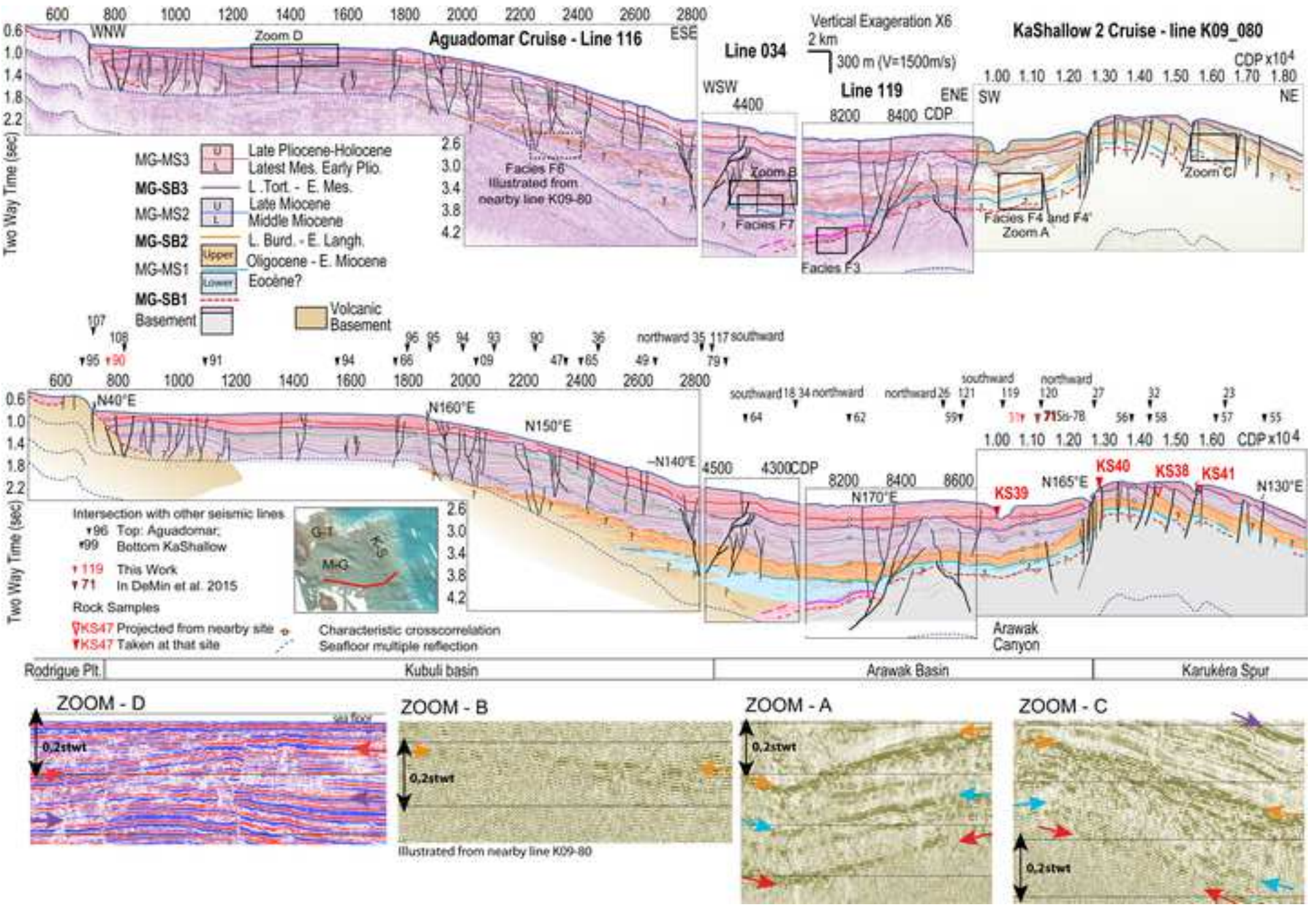
De Min, 2014

Münch et al., (2013)

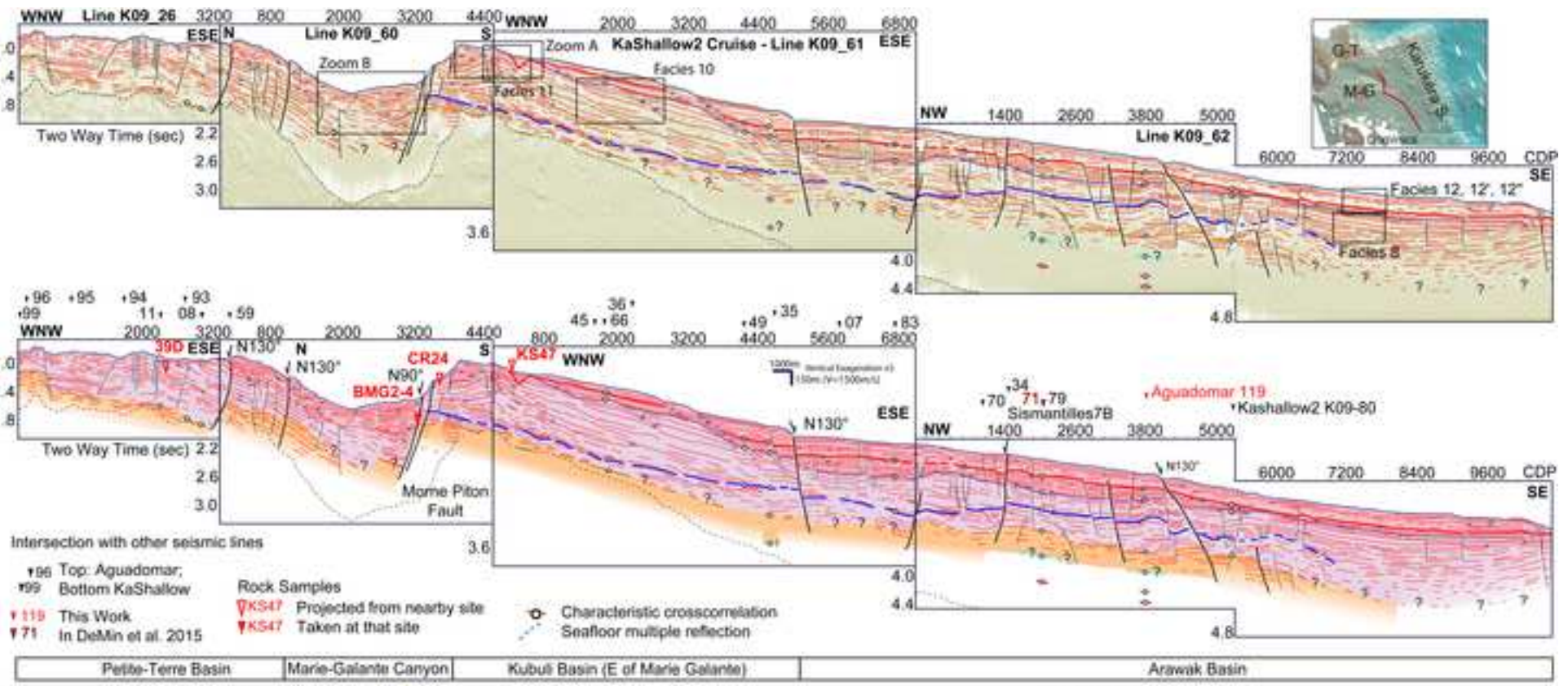
De Min et al., 2015



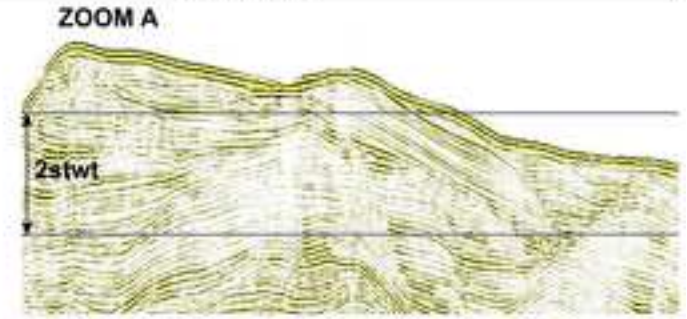
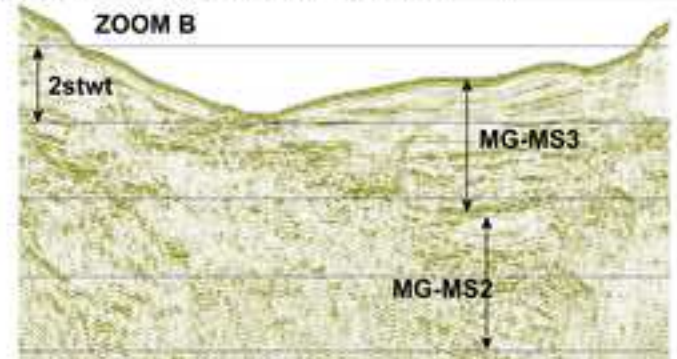
1
2
3
4
5
6
7
8
9
10
11
12
13
14
15
16
17
18
19
20
21
22
23
24
25
26
27
28
29
30
31
32
33
34
35
36
37
38
39
40
41
42
43
44
45
46
47
48
49

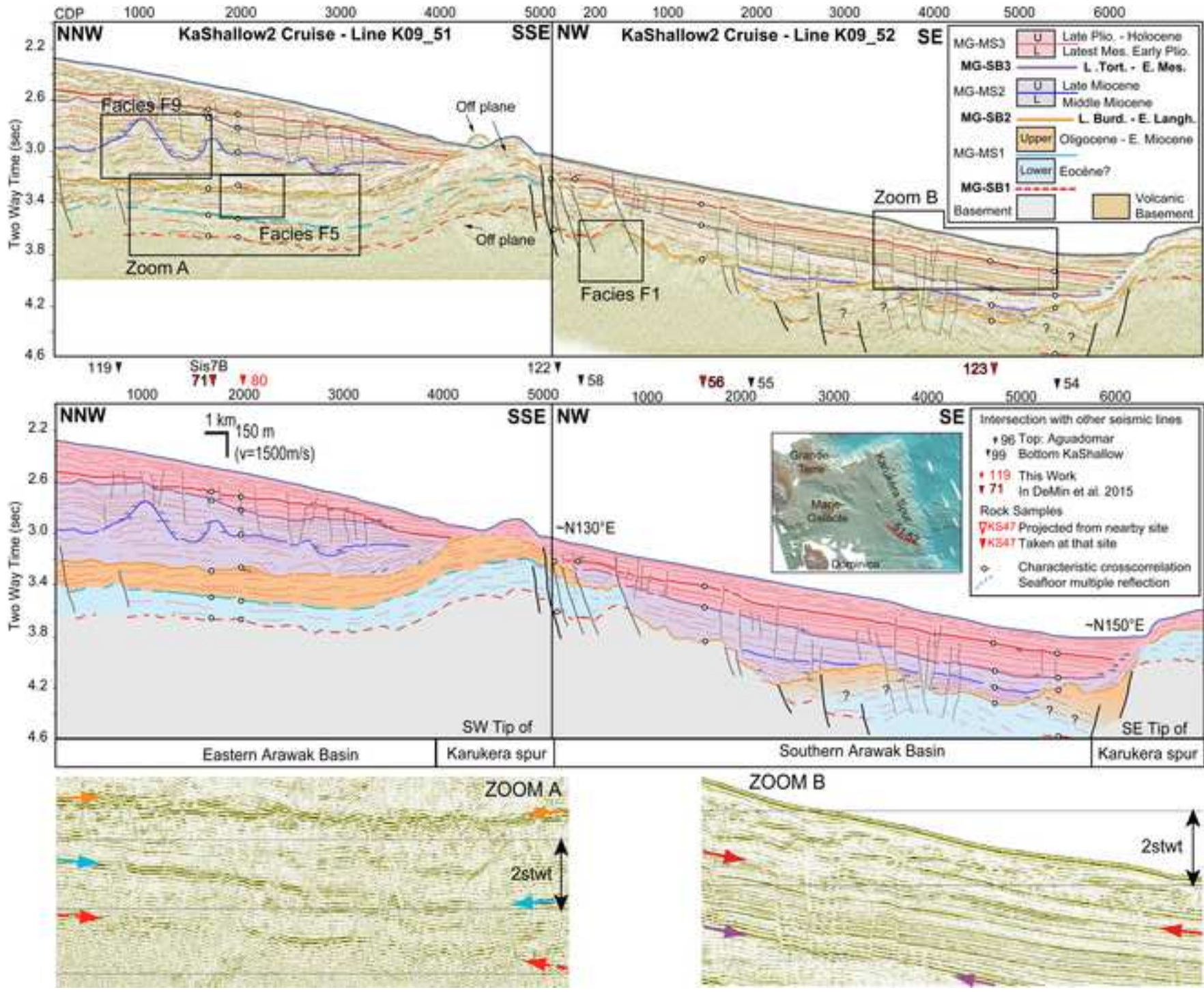


1
2
3
4
5
6
7
8
9
10
11
12
13
14
15
16
17
18
19
20
21
22
23
24
25
26
27
28
29
30
31
32
33
34
35
36
37
38
39
40
41
42
43
44
45
46
47
48
49



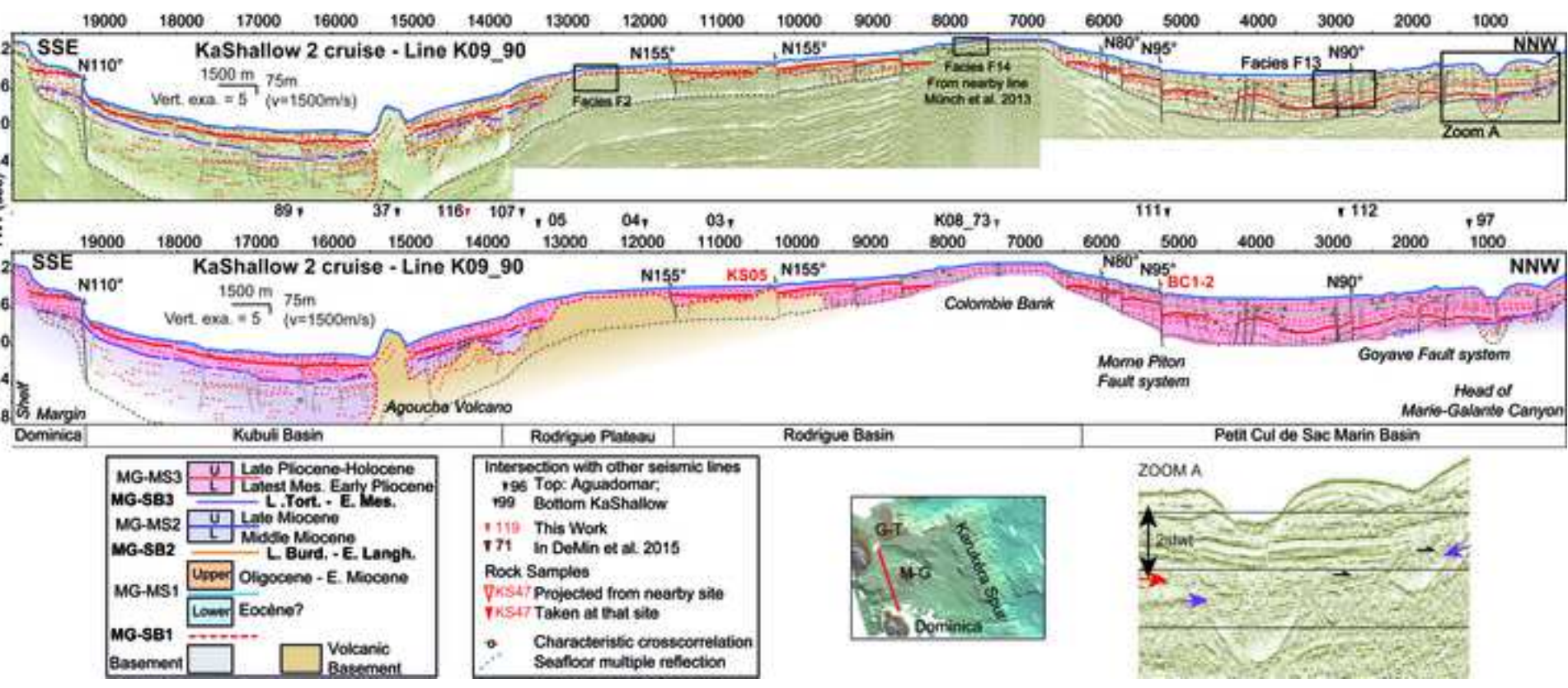
MG-MS3	U	Late Pliocene-Holocene
MG-SB3	L	Latest Mes. Early Pliocene
MG-MS2	U	L. Tort. - E. Mes.
MG-SB2	L	Late Miocene
MG-MS1	U	Middle Miocene
MG-SB1	L	L. Burd. - E. Langh.
	U	Upper Oligocene - E. Miocene
	L	Lower Eocene?
Basement		Volcanic Basement



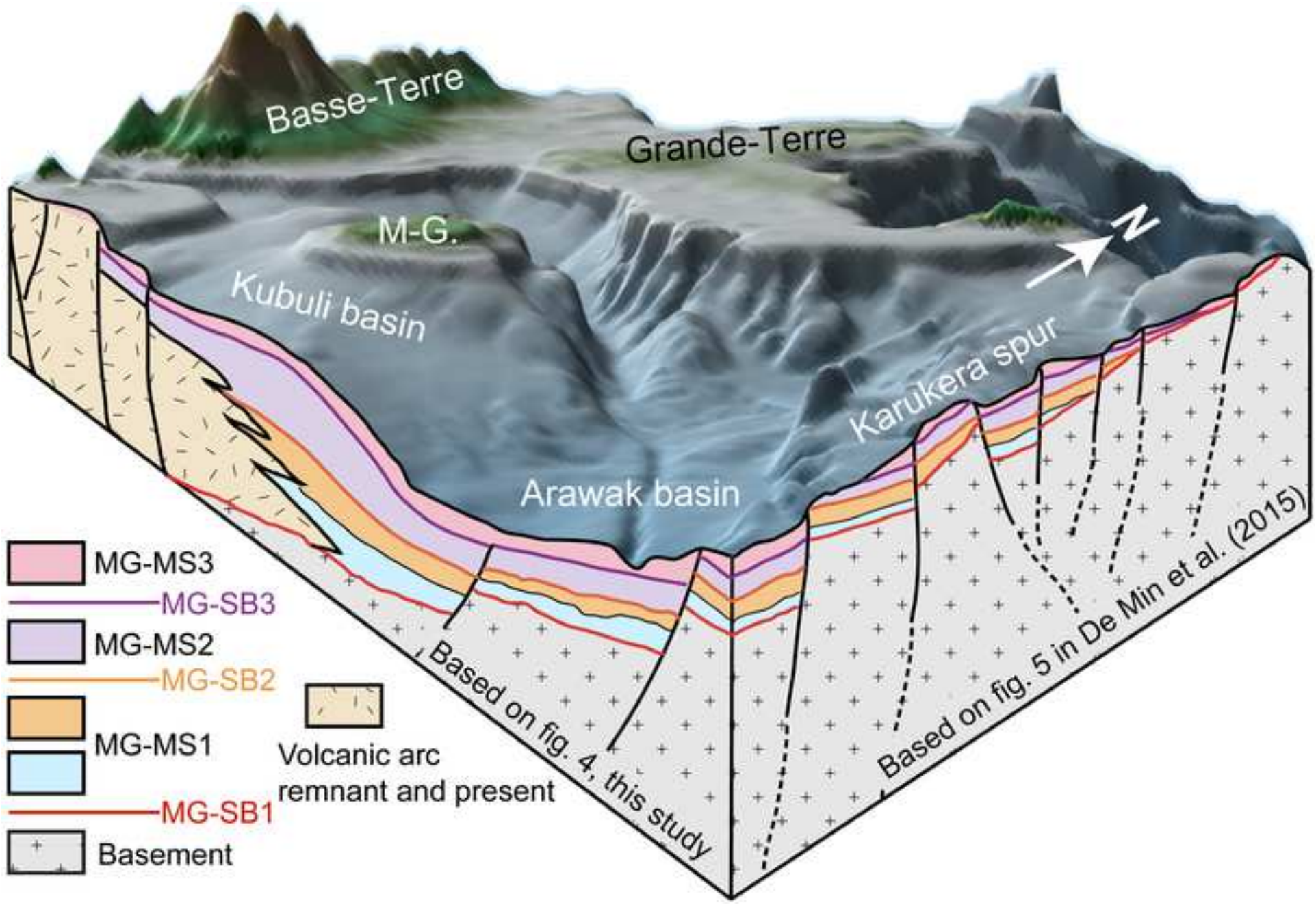


1
2
3
4
5
6
7
8
9
10
11
12
13
14
15
16
17
18
19
20
21
22
23
24
25
26
27
28
29
30
31
32
33
34
35
36
37
38
39
40
41
42
43
44
45
46
47
48
49

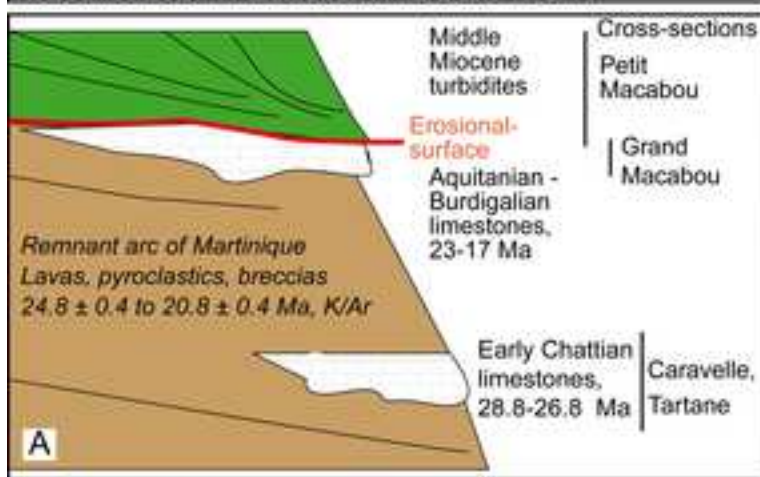
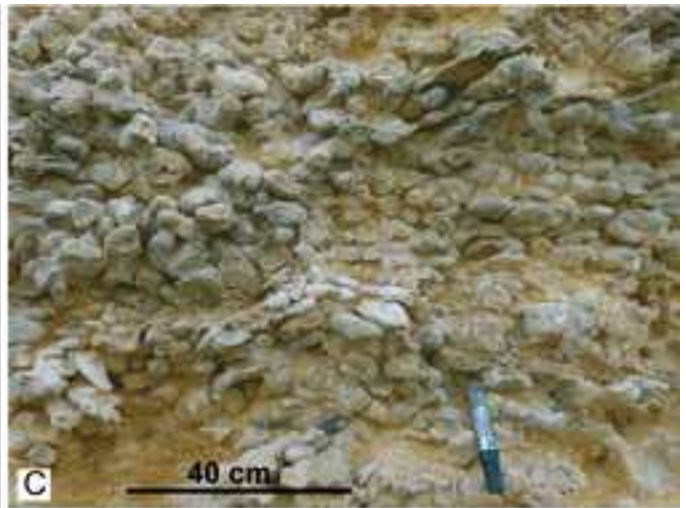
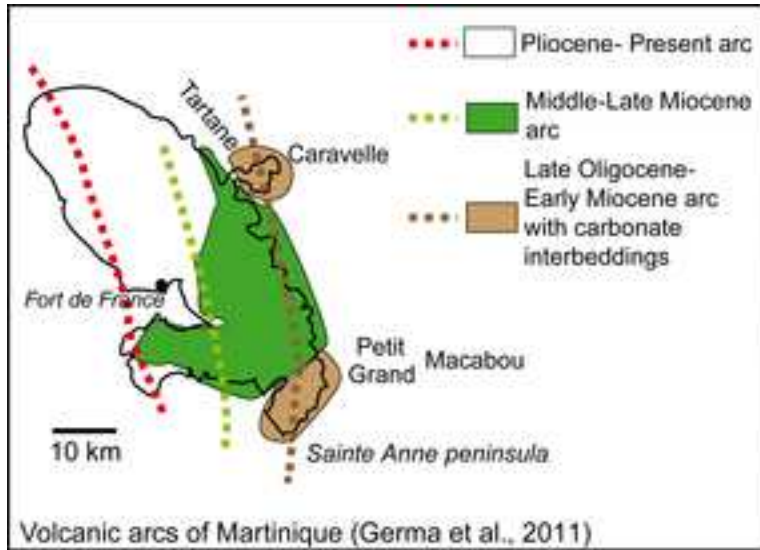
1
2
3
4
5
6
7
8
9
10
11
12
13
14
15
16
17
18
19
20
21
22
23
24
25
26
27
28
29
30
31
32
33
34
35
36
37
38
39
40
41
42
43
44
45
46
47
48
49



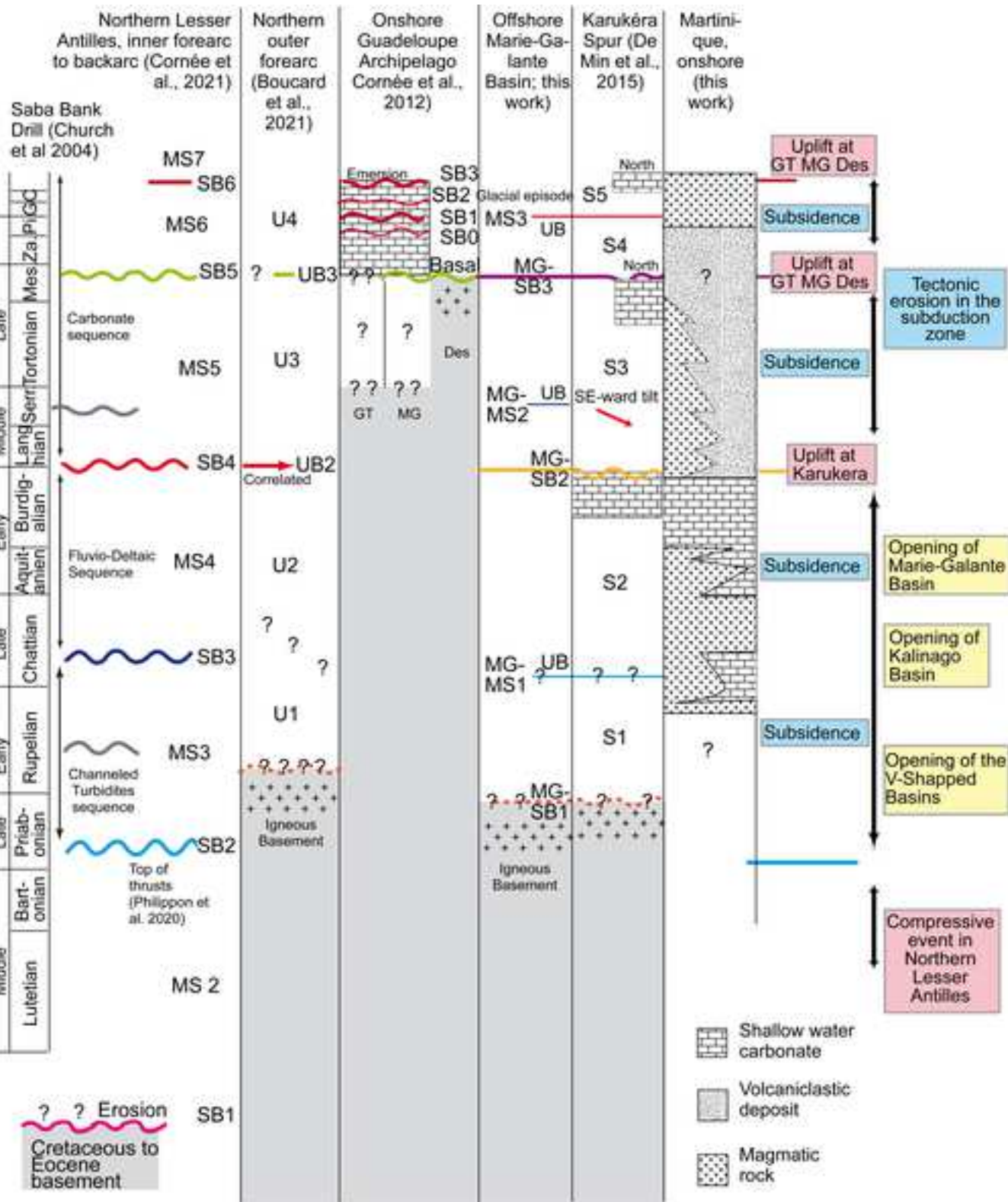
1
2
3
4
5
6
7
8
9
10
11
12
13
14
15
16
17
18
19
20
21
22
23
24
25
26
27
28
29
30
31
32
33
34
35
36
37
38
39
40
41
42
43
44
45
46
47
48
49

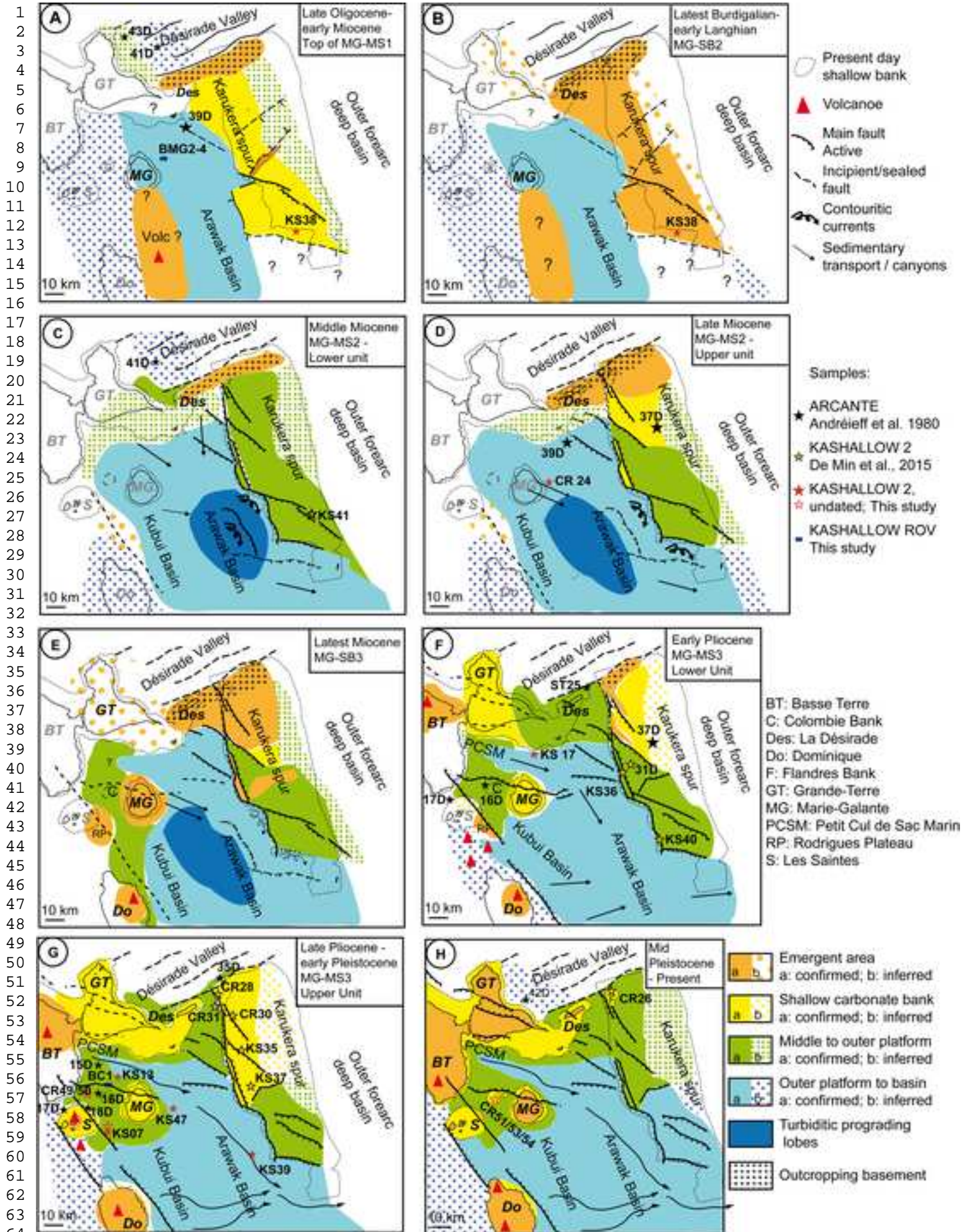


1
2
3
4
5
6
7
8
9
10
11
12
13
14
15
16
17
18
19
20
21
22
23
24
25
26
27
28
29
30
31
32
33
34
35
36
37
38
39
40
41
42
43
44
45
46
47
48
49
50
51
52
53
54
55
56
57
58
59
60
61
62
63
64
65

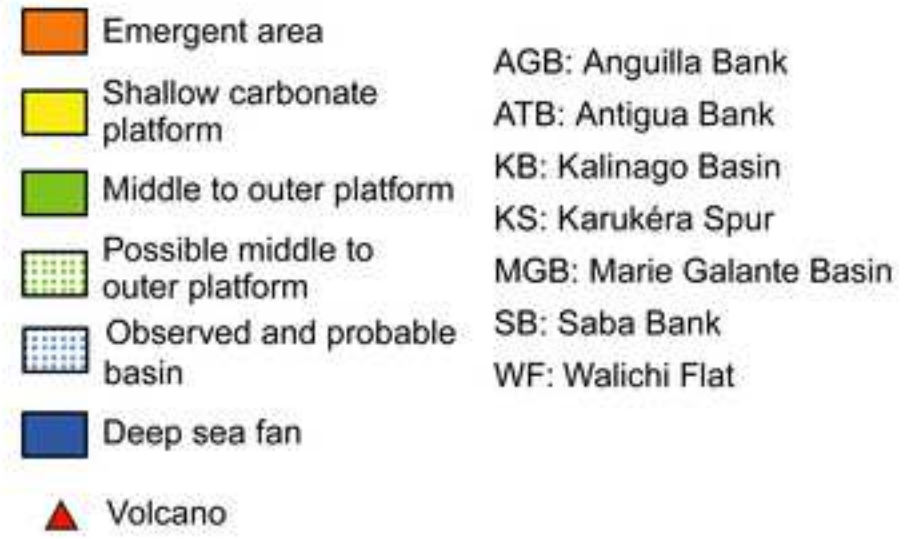
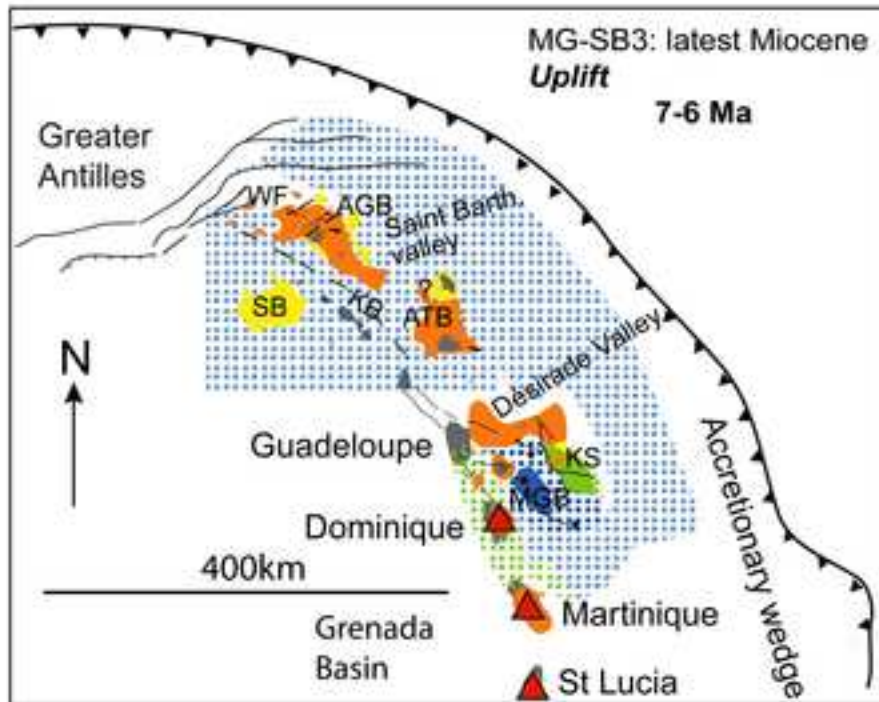
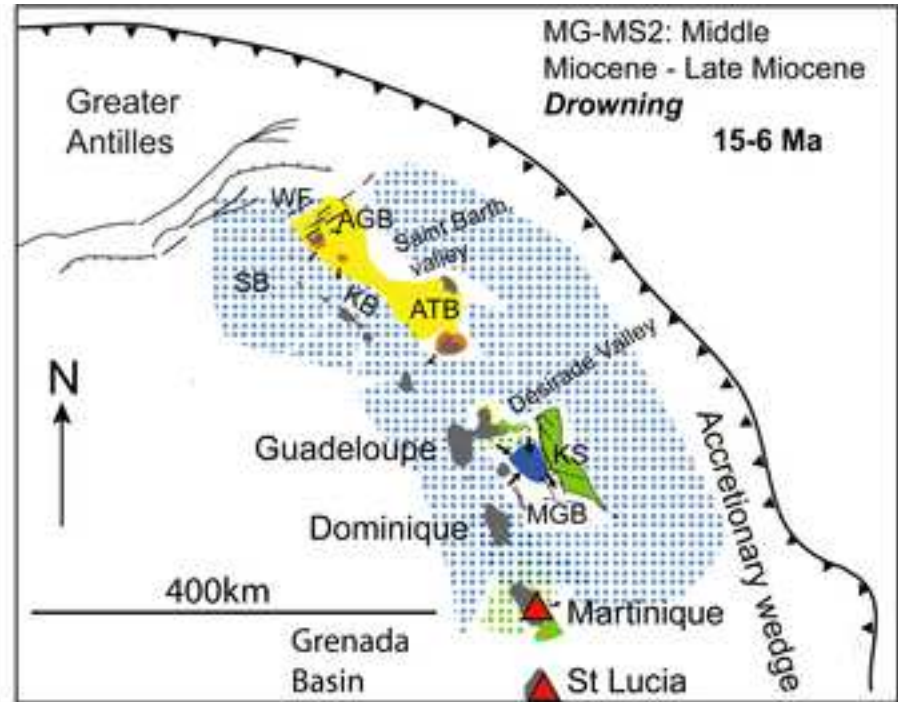
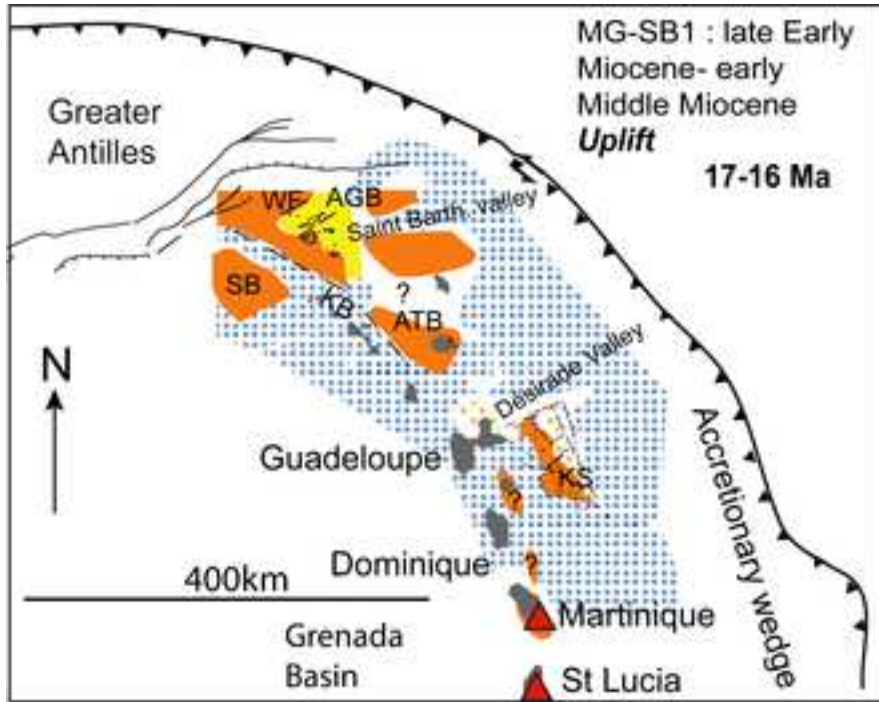


1
2
3
4
5
6
7
8
9
10
11
12
13
14
15
16
17
18
19
20
21
22
23
24
25
26
27
28
29
30
31
32
33
34
35
36
37
38
39
40
41
42
43
44
45
46
47
48
49
50
51
52
53
54
55
56
57
58
59
60
61
62
63
64
65





1
2
3
4
5
6
7
8
9
10
11
12
13
14
15
16
17
18
19
20
21
22
23
24
25
26
27
28
29
30
31
32
33
34
35
36
37
38
39
40
41
42
43
44
45
46
47
48
49

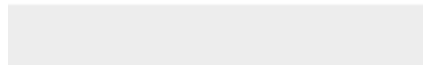




[Click here to access/download](#)

Supplementary Material (for online publication only)

Figure S1 DREDGES.pdf

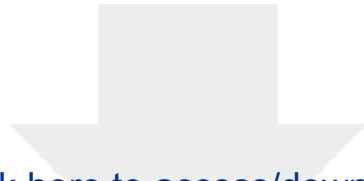




[Click here to access/download](#)

Supplementary Material (for online publication only)
Figure S2-Seismic-facies.pdf

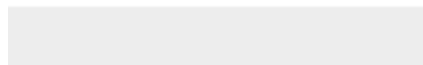


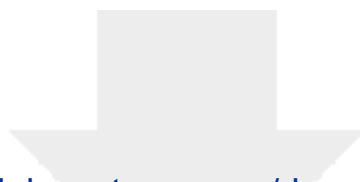


[Click here to access/download](#)

Supplementary Material (for online publication only)

Figure S3-Agua_116-34-119-080-A3.jpg

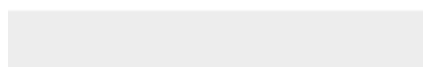
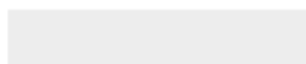


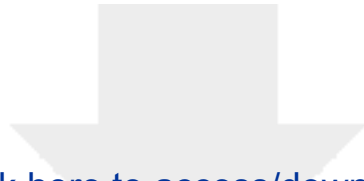


[Click here to access/download](#)

Supplementary Material (for online publication only)

Figure S4-K09_26-60-61-62-A3.jpg

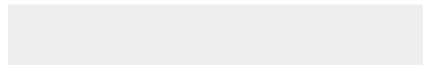


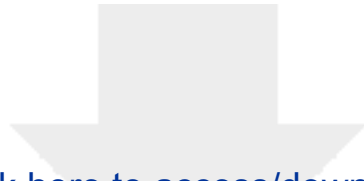


[Click here to access/download](#)

Supplementary Material (for online publication only)

Figure S5-K09_51-52-A3.jpg

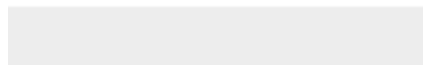
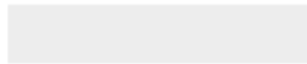


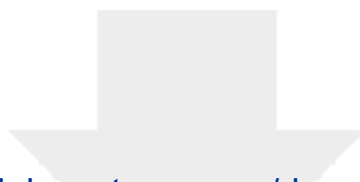


[Click here to access/download](#)

Supplementary Material (for online publication only)

Figure S6-K09_90-A3.jpg

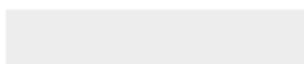




[Click here to access/download](#)

Supplementary Material (for online publication only)

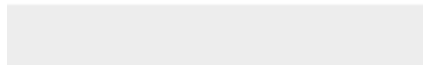
Figure S7-Martinique.pdf





[Click here to access/download](#)

Supplementary Material (for online publication only)
Figure S8-Guadeloupe.pdf



Declaration of interests

The authors declare that they have no known competing financial interests or personal relationships that could have appeared to influence the work reported in this paper.

The authors declare the following financial interests/personal relationships which may be considered as potential competing interests: